UNIVERSITY OF SOUTHAMPTON

ABSTRACT

FACULTY OF ENGINEERING, SCIENCE AND MATHEMATICS

SCHOOL OF MATHEMATICS

Doctor of Philosophy

Modelling the spreading and draining of viscous films

Jamie Michael Foster

The focus of the work in this thesis is to gain new insight into the fluid behaviour observed in a float glass furnace by means of simplified mathematical models. In particular, the models explore the dynamics of films of foam, known as logs, that spread across the surface of a pool of molten glass. The model employed throughout is the two dimensional Navier-Stokes equations, in the limit of zero Reynolds number, together with appropriate conditions at moving boundaries. Throughout the thesis, the slender geometry of the films is exploited using asymptotic techniques to simplify the models. In the introductory chapter, the motivating float glass manufacturing process is described, then the mathematical techniques and modelling assumptions that are used throughout the thesis are introduced. In the first technical chapter a model for the spreading of viscous films on the surface of a deep viscous pool is considered. Although this model neglects the effects of drainage it enables analytical progress to be made. As such, insight is gained into how the spreading logs interact with one another as they spread across the surface of the underlying pool. Analytic expressions for the evolution of a single spreading film, two spreading films and an infinite array of films are obtained. In addition, some comments on a general configuration of films are made. In the next technical chapter a model for the spreading and draining of a viscous film on a flat surface is considered. Although the model is simplistic, and neglects the interaction of logs via the underlying pool, it does allow some initial ideas on the effects of drainage to be explored. The model is systematically reduced to a nonlinear diffusion PDE. The subsequent analysis is applicable to a broad family of PDEs, hence the analysis is presented in some generality. Solutions to the PDEs under consideration exhibit an interesting behaviour in which the front of a compactly supported solution changes its direction of propagation. To explore this phenomenon, the behaviour of the front of the film as it advances (due to gravity driven spreading) and recedes (due to drainage) is examined. In particular, asymptotic solutions local to a time at which the front of the film changes its direction of propagation are obtained and their implications discussed. In the final technical chapter, the ideas from the previous two chapters are drawn together. A model is considered that incorporates both drainage, and allows the spreading logs to interact via the molten glass pool. It is shown that the model can be systematically reduced to a singular integro-differential equation (SIDE). In a special case, a steady state solution to this SIDE is obtained using a combination of asymptotic and numerical techniques. To complement the analysis in the previous chapters, advancing and receding fronts of solutions to the model are also examined. In the final chapter, the results of the previous chapters are summarised, and the practical implementation of the modelling is discussed. The work not only gives rise to a number of novel mathematical results, but also provides new understanding on the behaviour of spreading viscous films and the industrial float glass process.

Contents

List of Figures

Declaration of ownership

I, Jamie Michael Foster, declare that this thesis entitled 'Modelling the spreading and draining of viscous films' and the work presented in it are both my own, and have been generated by me as the result of my own research. I confirm that:

- this work was done wholly or mainly while in candidature for a research degree at this University;
- if any part of this thesis has previously been submitted for a degree or any other qualification at this University or any other institution, this has been clearly stated;
- where I have consulted the published work of others, this is always clearly attributed;
- where I have quoted from the work of others, the source is always given. With the exception of such quotations this thesis entirely my own work;
- I have acknowledged all main sources of help;
- where the thesis is based on work done by myself jointly with others, I have made clear exactly what was done by others and what I have contributed myself;
- parts of this work have been published as
  1. *The slow spreading of a viscous fluid film over a deep viscous pool*, to appear in the Journal of Engineering Mathematics.
  2. *The slow spreading of several viscous films over a deep viscous pool*, under consideration for publication in Physics of Fluids.
  3. *The reversing of interfaces in slow diffusion processes with strong absorption*, under consideration for publication in the SIAM journal of Applied Mathematics.
  4. *An SIDE model for the spreading and draining of viscous films on the surface of a deep viscous pool*, in preparation for submission.

Signed: Date:

Acknowledgements

I would first like to thank my supervisors Colin Please and Alistair Fitt for their insight, encouragement, patience and infectious enthusiasm throughout the project. They have made my time at Southampton not only educational but also extremely enjoyable. I am also very grateful to Giles Richardson, Giampaolo D'Alessandro, Marvin Jones and David Gelder for their input in numerous technical discussions. Thanks to David Martlew, David Collins, Graham Unwin, Keith Hyland, Andrew Keeley and Ian Williams for their helpful discussions regarding the industrial processes that motivated this study. I would also like to express my gratitude to the EPSRC for funding the project via a CASE award in collaboration with Pilkington Glass and to Vera Hazelwood from the Smith Institute for facilitating the partnership.

A wholehearted thank you to my family, girlfriend and all the friends (of which there are too many to mention by name) I have been fortunate enough have during the last three years. Without them I am quite sure I would not be in the position I am today.

Chapter 1

Introduction

This thesis is concerned with modelling the spreading and draining of films of slowly flowing incompressible viscous fluid. The problems presented here have three broad properties in common that make them susceptible to mathematical modelling (i) each flow has a small Reynolds' number, which enables the use of the Stokes flow simplification to the Navier-Stokes equations (ii) the slender geometry of the films mean that the models also admit the use of asymptotic perturbation schemes based on the inverse aspect ratio of the films (iii) the two dimensional nature of the flows allow boundary integral methods to be employed where appropriate. The presented models were originally motivated by fluid dynamic processes that occur in float glass furnaces (see section 1.1). However, the resulting models are studied in some generality and it is anticipated that many of the results will have applications in other physical processes (e.g. the flow of lava, the evolution of glaciers, optical fibre manufacture and the dispersion of populations [9], [10], [20], [32], [34], [59]).

In the remainder of this chapter an outline of the contents of this thesis is given. Next, a description of the float glass process is presented, and the need for the development of mathematical models is discussed. Following this, the key modelling assumptions that shall be used throughout this thesis are discussed. Finally, a paradigm model for the spreading of a viscous film over a flat surface is considered. This model, albeit unphysical, gives an introduction to the mathematical techniques that will be used throughout this thesis and serves as a simple analogy to the more complex models considered in chapters 2, 3 and 4.

In chapter 2, a model for the spreading of films of viscous fluid on the surface of a deep viscous pool is considered. The slender geometry of such films is exploited to employ asymptotic techniques to study the flow in these films. It is shown that when the viscosities and densities of the films and pool are comparable, the two dominant forces controlling the spreading are gravity, and the tangential stress induced in the films by underlying pool. As a consequence the rate of spreading does not depend on the viscosity of the films. Boundary integral techniques are used to determine the form of the flow in the pool. An analytic expression for the evolution of three scenarios is given; a single spreading film, two separate spreading films and an infinite periodic array of separate films. Chapter 2 concludes with the derivation of some results that apply to a general configuration of films.

Chapter 3 explores a family of nonlinear diffusion PDEs with drainage. One of the PDEs in this family is shown to be the equation that governs the spreading of a viscous film over a flat surface, subject to drainage. It is well known that solutions to the family of PDEs under consideration can exhibit behaviour in which a front of the compact support of the solution changes its direction of propagation. This corresponds to a film initially spreading and subsequently retreating due to drainage. Previously, no analytical explanation of how this change in the direction of the film front existed. To this end an analysis local to the time at which a front reverses is carried out by looking for self-similar solutions that change their direction of propagation. Using a combination of asymptotic and numerical techniques, solutions are found for the special case of a constant rate of drainage. Comments are also made on the more general case when the drainage is related to the film depth by a power law.

Chapter 4 presents a model for the spreading and draining of viscous films over a deep viscous pool. In a similar manner to the analysis in chapter 2, the slender geometry of the films is exploited to study the flow. It is shown that gravity and the tangential stress of the underlying pool are the dominant forces controlling the spreading of the films, provided; the viscosities and densities of the films and pool are assumed to be comparable, and the drainage rate is comparable to the typical vertical component of the fluid velocity in the films. The model is systematically reduced to a singular integro-differential equation (SIDE). For the special case of a constant rate of drainage, a steady solution is obtained using a combination of asymptotic and numerical techniques. Finally, to complement the analysis in chapter 3 solutions local to a travelling front of this SIDE are examined.

Chapter 5 concludes this thesis by summarising the results from the work presented in chapters 2, 3 and 4. Finally, a discussion on possible directions for future work, and the application of the models in the context of the float glass process is given.

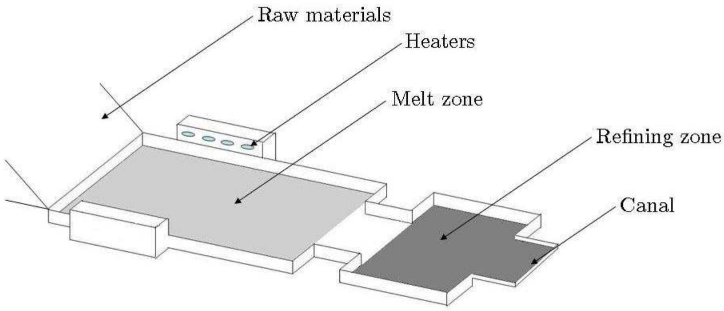

Figure 1.1: Schematic of a float glass furnace.

1.1 The float glass process, motivation and simplifying assumptions

A float glass furnace is the modern way of producing large quantities of flat sheets of glass. A schematic of a float glass furnace is shown in figure 1.1. On the left is a hopper that contains the raw materials, namely a granular substance consisting of recycled glass, sand and small traces of other minerals used to alter the optical properties of the end product. The grains fall from the hopper and are pushed into the main melting bath (shown in light grey). This is filled with molten glass over which the grains float. This layer of grains, known as the blanket, melts due to overhead heaters and heat from the underlying glass. As the grains in the blanket melt chemical reactions occur causing gases to be released and a glass foam to form. This foam is very wet (around 25% gas by volume) and the constituent bubbles have a typical diameter of 5×10^{-4}m. The fluid in this glass foam drains and the newly molten glass is subducted into the underlying molten glass below, so that it can then move from the melt zone into the refining area (shown in dark grey). The molten glass then flows out of the furnace via the canal (the thin outlet on the far right), where the thin layer of glass is allowed to slowly cool and solidify to form sheet glass.

One reason to model this process is to try to improve the efficiency of such glass furnaces. Materials that enter the furnace require a large amount of energy to be heated to a sufficiently high temperature for the glass to be refined properly. It is therefore desirable in terms of furnace efficiency (and of environmental interest) that as much of the end product as possible is of a usable quality. A major reason that the glass may not be usable is the presence of small

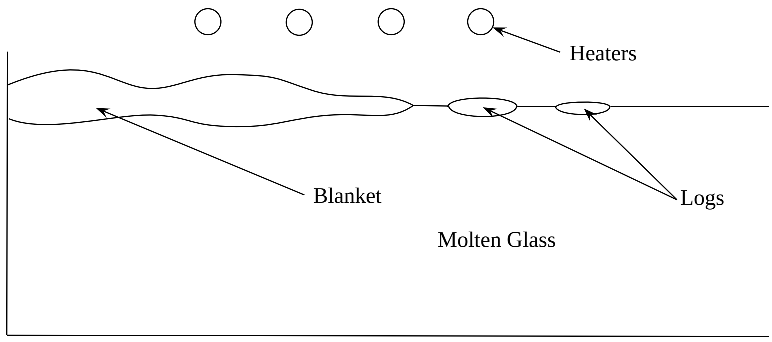

Figure 1.2: A schematic of the blanket and logs floating on the molten glass pool.

bubbles in the end product. As the grains in the blanket initially melt, chemical reactions occur which cause the release of gases. These become partially trapped within the newly melted fluid, causing a glass foam to form. As this foam is heated further, most of the bubbles rise and are liberated from the top of the foam blanket. Some, however, do not rise in time to burst before the new glass is subducted into the melt. These bubbles can then remain in the glass after it has solidified. The final stage of melting before the new glass is subducted often occurs on a piece of blanket that has detached from the main portion of the floating layer (the detached pieces of blanket are known as logs), see figure 1.2. Therefore, it is important to understand in detail the behaviour of these logs as they spread across the surface of the glass pool.

The float glass process involves many interacting physical processes, and so the mathematical modelling of the flow is challenging. One could incorporate processes such as; heating (by conduction or radiation), the resulting convective flows that are driven in the underlying pool, chemical reactions and the changes in phase of the melting blanket into a model. The studies [11] and [25] have considered in detail the convective flow in the pool that is driven by thermal gradients. In [25], it is shown that an estimate for the magnitude of the velocities induced in the molten glass pool due to thermally driven convective flows is given by

$$\frac{\kappa}{L}\sqrt{Ra} = \frac{\kappa}{L}\sqrt{\frac{\alpha g_r L^3 \Delta T}{\nu\kappa}} \sim 3 \times 10^{-3}\text{m s}^{-1}. \tag{1.1}$$

Here g_r is the acceleration due to gravity and Ra is the Rayleigh number, the other physical parameters used in calculation (1.1) are taken from table 1.1. In this study it is argued that, under certain circumstances, an appreciable contribution to the flow in the furnace may be due to the spreading of logs. Some order of magnitude calculations strongly support this idea.

In what follows ρ_f is the density of a log, u_0 is a typical horizontal velocity, W is a typical surface height of a log above the glass pool and all parameters are taken from table 1.1. First it is observed that an estimate for the magnitude of the horizontal hydrostatic pressure gradient ($= \partial p/\partial x$) in a film is given $\rho_f g_r W L^{-1}$ kg m^{-2} s^{-2}. Hence the magnitude of the horizontal force due to the hydrostatic pressure acting along a film (of depth W) is given by $\rho_f g_r W^2 L^{-1}$ kg m^{-1} s^{-2}. Next it is observed that an estimate for the magnitude of the horizontal forces acting on a film due to the viscous stress of a pool ($= \mu\, \partial u/\partial y$) of depth L is given by $\nu \rho u_0 L^{-1}$ kg m^{-1} s^{-2}. Note that these estimates are in agreement with the non-dimensionalisation used in the subsequent models in chapters 2, 3 and 4, however, there the assumption that the densities of the logs and glass pool are comparable is exploited. Under this assumption $d(\rho - \rho_f)/\rho \sim W$. The exact values of the parameters (ν, d, ρ and ρ_f) that should be used in this estimate are not obvious. However, working on the basis that a log (that has been sufficiently melted to ensure its viscosity and density are comparable to that of the glass pool) will have spread so that its depth is approximately 1cm and has 25% gas content by volume, the following estimate for the velocity induced in the pool due to the spreading of logs is derived

$$u_0 \sim \frac{\rho_f g_r d^2}{\rho \nu} \left(\frac{\rho - \rho_f}{\rho} \right)^2 \sim 4.5 \times 10^{-3} \text{m s}^{-1}. \tag{1.2}$$

Of course, this estimate is highly sensitive to the values that are taken for ν, d, ρ and ρ_f, but it does indicate that under certain circumstances an appreciable contribution to the flow in the pool may be due to the spreading of logs. The spreading of logs is an important aspect of the flow to understand, since it is thought to be one of the main sources of defects in the glass. This study takes an alternative approach to previous work and here the aim is to understand solely the interactions between isolated logs and the flow induced in the underlying pool. Note that by doing this, the models presented here are relevant to any logs where the dominant velocities locally in the pool are those induced by the spreading of the logs rather than by convectional flows.

The ethos of the the work in this thesis will be to simplify the complex physics of the flow using a series of modelling assumptions in order that analytical progress can be made, yet the essence of the fluid behaviour should be retained. Before continuing, it is therefore relevant to discuss the assumptions that shall be made in the following chapters. The model employed

Table 1.1: A table of values of physical parameters typically observed in a glass furnace, see [42]. Here ρ is density, T is temperature, α is the thermal expansion coefficient, d is the depth of a log, w is the width of the glass pool, L is the depth of the glass pool, M is the mass flow rate both into and out of the furnace, κ is thermal diffusivity and ν is the kinematic viscosity.

$\rho \sim 2 \times 10^3$ kg m^{-3}	$T \sim 2600 - 1400$ K	$\alpha \sim 8.5 \times 10^{-6}$ K^{-1}
$d \sim 10^{-2}$ m	$w \sim 10$ m	$L \sim 1$ m
$M \sim 6$ kg s^{-1}	$\kappa \sim 10^{-5}$ m^2 s^{-1}	$\nu \sim 10^{-2}$ m^2 s^{-1}

throughout this thesis is Navier-Stokes equations. Only parts of the blanket and logs that have been sufficiently melted so that their effective viscosity is comparable to the viscosity of the underlying pool are considered. A further mechanism that the models must capture is the draining of the fluid in the foam films into the pool. The position of the interface between the films and pool is difficult to define since the constituent fluid in the foam is the same fluid as in the pool. One could argue that the position of the film-pool interface is defined by the position of the lowest bubbles in the films. Alternatively, one could argue that the film-pool interface does not have a sharp, well defined position and so a phase field model is appropriate. Here the modelling assumption will be to treat the foam and pool as two seperate fluids, with comparable but different viscosities and densities, seperated by a sharp interface. The drainage of the fluid from the films into the pool will be modelled by imposing mass flux conditions and the condition of conservation across the film-pool interface. Since the constituent fluid in the foam logs and the fluid in the glass pool are the same it shall also be assumed that surface tension effects are negligible.

1.2 The slow spreading of a viscous fluid on a flat surface

This section considers a model for a flow, albeit unphysical, that exhibits very similar mathematical characteristics to those that will be studied in chapters 2, 3 and 4. The model presented here can be thought of as a model for a film spreading over a lubricating layer of fluid when the interface between the spreading film and lubricating layer is held horizontal. Alternatively, it can also be thought of as a model for a film spreading over a plate in which the fluid is allowed to *slip* over the plate. In either case, the Navier slip condition (1.3) is the kinematic constraint to be imposed at the flat interface at the bottom of the spreading film. See figure 1.3 for a schematic of the flow.

The spreading fluid is modelled using the Navier-Stokes equations in the limit of zero Reynolds number. As is the case in chapters 2, 3 and 4 it is assumed that surface tension effects are negligible. The governing Stokes flow equations can be simplified further by exploiting the slender aspect ratio of the film. Asymptotic techniques are used to expand the Stokes flow equations in the parameter representing the inverse aspect ratio, and (to leading order) the lubrication equations are used to govern the spreading. The free surface of the film satisfies a stress free and kinematic condition, whilst between the plate and film, no penetration, and the Navier slip condition are imposed. This regime shall be analysed for different values of the shear length. It is therefore worth discussing the details of this condition further. On the interface between the film and the plate

$$\mathbf{t}'\mathbf{T}\mathbf{n} = \frac{\mu}{\delta}u. \tag{1.3}$$

is imposed. Where $\mathbf{T}$ is the stress tensor (defined in the usual way), $\mathbf{t}$ and $\mathbf{n}$ are unit vectors tangential and normal to the plate, u is the horizontal component of the velocity of the fluid, μ is the viscosity of the fluid, δ is the dimensional shear length and a prime denotes the usual vector transpose operation. This condition requires that the shear stress exerted on the fluid by the plate is proportional to the velocity of the fluid at that point. The constant of proportionality is the quotient μ/δ. It is found that different spreading regimes may be observed for different values of δ, the shear length. Later it will be shown that the size of this shear length determines the dominant physical mechanisms that govern the spreading behaviour. Understanding the relationship between the size of the shear length and the spreading dynamics is straightforward for the case of a fluid moving over a plate, but this is worth reiterating in order to gain insight into more complex examples that shall be examined in the subsequent chapters.

The problem for a fluid film spreading over a plate is scaled in the natural way with $x = L\bar{x}$, $y = W\bar{y}$, $u = u_0\epsilon^{\beta}\bar{u}$, $v = u_0\epsilon^{\beta+1}\bar{v}$, $p = \rho g_r W\epsilon^{\beta}\bar{p}$, $t = Lu_0^{-1}\epsilon^{-\beta}\bar{t}$ and $\delta = W\bar{\delta}$ with $u_0 = \rho g_r W^3\mu^{-1}L^{-1}$ and $\epsilon = WL^{-1}$. Here v is the vertical component of the fluid velocity, p is the pressure, t is time and β is a constant that must be chosen in agreement with the shear length. The non-dimensional PDEs and boundary conditions may then be written as

$$\begin{aligned} &\frac{\partial \bar{p}}{\partial \bar{x}} = \epsilon^2\frac{\partial^2 \bar{u}}{\partial \bar{x}^2} + \frac{\partial^2 \bar{u}}{\partial \bar{y}^2}, \quad \frac{\partial \bar{p}}{\partial \bar{y}} = \epsilon^4\frac{\partial^2 \bar{v}}{\partial \bar{x}^2} + \epsilon^2\frac{\partial^2 \bar{v}}{\partial \bar{y}^2} - \epsilon^{-\beta}, \\ &\frac{\partial \bar{u}}{\partial \bar{x}} + \frac{\partial \bar{v}}{\partial \bar{y}} = 0, \end{aligned} \tag{1.4}$$

subject to

$$\bar{\mathbf{t}}_h'\bar{\mathbf{T}}\bar{\mathbf{n}}_h = \bar{\mathbf{n}}_{\mathbf{h}}'\bar{\mathbf{T}}\bar{\mathbf{n}}_{\mathbf{h}} = 0 \quad \text{and} \quad \frac{\partial \bar{h}}{\partial \bar{t}} + \frac{\partial \bar{h}}{\partial \bar{x}}\bar{u} = \bar{v} \quad \text{on} \quad \bar{y} = \bar{h}(\bar{x}, \bar{t}) \tag{1.5}$$

and

$$\bar{\mathbf{t}}'\bar{\mathbf{T}}\bar{\mathbf{n}} = \frac{1}{\bar{\delta}}\bar{u} \quad \text{and} \quad \bar{v} = 0 \quad \text{on} \quad \bar{y} = 0. \tag{1.6}$$

Here the quantities, $\bar{\mathbf{t}}$, $\bar{\mathbf{n}}$, $\bar{\mathbf{t}}_{\mathbf{h}}$, $\bar{\mathbf{n}}_{\mathbf{h}}$ and $\bar{\mathbf{T}}$ depend on the parameter ϵ. However, for brevity the full expressions have not been shown explicitly.

The slender aspect ratio of the problem means that it is appropriate to consider the system in the limit that ϵ tends to zero, and examine the differences in spreading dynamics for different orders of magnitude of the non-dimensional shear length, $\bar{\delta}$ (relative to ϵ).

In section 1.2.1 it will be shown that when the shear length is comparable to the depth of the spreading film (i.e. $\delta = O(W)$) there are three dominant effects that control the spreading. These are; gravity, the shear induced in the film by the plate and the internal shear of the film. However, in section 1.2.2 it will be shown that when the shear length is increased to $O(L^2W^{-1})$ (and hence the velocity of the spreading is increased) the three dominant effects that control the spreading are gravity, the shear induced by the plate and resistance due to extensional forces. Then in section 1.2.3 it will be shown that for intermediate shear lengths (i.e. $O(W) < \delta < O(L^2W^{-1})$) the velocity of the spreading is not large enough to allow the resistance due to extensional forces to enter the dominant force balance, yet the spreading velocity is not small enough to allow the internal shear of the film to enter the dominant force balance. Hence, in this intermediate regime the spreading is largely controlled by gravity and the shear induced by the plate.

1.2.1 $\epsilon \to 0$, $\bar{\delta} = O(1)$

The problem may be analysed when $\bar{\delta} = O(1)$ by scaling with $\beta = 0$ (this scaling is represented with hatted variables). The PDEs and boundary conditions (1.4) - (1.6) may then be balanced at leading order to give, for the evolution of the free surface $y = h(x, t)$,

$$\frac{\partial \hat{h}}{\partial \hat{t}} + \frac{\partial}{\partial \hat{x}}\left(\hat{u}\hat{h}\right) = 0 \tag{1.7}$$

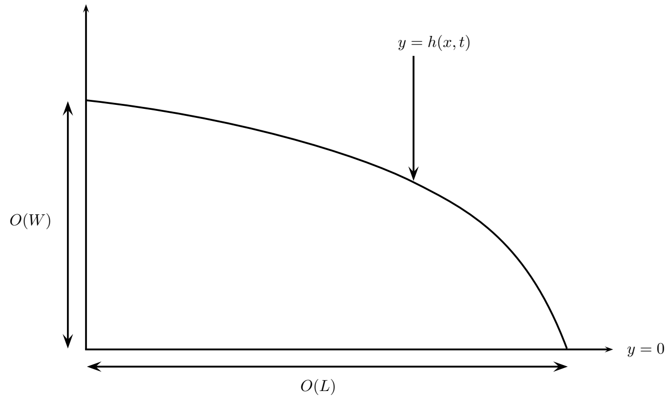

Figure 1.3: A schematic diagram of the flow showing the characteristic length scales.

and

$$0 = \hat{h}\frac{\partial \hat{h}}{\partial \hat{x}} + \frac{1}{\bar{\delta}}\hat{u} + \frac{1}{\bar{\delta}}\frac{\hat{h}^2}{3}\frac{\partial \hat{h}}{\partial \hat{x}}. \tag{1.8}$$

Equations (1.7) and (1.8) can be interpreted as the equation of mass conservation and a force balance. Together, (1.7) and (1.8) define a nonlinear diffusion equation for $\hat{h}$. In (1.8) there is a balance between the effect of gravity (represented by the first term), the shear induced by the plate (represented by the second term) and the internal shear of the film (represented by the third term). It can also be observed that by eliminating $\hat{u}$ from (1.7) and (1.8), and taking the limit that $\bar{\delta} \to 0$ the familiar result of Reynolds' equation is recovered, the well-known result for the condition of no slip along the plate [51].

1.2.2 $\epsilon \to 0$, $\bar{\delta} = O(\epsilon^{-2})$

The case $\bar{\delta} = O(\epsilon^{-2})$ may be considered by scaling the problem with $\beta = -2$ (this scaling is represented by variables marked with a tilde), and writing $\epsilon^{-2}\tilde{\bar{\delta}} = \bar{\delta}$ so that $\tilde{\bar{\delta}} = O(1)$. The leading order problem can then be solved to derive the mass conservation equation.

$$\frac{\partial \tilde{h}}{\partial \tilde{t}} + \frac{\partial}{\partial \tilde{x}}\left(\tilde{u}\tilde{h}\right) = 0. \tag{1.9}$$

In this case however, the problem for $\tilde{h}$ cannot be closed by consideration of the leading order balances alone. It is therefore necessary to use the Fredholm alternative [52] and continue to balance the system at $O(\epsilon^2)$. It may then be shown that

$$\tilde{h}\frac{\partial \tilde{h}}{\partial \tilde{x}} + \frac{1}{\tilde{\bar{\delta}}}\tilde{u} = 4\frac{\partial}{\partial \tilde{x}}\left(\tilde{h}\frac{\partial \tilde{u}}{\partial \tilde{x}}\right). \tag{1.10}$$

Equation (1.10) can be interpreted as a force balance between the effects of gravity (represented by the first term on the left-hand side), the shear stress induced by the plate (represented by the second term on the left-hand side) and the resistance due to extensional forces (represented by the term on the right-hand side). The factor of 4 on the RHS of (1.10) arises as a Trouton viscosity [33].

1.2.3 Intermediate $\bar{\delta}$

Having analysed the flow in the two distinguished limits ($\bar{\delta} = O(1)$ and $\bar{\delta} = O(\epsilon^{-2})$), there is also a further type of solution in the intermediate region between these where $1 \ll \bar{\delta} \ll \epsilon^{-2}$, for example $\bar{\delta} = O(\epsilon^{-1})$. This problem is studied by putting $\epsilon^{-1}\check{\delta} = \bar{\delta}$ so that $\check{\delta} = O(1)$ and the variables are scaled with $\beta = -1$ (this scaling is represented with checked variables). It may then be shown that

$$\frac{\partial \check{h}}{\partial \check{t}} + \frac{\partial}{\partial \check{x}} \left(\check{u}\check{h} \right) = 0, \tag{1.11}$$

and

$$0 = \check{h}\frac{\partial \check{h}}{\partial \check{x}} + \frac{1}{\check{\delta}}\check{u}. \tag{1.12}$$

Again, these equations may be interpreted as a mass conservation law and a force balance. The latter (1.12) can be seen to be a balance between the effects of gravity (represented by the first term) and the shear stress induced by the plate (represented by the second term). This is the same balance of forces that was shown to govern the spreading in sections 2.3.2 and 4.1.

1.2.4 Summary of Spreading over a Flat Surface

From the force balance equations in each regime (1.8), (1.10) and (1.12) the physical mechanisms that are dominant in controlling the spreading may be interpreted. When the shear length $\bar{\delta}$ in (1.6) is $O(1)$ the dominant effects are gravity, the shear stress induced by the plate and the internal shear stress within the film. As $\bar{\delta}$ increases to $O(\epsilon^{-1})$ (corresponding to a value of $\delta = O(L)$) the internal stress within the film is no longer part of the dominant force balance. Instead, gravity and the shear stress induced by the plate become the two dominating effects. Then as $\bar{\delta}$ increases further to $O(\epsilon^{-2})$, the resistance due to extensional flow becomes part of the dominant force balance, which is then between gravity, the shear induced by the plate and resistance due to extensional flow.

In the subsequent chapters 2 and 4 the dominant forces controlling the spreading of viscous films on the surface of a deep viscous pool will be shown to be the effects of gravity and the shear stress induced in the films by the underlying pool. This result may be anticipated if one considers that the shear length associated with the deep viscous pool in the later chapters is $O(L)$. Hence there is analogy with the results for the models in chapters 2 and 4 and the model considered in section 1.2.3.

Chapter 2

The spreading of viscous films on a deep viscous pool

In this chapter, a model for the slow spreading of viscous films on the surface of a quiescent deep viscous pool is considered. It is assumed that the densities and viscosities of the fluids in the films and pool are comparable, but may be different. It is also assumed that surface tension effects are negligible. The fluid in the films and in the pool are both modelled using the Stokes flow equations. By exploiting the slender geometry of the spreading films, asymptotic techniques are used to analyse the flow. It is shown that the two dominant forces controlling the spreading are gravity and the tangential stress induced in the films by the pool. As a consequence, the rate of spreading of the films is independent of their viscosity. For the special case of a symmetric configuration of films on the surface of the pool, the flow is studied by assuming the solution becomes self-similar and hence the problem is recast in a self-similar co-ordinate system. Stokeslet analysis is used to derive a singular integral equation for the stresses on the interfaces between the films and the pool. The form of this integral equation depends on the configuration of spreading films that are being considered. A number of different cases are then studied, namely; a single film, two separate films and an infinite periodic array of separate films. Lastly, some results are derived that apply to a general symmetric configuration of films. It is shown that the profile of a film close to its front is proportional to $x^{1/4}$. It is also shown that fronts move, and hence, the distance between adjacent fronts increase proportional to $t^{1/3}$.

2.1 Introduction

The spreading of fluid films over fluid pools is an example of a problem in the field of gravity currents. Such flows are driven by differences in density and arise in many natural and industrial situations. Gravity currents have been thoroughly studied in fluid mechanics since the 1940's. A review of the progress that has been made is given in Huppert [36], which describes not only theoretical results but also natural and industrial applications of such flows. Examples of gravity currents that occur in nature include the propagation of air currents, the spreading of oil slicks, saline currents in the ocean, intrusion of clouds in the atmosphere, the spreading of lava, and the evolution of snow avalanches [9], [10], [32], [59]. Some industrial examples include accidents in which dense gases are released, the flows in glass furnaces and other areas of glass manufacture including optical fibres [20], [34].

The spreading of viscous fluids under gravity has been considered by many authors. In most analyses the slenderness of the spreading current has been exploited to make the lubrication theory simplification to the governing flow equations. A compelling explanation of this is given in [2]. In the classic paper [35] (and its accompanying paper [16]) the lubrication theory simplification is used to study the spreading of a viscous gravity current along a rigid horizontal plate, below a fluid of lesser density. It is shown, in this case, that the stress condition due to the presence of the ambient fluid can be approximated as a condition of zero shear on the top surface of the gravity current. An analytic description of the shape and the speed of the propagating current is found by means of a self-similar solution by assuming that the total volume of the fluid in the current increases proportional to t^{α}. Other studies have considered similar problems in which a gravity current is allowed to intrude into a linearly stratified fluid [46]. Further authors have also examined the effects on a current intruding into a two-layer fluid [31], and many studies have considered the problem of oil spreading over the sea [9] [32]. A good example of this type of flow is found in [21] which studies the spreading of thin liquid films on an air-water interface. Another relevant study, [48], considers the dynamics of an incompressible fluid film spreading over solid substrates. Using asymptotic analysis, the differences in behaviour are studied as the slip condition between the substrate and the fluid is changed. All of this previous work is predicated upon a viscous fluid spreading over an inviscid pool. As far as the author is aware, much less work has investigated how viscous films spreads over a viscous pool. Therefore, the remainder of this chapter considers a model for the slow spreading of a film of incompressible viscous fluid over a slowly flowing deep incompressible

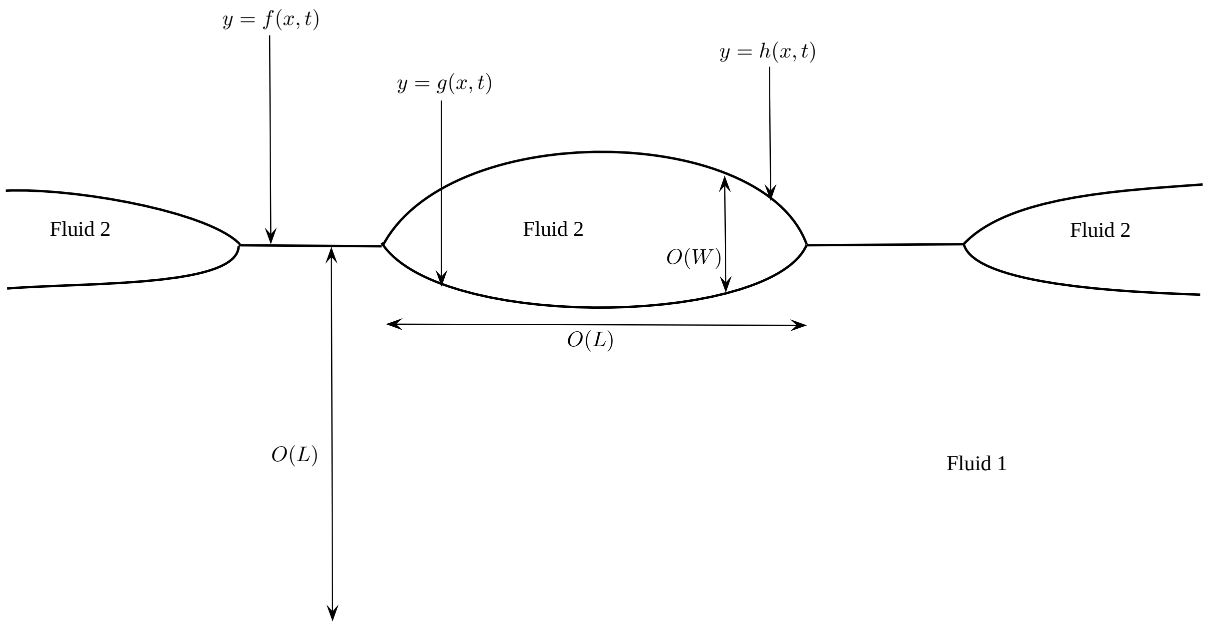

Figure 2.1: A schematic diagram of the flow showing the characteristic length scales.

viscous pool.

2.2 Problem formulation

Consider the slow spreading of a film of incompressible viscous fluid over a slowly flowing deep incompressible viscous pool. The deep pool has a stress free top surface (denoted by $y = f(x,t)$) and is perturbed only in the region covered by the spreading films. The flow is driven by the spreading of the non-flat top films under the action of gravity. The fluid in the deep pool is referred to as fluid 1, and the fluid in the films as fluid 2. The density and viscosity of fluids 1 and 2 are defined to be ρ_1, μ_1, ρ_2 and μ_2 respectively, with $\rho_1 > \rho_2$ so that the spreading films float. Here the regime in which both phases are well represented by slow-viscous flows is considered, and so the Stokes flow equations are used to govern the flow in each phase. Across the interface between fluids 1 and 2 (denoted by $y = g(x,t)$), both continuity of stresses and velocity, and a kinematic condition are required. The free surface at the top of fluid 2 (denoted by $y = h(x,t)$) is stress free and also satisfies a kinematic condition. A schematic diagram of this problem with its characteristic length scales is shown in figure 2.1.

Using dimensional variables the problem is modelled in the following way. On $y = h(x,t)$ it is imposed that

$$\mathbf{t_h'}\mathbf{T}\mathbf{n_h} = \mathbf{n_h'}\mathbf{T}\mathbf{n_h} = 0 \quad \text{and} \quad \frac{D}{Dt}(y - h) = 0, \tag{2.1}$$

whilst

$$\nabla p = \mu_2 \nabla^2 \mathbf{u} - \rho_2 \mathbf{g_r} \quad \text{and} \quad \nabla \cdot \mathbf{u} = 0, \tag{2.2}$$

hold in fluid phase 2. The jump conditions on the interface between the two fluids ($y = g(x, t)$) are written as

$$[\mathbf{t_g'}\mathbf{T}\mathbf{n_g}] = [\mathbf{n_g'}\mathbf{T}\mathbf{n_g}] = [u] = [v] = 0 \quad \text{and} \quad \frac{D}{Dt}(y - g) = 0 \tag{2.3}$$

whilst

$$\nabla p = \mu_2 \nabla^2 \mathbf{u} - \rho_1 \mathbf{g_r} \quad \text{and} \quad \nabla \cdot \mathbf{u} = 0, \tag{2.4}$$

hold in fluid phase 1. Here $\mathbf{T}$ is the stress tensor (defined in the usual way), a prime denotes the usual vector transpose operation, D/Dt is the material derivative with respect to the fluid velocity, $\mathbf{g_r} = (0, g_r)$ is the acceleration due to gravity, $\mathbf{n_h}$, $\mathbf{n_g}$, $\mathbf{t_h}$, $\mathbf{t_g}$ are the unit vectors normal and tangential to the surfaces $h(x, t)$ and $g(x, t)$ respectively, $\mathbf{u} = (u, v)$ is the vector of the fluid velocity, p is the pressure and square brackets denote the jump in the enclosed quantity across the interface $y = g(x, t)$. It shall also be imposed that the velocities in fluid 1 far from the surface or away from the spreading film should vanish. Problem closure is achieved by specification of the initial conditions.

The problem may now be non-dimensionalised by setting $x = L\bar{x}$, $y = W\bar{y}$, $g = W\bar{g}$, $h = W\bar{h}$, $u = u_0\bar{u}$, $v = \epsilon u_0\bar{v}$, $p = \rho_2 g_r W\bar{p}$ and $t = Lu_0^{-1}\bar{t}$ in fluid 2 and $x = L\hat{x}$, $y = L\hat{y}$, $f = L\hat{f}$, $g = L\hat{g}$, $u = u_0\hat{u}$, $v = u_0\hat{v}$ and $p = \rho_2 g_r L\hat{p}$ in fluid 1. Where $\epsilon = WL^{-1}$ and $u_0 = \rho_2 g_r W^2 \mu_2^{-1}$. By scaling in this manner three dimensionless parameters that characterise the flow have been introduced, $\epsilon = WL^{-1}$, is the inverse aspect ratio of the spreading film, whilst $\mu = \mu_1\mu_2^{-1}$ and $\rho = \rho_1\rho_2^{-1}$ are the ratios of the viscosities and densities of the two fluids. In the following analysis, the limit that ϵ tends to zero is taken while the parameters μ and ρ are both assumed to be $O(1)$. Hence, the results are relevant to flow in which both the viscosities and densities of the fluids in the films and pool are comparable. In the subsequent analysis the limit that ϵ tends to zero will be taken, hence, in the interests of brevity, terms that are sufficiently small that they do not enter the subsequent analysis will not be shown explicitly.

In fluid 1 the governing PDEs of the flow become

$$\frac{\partial \hat{p}}{\partial \hat{x}} = \epsilon^2 \mu \frac{\partial^2 \hat{u}}{\partial \hat{x}^2} + \epsilon^2 \mu \frac{\partial^2 \hat{u}}{\partial \hat{y}^2}, \quad \frac{\partial \hat{p}}{\partial \hat{y}} = \epsilon^2 \mu \frac{\partial^2 \hat{v}}{\partial \hat{x}^2} + \epsilon^2 \mu \frac{\partial^2 \hat{v}}{\partial \hat{y}^2} - \rho, \quad \frac{\partial \hat{u}}{\partial \hat{x}} + \frac{\partial \hat{v}}{\partial \hat{y}} = 0, \tag{2.5}$$

whilst in fluid 2

$$\epsilon \frac{\partial \bar{p}}{\partial \bar{x}} = \epsilon^2 \frac{\partial^2 \bar{u}}{\partial \bar{x}^2} + \frac{\partial^2 \bar{u}}{\partial \bar{y}^2}, \quad \frac{\partial \bar{p}}{\partial \bar{y}} = \epsilon \frac{\partial^2 \bar{v}}{\partial \bar{y}^2} - 1 + O(\epsilon^2), \quad \frac{\partial \bar{u}}{\partial \bar{x}} + \frac{\partial \bar{v}}{\partial \bar{y}} = 0 \tag{2.6}$$

govern the flow. In non-dimensional form the conditions on the interface $y = g(x,t)$ between the two fluids are

$$\bar{u} = \hat{u}, \tag{2.7}$$

$$\epsilon \bar{v} = \hat{v}, \tag{2.8}$$

$$\epsilon \bar{p} = \left(1 + \left(\frac{\partial \hat{g}}{\partial \hat{x}}\right)^2\right) \hat{p} + O(\epsilon^2) \tag{2.9}$$

$$\frac{\partial \bar{u}}{\partial \bar{y}} = \epsilon \mu \left(\frac{\partial \hat{u}}{\partial \hat{y}} + \frac{\partial \hat{v}}{\partial \hat{x}}\right) + O(\epsilon^2), \tag{2.10}$$

$$\bar{v} = \bar{u} \frac{\partial \bar{g}}{\partial \bar{x}} + \frac{\partial \bar{g}}{\partial \bar{t}}. \tag{2.11}$$

On the free surface $y = h(x,t)$

$$\frac{\partial \bar{u}}{\partial \bar{y}} = O(\epsilon^2), \tag{2.12}$$

$$\bar{p} = 2\epsilon \left(\frac{\partial \bar{v}}{\partial \bar{y}} - \frac{\partial \bar{h}}{\partial \bar{x}} \frac{\partial \bar{u}}{\partial \bar{y}}\right) + O(\epsilon^2), \tag{2.13}$$

$$\bar{v} = \bar{u} \frac{\partial \bar{h}}{\partial \bar{x}} + \frac{\partial \bar{h}}{\partial \bar{t}}, \tag{2.14}$$

and on the free surface $y = f(x,t)$

$$\frac{\partial \hat{u}}{\partial \hat{y}} = O(\epsilon^2) \tag{2.15}$$

$$\hat{p} = O(\epsilon). \tag{2.16}$$

Motivated by the presence of the small parameter ϵ, it is assumed that regular asymptotic expansions can be made for the dependent variables in the problem. These are presented in detail as the scalings used are different in the two regions. In the two regions these are

Region 1:	Region 2:
$\hat{u} \sim \hat{u}_0 + \epsilon \hat{u}_1 + \cdots$	$\bar{u} \sim \bar{u}_0 + \epsilon \bar{u}_1 + \cdots$
$\hat{v} \sim \hat{v}_0 + \epsilon \hat{v}_1 + \cdots$	$\bar{v} \sim \bar{v}_0 + \epsilon \bar{v}_1 + \cdots$
$\hat{p} \sim \hat{p}_0 + \epsilon \hat{p}_1 + \cdots$	$\bar{p} \sim \bar{p}_0 + \epsilon \bar{p}_1 + \cdots$
$\hat{g} \sim -\epsilon g_0 - \epsilon^2 g_1 + \cdots$	$\bar{g} \sim -g_0 - \epsilon g_1 + \cdots$
$\hat{f} \sim \epsilon f_0 + \epsilon^2 f_1 + \cdots$	$\bar{h} \sim h_0 + \epsilon h_1 + \cdots$

The flows in the two different regions are now analysed in turn.

2.3 Fluid 2: The spreading films

First the behaviour of the spreading films is analysed. On substitution of the assumed asymptotic forms the system can be balanced at increasing orders of ϵ.

2.3.1 Fluid 2: $O(1)$ Problem

The system of PDEs and boundary conditions derived from equating terms of $O(1)$ in equations (2.6) - (2.14) may be solved to give the mass conservation equation.

$$\frac{\partial}{\partial \bar{t}} (h_0 + g_0) + \frac{\partial}{\partial \bar{x}} \left((h_0 + g_0) \, \hat{u}_0(\hat{x}, 0, \hat{t}) \right) = 0. \tag{2.17}$$

At this stage it is important to note that at $O(1)$, despite making use of all the relevant boundary conditions, it is not possible to close the problem for finding the evolution of the two free surfaces. This is due to the degenerate nature of the tangential stress conditions on the two surfaces (at $O(1)$). A solvability condition using the Fredholm alternative [52] is therefore sought at higher order.

2.3.2 Fluid 2: $O(\epsilon)$ Problem

Proceeding to equate terms of $O(\epsilon)$ in equations (2.6) - (2.14) allows the solvability condition

$$(g_0 + h_0) \frac{\partial h_0}{\partial \bar{x}} + \mu \frac{\partial \hat{u}_0}{\partial \hat{y}} (\hat{x}, 0, \hat{t}) = 0 \tag{2.18}$$

to be derived. This condition may be interpreted as a simplified (leading order in ϵ) balance of horizontal forces in the spreading films. The first term in (2.18) represents the horizontal force due to the hydrostatic pressure in the film. The second term in (2.18) represents the horizontal shear stress induced on the film due to the underlying pool. It is at this stage that an analogy may be drawn between the dynamics observed in this model, and those observed in section 1.2.4. It has been shown that the same force balance between gravity and externally induced stress occurred for the spreading of a fluid film over a flat surface in the case that the shear length was $O(L)$. The analogous mass conservation (2.17) and force balance (2.18) equations have now been shown to hold for the problem of a fluid film spreading over a deep pool. This may not come as a surprise when considering the form of the boundary conditions for the shear stress on the lower boundary of the films ((2.10) and (1.6)). In each case the shear stress exerted on the lower boundary of the spreading film is a quantity proportional to $1/L$, the inverse horizontal length scale of the film.

This analysis at $O(\epsilon)$ has given sufficient information to derive two PDEs for g_0 and h_0 (the free surfaces), $\hat{u}_0(\hat{x}, 0, \hat{t})$ (the interfacial velocity) and $\partial\hat{u}_0/\partial\hat{y}\,(\hat{x}, 0, \hat{t})$ (the interfacial stress). Analysing the flow in fluid phase 2 at higher order does not aid in closing the system for the aforementioned leading order variables. Hence, the flow in fluid phase 1 is now analysed in an effort to derive two further relationships between g_0, h_0, $\hat{u}_0(\hat{x}, 0, \hat{t})$ and $\partial\hat{u}_0/\partial\hat{y}\,(\hat{x}, 0, \hat{t})$.

2.4 Fluid 1: The underlying pool

In a similar manner to section 2.3 equations (2.5) and (2.7) - (2.16) are balanced at increasing orders of ϵ.

2.4.1 Fluid 1: $O(1)$ Problem

Equating terms of $O(1)$ in equations (2.5) and (2.7) - (2.16) a system is derived that has solution

$$\hat{p_0} = -\rho\hat{y}. \tag{2.19}$$

This analysis shows that, to leading order, the pressure in the pool is hydrostatic. From this balance, no information is obtained about g_0, h_0, $\hat{u}_0(\hat{x}, 0, \hat{t})$ or $\partial\hat{u}_0/\partial\hat{y}\,(\hat{x}, 0, \hat{t})$. Hence, in an effort to close the system of equations, the problem for the flow in the pool is balanced at $O(\epsilon)$.

2.4.2 Fluid 1: $O(\epsilon)$ Problem

Equating terms of $O(\epsilon)$ in equations (2.5) and (2.7) - (2.16) yields a system of equations that has a solution provided

$$h_0 = (\rho - 1)g_0. \tag{2.20}$$

This may be rewritten as

$$\rho_2\left(h_0 + g_0\right) = \rho_1 g_0, \tag{2.21}$$

which may then be seen to be consistent with Archimedes' principle, determining the level at which the foam floats over the pool. Equation (2.20) provides one of the additional relationships between g_0, h_0, $\hat{u}_0(\hat{x}, 0, \hat{t})$ and $\partial\hat{u}_0/\partial\hat{y}\,(\hat{x}, 0, \hat{t})$. However, one further condition is still required. To this end, the system is analysed at $O(\epsilon^2)$.

2.4.3 Fluid 1: $O(\epsilon^2)$ Problem

Equating $O(\epsilon^2)$ terms in (2.5) and (2.7) - (2.16) yields the equations

$$\frac{\partial\hat{p}_2}{\partial\hat{x}} = \mu\frac{\partial^2\hat{u}_0}{\partial\hat{x}^2} + \mu\frac{\partial^2\hat{u}_0}{\partial\hat{y}^2}, \quad \frac{\partial\hat{p}_2}{\partial\hat{y}} = \mu\frac{\partial^2\hat{v}_0}{\partial\hat{x}^2} + \mu\frac{\partial^2\hat{v}_0}{\partial\hat{y}^2}, \quad \frac{\partial\hat{u}_0}{\partial\hat{x}} + \frac{\partial^2\hat{v}_0}{\partial\hat{y}} = 0. \tag{2.22}$$

In order to write the boundary conditions in a convenient way, $s_n(\bar{t})$ and $s_{n+1/2}(\bar{t})$ are defined as the locations of the left and right fronts of the n^{th} film along $\hat{y} = 0$. The author also writes $\digamma = \cup_{n=0}^{n=N}(s_n(\bar{t}), s_{n+1/2}(\bar{t}))$ so that $\digamma$ is the union of intervals along the line $\hat{y} = 0$ for which g_0 and h_0 are non-zero. Since the surface of the pool away from the spreading films has been assumed stress free (2.22), must be solved subject to

$$\frac{\partial\hat{u}_0}{\partial\hat{y}} = 0, \tag{2.23}$$

$$\hat{p}_2 = 0 \quad \text{on} \quad \hat{y} = 0 \quad \text{for} \quad \hat{x} \notin \digamma, \tag{2.24}$$

$$\frac{\partial h_0}{\partial\hat{t}} + \frac{\partial}{\partial\hat{x}}\left(\hat{u}_0 h_0\right) = 0 \tag{2.25}$$

$$h_0\frac{\partial h_0}{\partial\hat{x}} = \frac{\mu(1-\rho)}{\rho}\frac{\partial\hat{u}_0}{\partial\hat{y}} \quad \text{on} \quad \hat{y} = 0 \quad \text{for} \quad \hat{x} \in \digamma \tag{2.26}$$

and

$$\hat{v}_0 = 0 \quad \text{on} \quad \hat{y} = 0 \quad \forall\hat{x}. \tag{2.27}$$

The boundary conditions in (2.25) and (2.26) are consequences of (2.17), (2.18) and (2.20). At this point it is also necessary to write equations to govern the motion of the points $s_n(\bar{t})$ and $s_{n+1/2}(\bar{t})$. As a consequence of the jump condition that conserves the horizontal component of velocity across the interface $y = g(x,t)$, and since the mass of the fluid must be conserved at any front, it can be written that

$$h_0 = 0 \quad \text{and} \quad \hat{u} = \frac{ds_n}{d\hat{t}} \quad \text{on} \quad \hat{y} = 0 \quad \text{at} \quad \hat{x} = s_n(\bar{t}). \tag{2.28}$$

In general (2.22), (2.23), (2.27) and (2.28) provide a fourth relationship between g_0, h_0, $\hat{u}_0(\hat{x},0,\bar{t})$ and $\partial\hat{u}_0/\partial\hat{y}\,(\hat{x},0,\bar{t})$. In this analysis, however, the three previous relationships ((2.17), (2.18) and (2.20)) have been used in order to write (2.25). By doing so, (2.22) - (2.28) close a system for the flow in fluid phase 1 and the two free surfaces (g_0 and h_0).

2.5 A symmetric configuration of films

In order to make further analytical progress with the problem, the special case when the configuration of spreading films have reflectional symmetry in the vertical axis is now considered. If the flow has this property then the equations may be reduced by seeking a reduction of the form

$$\begin{aligned} \hat{u} &= \hat{t}^{\alpha_1} U(\phi,\theta), \\ \hat{v} &= \hat{t}^{\alpha_1} V(\phi,\theta), \\ \hat{p} &= \hat{t}^{\alpha_2} P(\phi,\theta), \\ g_0 &= \hat{t}^{\alpha_3} G(\phi), \\ h_0 &= \hat{t}^{\alpha_3} H(\phi), \end{aligned} \tag{2.29}$$

with

$$\phi = \hat{x}\hat{t}^{\beta} \quad \text{and} \quad \theta = \hat{y}\hat{t}^{\beta}. \tag{2.30}$$

In the (ϕ,θ) coordinate system the equations are reduced to a steady problem by setting $\alpha_1 = -2/3$, $\alpha_2 = -1$, $\alpha_3 = -1/3$ and $\beta = -1/3$. Note that by using this reduction some information about the initial configuration of films is inherently imposed (i.e. $g_0(\hat{x},0) = h_0(\hat{x},0) = \delta(\hat{x})$ where $\delta(\hat{x})$ is the Dirac delta function). Note also that the author anticipates that self-similar

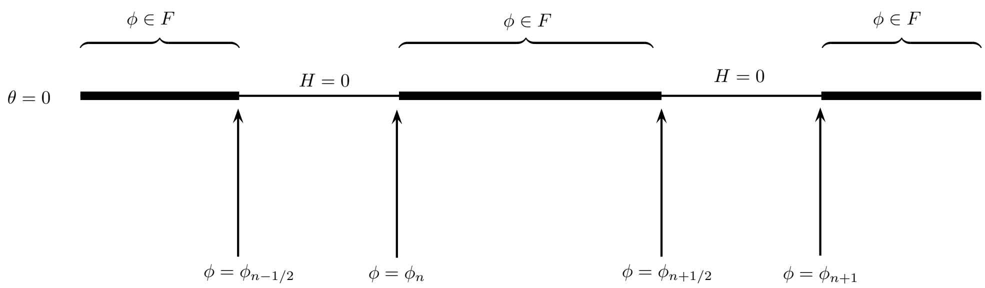

Figure 2.2: A schematic of the problem in the self-similar coordinate system.

solutions of the form (2.29) may be attractors (at large times) for solutions with more general initial conditions. This however is conjecture and a rigorous proof of this result is not given here. In order to close the reduced problem, it is sufficient to specify the quantity of fluid in each film and one further condition on the location of one of the fronts of each of the films at some reference time (or equivalently the distance between adjacent films at some reference time). Therefore, it is useful to introduce the notation shown in figure 2.2 that $\phi = \phi_n$ and $\phi = \phi_{n+1/2}$ are the locations of the left and right fronts of the n^{th} film along the line $\theta = 0$. Hence $H(\phi_n) = H(\phi_{n+1/2}) = 0$. The author also writes $F = \cup_{n=-N}^{n=N}(\phi_n, \phi_{n+1/2})$ so that F is the union of intervals along the line $\theta = 0$ for which G and H are non-zero. Due to the form of (2.29), the position of the fronts of the n^{th} film are $\phi_n = x_n t^{-1/3}$. Hence, the front's positions move proportional to $t^{1/3}$, and, adjacent fronts separate proportional to $t^{1/3}$.

Using the reduction (2.29) the conditions (2.25) may be written as

$$\frac{d}{d\phi}\left(H\left(U - \frac{1}{3}\phi\right)\right) = 0 \tag{2.31}$$

and

$$\frac{d}{d\phi}\left(\frac{H^2}{2}\right) = \frac{\mu(1-\rho)}{\rho}\frac{\partial U}{\partial \theta} \tag{2.32}$$

$$\text{on} \quad \theta = 0 \quad \text{for} \quad \phi \in F.$$

Since equation (2.31) holds along the line $\theta = 0$ this may be integrated with respect to ϕ. Owing to the symmetric nature of the flow $U(0,0) = 0$, hence, equation (2.31) may be written as

$$U = \frac{1}{3}\phi \quad \text{on} \quad \theta = 0 \quad \text{for} \quad \phi \in F. \tag{2.33}$$

A stream function, $\psi(\phi, \theta)$, defined by

$$\frac{\partial \psi}{\partial \theta} = U, \quad -\frac{\partial \psi}{\partial \phi} = V, \tag{2.34}$$

is introduced so that the problem for the flow in the pool under a general symmetric configuration of spreading films may be written as

$$\nabla^4 \psi = 0 \tag{2.35}$$

subject to

$$\frac{\partial^2 \psi}{\partial \theta^2} = 0 \quad \text{and} \quad \psi = 0 \quad \text{on} \quad \theta = 0 \quad \text{for} \quad \phi \notin F, \tag{2.36}$$

$$\frac{\partial \psi}{\partial \theta} = \frac{1}{3}\phi \quad \text{and} \quad \psi = 0 \quad \text{on} \quad \theta = 0 \quad \text{for} \quad \phi \in F, \tag{2.37}$$

$$\frac{\partial \psi}{\partial \theta} \to 0\,, \; \frac{\partial \psi}{\partial \phi} \to 0 \quad \text{as} \quad \phi \to \pm\infty \quad \text{and} \tag{2.38}$$

$$\frac{\partial \psi}{\partial \theta} \to 0\,, \; \frac{\partial \psi}{\partial \phi} \to 0 \quad \text{as} \quad \theta \to -\infty. \tag{2.39}$$

Note that the first condition in (2.37) is (2.33) written in terms of the stream function ψ. To solve the problem posed by (2.35) - (2.39), Stokeslet analysis is used. Consider the stream function of a Stokeslet oriented in the direction of positive ϕ on the line $\theta = 0$ positioned at the point $\phi = \Phi$,

$$\psi_s(\phi, \theta, \Phi) = -\frac{\theta}{2} \ln\left((\phi - \Phi)^2 + \theta^2\right). \tag{2.40}$$

Provided $\Phi \in F$, ψ_s satisfies equations (2.35), (2.36), (2.38) and (2.39). Hence, to solve the problem posed by (2.35) - (2.39), a superposition of Stokeslets must be chosen such that (2.37) is satisfied. Using equation (2.37), this requirement may be written as

$$\lim_{\theta \to 0^-} \fint_F s(\Phi) \frac{\partial \psi_s}{\partial \theta}(\phi, \theta, \Phi)\, d\Phi = \frac{1}{3}\phi \quad \text{for} \quad \phi \in F, \tag{2.41}$$

where s is a function that describes the Stokeslet concentration in F. Note that this equation cannot simply be evaluated on $\theta = 0$ due to the singular nature of (2.40), and instead the limit that $\theta \to 0^-$ must be taken. Note also that the *dashed* integral sign indicates that the integral is to be understood in the Cauchy Principal value sense. Taking the derivative of (2.41) with respect to ϕ and taking the limit that $\theta \to 0^-$, equation (2.41) may be written as

$$\fint_F \frac{s(\Phi)}{\Phi - \phi} d\Phi = \frac{1}{3} \quad \text{for} \quad \phi \in F. \tag{2.42}$$

The solution to equation (2.42) depends on the form of the domain of integration F. In sections 2.6, 2.7, 2.8 and 2.9 the function s will be computed for a number of different examples. In the interests of brevity and clarity of the problem structure the author continues to solve the problem assuming that s may be determined from equation (2.42).

The tangential stress on the fluid-fluid surface can be found by noting that the Stokeslet solution, ψ_s, is the flow generated by a stress singularity of strength 2π. Hence

$$\left.\frac{\partial U}{\partial \theta}\right|_{\theta=0} = 2\pi s(\phi) \quad \text{for} \quad \phi \in F. \tag{2.43}$$

Substitution of equation (2.43) into (2.32) and integrating with respect to ϕ gives

$$H^2 = 4\pi \frac{\mu(1-\rho)}{\rho} \int_F s(\phi) d\phi \quad \text{for} \quad \phi \in F \tag{2.44}$$

as an expression for H^2. A number of examples of different configurations are studied in the following sections.

2.6 A single spreading film

In the case of a single spreading film, F takes a particularly simple form, a single section of the line $\theta = 0$. Due to the assumed symmetric nature of the problem, $\phi_1 = -\phi_{3/2}$. Hence, equation (2.42) takes the form

$$\frac{1}{3} = \fint_{-\phi_1}^{+\phi_1} \frac{s(\Phi)}{\Phi - \phi} d\Phi \quad \text{for} \quad -\phi_1 < \phi < +\phi_1. \tag{2.45}$$

Equation (2.45) may be solved using standard results, see [49], to give

$$s(\phi) = \frac{1}{3\pi} \frac{\phi}{\sqrt{\phi_1^2 - \phi^2}} \quad \text{for} \quad -\phi_1 < \phi < +\phi_1. \tag{2.46}$$

Following the steps outlined between equations (2.42) and (2.44), and imposing the conditions $H(-\phi_1) = H(+\phi_1) = 0$, the profile of the film can be shown to take the form

$$H^2 = \frac{4}{3}\frac{\mu(\rho-1)}{\rho}\sqrt{\phi_1^2 - \phi^2} \quad \text{for} \quad -\phi_1 < \phi < +\phi_1. \tag{2.47}$$

Closure of the problem (finding ϕ_1) is completed by specifying the total amount of fluid in the film. This is imposed by consideration of the equation

$$\int_{-\phi_1}^{+\phi_1} H d\phi = M_1, \tag{2.48}$$

where M_1 is the quantity of fluid in the film.

For the purposes of demonstration the example of $M_1 = 1$ and $2\frac{\mu}{3}\frac{\rho-1}{\rho} = 1$ is used. In this case it can be shown numerically that $\phi_1 \approx 0.5481$. The predicted profile for H and streamlines of the flow generated in the pool are shown in figures 2.3 and 2.4.

2.7 A finite number of symmetric films

In this section the problem for a finite number of symmetrically arranged films is studied. In this case equation (2.42) may be written as

$$\frac{1}{3} = \fint_{F^-} \frac{s(\Phi)}{\Phi - \phi} d\Phi + \fint_{F^+} \frac{s(\Phi)}{\Phi - \phi} d\Phi \quad \text{for} \quad \phi \in F. \tag{2.49}$$

Here $F^+ = \{\phi \in F | \phi \geq 0\}$ and $F^- = \{\phi \in F | \phi < 0\}$. The symmetry of the problem may then be exploited by substituting $z = -z$ in the first term on the RHS of (2.49). Hence

$$\frac{1}{3} = \fint_{F^+} s(\Phi) \frac{2\Phi}{\Phi^2 - \phi^2} d\Phi \quad \text{for} \quad \phi \in F^+. \tag{2.50}$$

To make further analytical progress the author puts $\Phi^2 = q$ and $\phi^2 = p$, and also defines $\phi_n^2 = p_n$, $s_1(q) = s(\Phi)$ and $\bar{F} = \cup_{n=1}^{n=N}(p_n, p_{n+1/2})$. Equation (2.50) may then be written as

$$\frac{1}{3} = \fint_{\bar{F}} \frac{s_1(q)}{q - p} dq \quad \text{for} \quad p \in \bar{F}. \tag{2.51}$$

Equation (2.51) takes the form of a Fredholm singular integral equation of the first kind, where the domain of integration, $\bar{F}$, is a union of disjoint sections of the real line. Equation (2.51)

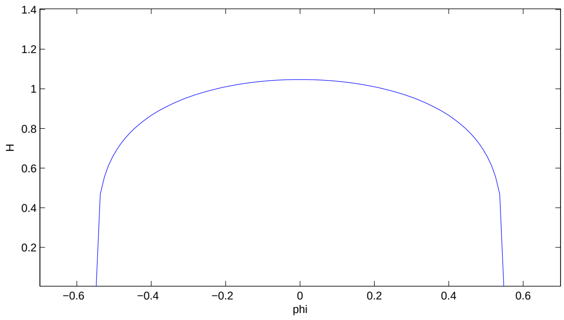

Figure 2.3: $H(\phi)$ for $M_1 = 1$ and $2\frac{\mu}{3}\frac{\rho-1}{\rho} = 1$.

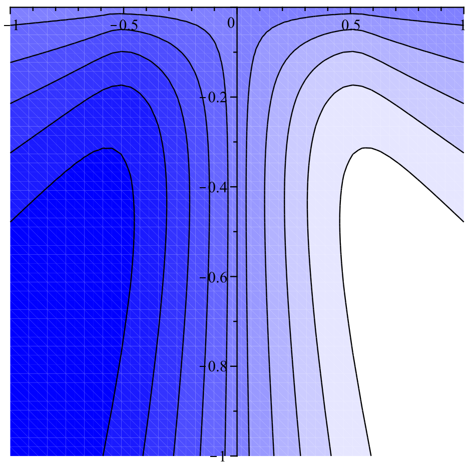

Figure 2.4: The streamlines of the flow in the pool in the (ϕ, θ) plane for $M_1 = 1$ and $2\frac{\mu}{3}\frac{\rho-1}{\rho} = 1$. These streamlines have been computed by numerically integrating the product of s and ψ_s on the domain F and plotting the contours of the resulting function.

can be inverted for s_1 using results in [49] to give

$$s_1(p) = -\frac{1}{3\pi^2}\prod_{n=1}^{n=N}\frac{1}{\sqrt{-(p_n - p)(p_{n+1/2} - p)}}\left(\fint_{\bar{F}}\frac{1}{q-p}\prod_{n=1}^{n=N}\sqrt{-(p_n - q)(p_{n+1/2} - q)}dq + c\right) \tag{2.52}$$

$$\text{for} \quad p \in \bar{F}.$$

Here c is a constant to be determined by insisting that the film thickness is zero at all points p_n and $p_{n+1/2}$. Calculating the integral in equation (2.53) is, in general, a problem that must be treated numerically. However, some analytical progress can be made by simplifying to some special cases. Note that aside from the example studied in section 2.8, some analytical progress can also be made with the cases of three and four spreading films. However these problems involve elliptic functions that must be computed numerically and they are not studied here.

2.8 Two symmetric films

For the case of two films, the integral in equation (2.53) can be calculated analytically by standard methods, see [1]. In terms of the ϕ coordinate system it may be written that

$$s(\phi) = \frac{1}{3\pi}\frac{\phi^2 + c_1}{\sqrt{(\phi^2 - \phi_1^2)(\phi_{3/2}^2 - \phi^2)}} \quad \text{for} \quad \phi \in (-\phi_{3/2}, -\phi_1) \cup (\phi_1, \phi_{3/2}). \tag{2.53}$$

Here c_1 is a constant that may be determined by requiring that $H(\pm\phi_1) = H(\pm\phi_{3/2}) = 0$. Hence, $c_1 = -((\phi_{3/2} - \phi_1)/2)^2$. Equation (2.44) becomes

$$H^2 = \frac{4}{3}\frac{\mu(1-\rho)}{\rho}\int \frac{\phi^2 - ((\phi_1 + \phi_{3/2})/2)^2}{\sqrt{(\phi^2 - \phi_1^2)(\phi_{3/2}^2 - \phi^2)}}d\phi \quad \text{for} \quad \phi \in (-\phi_{3/2}, -\phi_1) \cup (\phi_1, \phi_{3/2}). \tag{2.54}$$

The integral in equation (2.54) must be computed numerically. However, some manipulations can be made to minimise the amount of computation. Since the film thickness is zero at the points $\phi = \pm\phi_1$ and $\phi = \pm\phi_{3/2}$ equation (2.54) may be be written as

$$H^2 = \frac{4}{3}\frac{\mu(\rho-1)}{\rho}\int_{\phi}^{\phi_{3/2}} \frac{\phi^2 - ((\phi_1 + \phi_{3/2})/2)^2}{\sqrt{(\phi^2 - \phi_1)(\phi_{3/2}^2 - \phi^2)}}d\phi \quad \text{for} \quad \phi \in (-\phi_{3/2}, -\phi_1) \cup (\phi_1, \phi_{3/2}). \tag{2.55}$$

The problem is then reduced to finding ϕ_1 and $\phi_{3/2}$. One condition on one of the fronts of each of the films must be given. In this example the author chooses to specify the value of ϕ_1, since this is the shortest distance between films at $\hat{t} = 1$. A second condition, sufficient to find $\phi_{3/2}$, is to specify the total amount of fluid in each film. In the same way as section 2.6 the equation

$$\int_{\phi_1}^{\phi_{3/2}} H d\phi = M_2 \tag{2.56}$$

is used. To determine $\phi_{3/2}$ from equations (2.55) and (2.56) a shooting method is employed using the following steps.

- A guess for $\phi_{3/2}$ is made.
- The RHS of (2.55) is then computed numerically using an adaptive Gauss-Kronrod quadrature [57] at a number of equally spaced values of ϕ on the interval $(\phi_1, \phi_{3/2})$.
- From this numerical approximation to H a value for the LHS of (2.56) is computed using a composite Simpson's rule. If the LHS of (2.56) is less than M_2 the guess for $\phi_{3/2}$ is

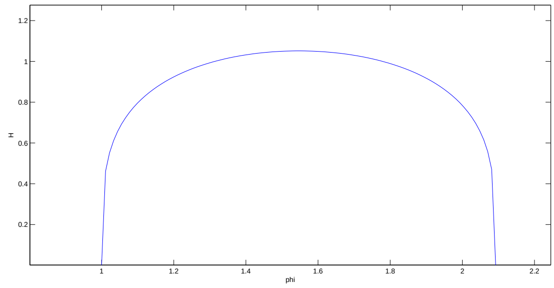

Figure 2.5: $H(\phi)$ for for $M_2 = 1$ and $2\frac{\mu}{3}\frac{\rho-1}{\rho} = 1$.

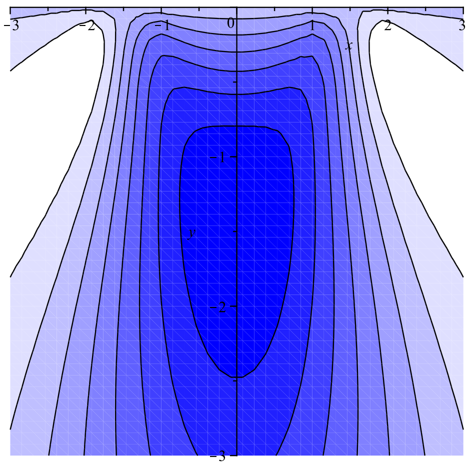

Figure 2.6: The streamlines of the flow in the pool in the (ϕ, θ) plane for $M_2 = 1$ and $2\frac{\mu}{3}\frac{\rho-1}{\rho} = 1$. These streamlines have been computed numerically integrating the product of s and ψ_s on the domain F and plotting the contours of the resulting function.

increased. However if the LHS of (2.56) is greater than M_2 the guess for $\phi_{3/2}$ is decreased (since the LHS of (2.56) is a monotonic increasing function of $\phi_{3/2}$).

- This process is repeated until the LHS of (2.56) is equal to $M_2 \pm E$, where E is some error tolerance.

For the purposes of demonstration, the example of $\phi_1 = 1$, $M_2 = 1$ and $2\frac{\mu}{3}\frac{\rho-1}{\rho} = 1$ is chosen. Using 100 equally spaced values of ϕ on the interval $(\phi_1, \phi_{3/2})$ and a value of $E = \pm 10^{-3}$ it is found that $\phi_{3/2} \approx 2.0924$, the predicted profile for H and streamlines of the flow generated in the pool are shown in figures 2.5 and 2.6.

2.9 An infinite periodic array of films

In this section a problem is considered for an infinite periodic array of spreading films. The distance between the centre of adjacent films at time $\hat{t} = 1$ is denoted by D and the length of each film at time $\hat{t} = 1$ is denoted by $2a$. In the interests of algebraic clarity the horizontal co-ordinate is scaled with D by putting $\phi = D\bar{\phi}$. This means that the distance between the centre of adjacent films in the $\bar{\phi}$ coordinate system is one, and the extent of each film is $2a/D = 2\bar{a}$. Without loss of generality, the position the centres of the films are chosen to be $\bar{\phi} = n + 1/2$ along the line $\theta = 0$, where $n \in \mathbb{Z}$. Equation (2.42) may be written as

$$\frac{1}{3} = \sum_{n=-\infty}^{n=+\infty} \fint_{(n+1/2)-\bar{a}}^{(n+1/2)+\bar{a}} \frac{s(\Phi)}{\Phi - \bar{\phi}} d\Phi \quad \text{for} \quad \bar{\phi} \in (n + 1/2 - \bar{a}, n + 1/2 + \bar{a}). \tag{2.57}$$

The author now puts $\Phi = n + 1/2 + q$ and $\bar{\phi} = m + 1/2 + p$ with $p, q \in (-\bar{a}, +\bar{a})$ and $m \in \mathbb{Z}$. Owing to the periodicity of the problem the function s has the property that $s(z) = s(z + k)$ for any $k \in \mathbb{Z}$. Therefore, the problem may be reduced to considering a single period of the function s by writing equation (2.57) as

$$\frac{1}{3} = \fint_{-\bar{a}}^{+\bar{a}} s(q) \sum_{n=-\infty}^{n=+\infty} \frac{1}{(n+q) - (m+p)} dq \quad \text{for} \quad p \in (-\bar{a}, +\bar{a}). \tag{2.58}$$

This is a singular Fredholm integral equation of the first kind for the function s. The form of the kernel in equation (2.58) may be manipulated into a simpler form by noting that the kernel is related to the Hurwitz-Zeta function [6]. The properties of this function have been considered previously, and it can be shown using standard techniques [37], [64] that

$$\sum_{n=-\infty}^{n=+\infty} \frac{1}{(n+q) - (m+p)} = \pi \cot \pi(q - p). \tag{2.59}$$

Hence equation (2.58) may be written as

$$\frac{1}{3} = \pi \fint_{-\bar{a}}^{+\bar{a}} s(q) \cot \pi(q - p) dq \quad \text{with} \quad p \in (-\bar{a}, +\bar{a}). \tag{2.60}$$

In order to progress with finding a solution to equation (2.60), the ideas in Muskhelishvili [49] are followed, and (2.60) is projected into the complex plane by making the substitutions $Q = \exp(2\pi i q)$, $P = \exp(2\pi i p)$, $S(Q) = s(q)$ and $\alpha_0 = \exp(2\pi i \bar{a})$. Then equation (2.60) may be written as

$$\frac{1}{3} = \fint_A \frac{S(Q)}{Q-P} dQ \quad \text{for} \quad P \in A. \tag{2.61}$$

Here, A is the part of the unit circle in the complex plane connecting α_0^* and α_0, where α_0^* is the complex conjugate of α_0. Equation (2.61) may be inverted using results in [18] to give

$$S(P) = \frac{1}{3\pi} \frac{P + c_2}{\sqrt{(P-\alpha_0)(\alpha_0^* - P)}} \quad \text{for} \quad P \in A, \tag{2.62}$$

where c_2 is an undetermined complex constant. So that the function s is real, and so that it is anti-symmetric on the domain $(-\bar{a}, +\bar{a})$, c_2 is set equal to minus one. This allows the function s to be written in terms of p as

$$s(p) = \frac{1}{3\pi} \frac{\sin(\pi p)}{\sqrt{\sin(\pi(a+p))\sin(\pi(\bar{a}-p))}}. \tag{2.63}$$

Using equations (2.44) and (2.63), and following the steps outlined in section 2.5 gives

$$H^2 = \frac{4}{3}\frac{\mu(1-\rho)}{\rho} \int_{-\bar{a}}^{+\bar{a}} \frac{\sin(\pi p)}{\sqrt{\sin(\pi(\bar{a}+p))\sin(\pi(\bar{a}-p))}} dp. \tag{2.64}$$

The integral in equation (2.64) may be calculated and imposing that $H(-p) = H(+p) = 0$ gives

$$H^2 = \frac{4}{3}\frac{\mu(\rho-1)}{\rho} \ln\left(\frac{\cos(\pi p) + \sqrt{\cos^2(\pi p) - \cos^2(\pi\bar{a})}}{\cos(\pi\bar{a})}\right). \tag{2.65}$$

In order to close the problem, a value for $\bar{a}$ must be found. Mimicking sections 2.6 and 2.8, the following condition on the total amount of fluid in each film is imposed

$$\int_{-\bar{a}}^{+\bar{a}} H dp = M_\infty. \tag{2.66}$$

For the purposes of demonstration the example of $M_\infty = 1$ and $2\frac{\mu}{3}\frac{\rho-1}{\rho} = 1$ is chosen. In this case it can be shown numerically that $\bar{a} \approx 0.3438$. The predicted profile for H is shown in figure 2.7.

Note that, by expanding equation (2.60) for small $\bar{a}$ (the limit that the films are well separated), it can be systematically shown that the problem studied in this section reduces to the problem for a single spreading film.

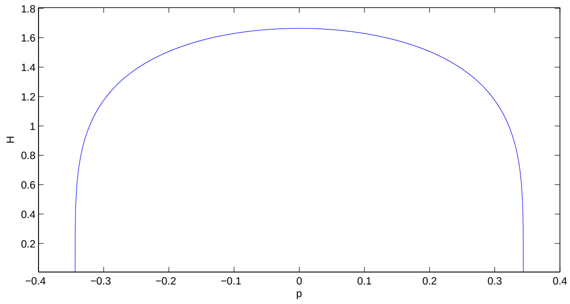

Figure 2.7: $H(p)$ for $M_\infty = 1$ and $2\frac{\mu}{3}\frac{\rho-1}{\rho} = 1$.

2.10 Behaviour at the front

In sections 2.6, 2.8 and 2.9, the problems of a single spreading film, two spreading films and an infinite periodic array of spreading films have been studied. Note that a challenge inherent in dealing with more general configurations of films comes when computing the more complex counterparts of the integrals derived from equations (2.42) and (2.44). Many of the integrands exhibit singular behaviour near the endpoints of the integral, and due to the absence of analytical solutions, the integrals may have to be computed numerically. It is therefore useful to understand the nature of these singularities analytically.

For the case of a single spreading film it is straightforward to determine these behaviours. Examination of equation (2.46) yields

$$s \sim K_0 \left(\phi_1 + \phi\right)^{-1/2} \quad \text{as} \quad \phi \to -\phi_1^+, \tag{2.67}$$

$$s \sim K_1 \left(\phi_1 - \phi\right)^{-1/2} \quad \text{as} \quad \phi \to +\phi_1^-. \tag{2.68}$$

Furthermore, direct inspection of equation (2.47) shows

$$H \sim K_2 \left(\phi_1 + \phi\right)^{1/4} \quad \text{as} \quad \phi \to -\phi_1^+, \tag{2.69}$$

$$H \sim K_3 \left(\phi_1 - \phi\right)^{1/4} \quad \text{as} \quad \phi \to +\phi_1^-. \tag{2.70}$$

Here K_i are constants (which, in this case, could be found from the exact solutions (2.46) and (2.47)). For the case of two spreading films equations (2.53) and (2.55) reveal that the asymptotic behaviours of both s and H also take the forms (2.67) - (2.70). This can also be shown to be true for an infinite periodic array of films by expanding trigonometric terms in equations (2.63) and (2.65).

In light of the fact that all the cases examined thus far appear to have a generic behaviour near the fronts of each film, one might anticipate that this is the case for any spreading film. In order to support this claim the author poses the following generalised problem.

Equation (2.42) is a relationship that has been derived by seeking a distribution of Stokeslets that will satisfy a given velocity condition along the fluid-fluid surface, see section 2.5. Thus far, in the current study, the velocity condition to be satisfied has been $U(\phi, 0) = \phi/3$ for $\phi \in F$. To answer the aforementioned question the author introduces a general, but well behaved function $U_G(\phi)$ (with the property that $U_G(0) = 0$) and assumes that the velocity condition to be satisfied is $U(\phi, 0) = U_G(\phi)$ for $\phi \in F$. A film that has a front at $\phi = \phi_G$ and lies in $\phi > \phi_G$ is also introduced. Following the working in section 2.5 and carrying out an analysis local to $\phi = \phi_G$ an equation that takes the form

$$\frac{dU_G}{d\phi} = \fint_{\phi_G}^{\infty} \frac{s(\Phi)}{\Phi - \phi} d\Phi \quad \text{with} \quad \phi \in (\phi_G, +\infty) \tag{2.71}$$

is derived. In order to understand the behaviour of the film near its front the behaviour of s as $\phi \to \phi_G^+$ must be determined. By introducing a constant δ, such that $\delta \ll 1$ but $\phi < \phi_G + \delta$ equation (2.71) may be written as

$$\frac{dU_G}{d\phi} = \fint_{\phi_G}^{\phi_G+\delta} \frac{s(\Phi)}{\Phi - \phi} d\Phi + \int_{\phi_G+\delta}^{\infty} \frac{s(\Phi)}{\Phi - \phi} d\Phi. \tag{2.72}$$

Assuming that s blows-up but is still integrable as $\phi \to \phi_G^+$ motivates expanding $s \sim K(\phi - \phi_G)^{-p}$ as $\phi \to \phi_G^+$ with $0 < p < 1$ and K a constant. This gives

$$\begin{aligned} \frac{dU_G}{d\phi} = \quad & \fint_{\phi_G}^{\infty} \frac{K(\Phi - \phi_G)^{-p}}{\Phi - \phi} d\Phi \\ & + \int_{\phi_G+\delta}^{\infty} \frac{f(\Phi) - K(\Phi - \phi_G)^{-p}}{\Phi - \phi} d\Phi. \end{aligned} \tag{2.73}$$

Substituting $z - \phi_G = \phi u$ in the first term on the RHS of equation (2.73) gives

$$\begin{aligned} \frac{dU_G}{d\phi} = \quad & -K\phi^{-p} \fint_{0}^{\infty} \frac{u^{-p}}{1-u} du \\ & + \int_{\phi_G+\delta}^{\infty} \frac{f(\Phi) - K(\Phi - \phi_G)^{-p}}{\Phi - \phi} dz. \end{aligned} \tag{2.74}$$

Recalling the result

$$\int_0^\infty \frac{u^{-p}}{1-u} du = -\pi \cot(\pi p), \tag{2.75}$$

allows equation (2.74) to be written as

$$\begin{aligned} \frac{dU_G}{d\phi} = \quad & K(\phi - \phi_G)^{-p} \pi \cot(\pi p) \\ & + \int_\delta^\infty \frac{f(\Phi) - K(\Phi - \phi_G)^{-p}}{\Phi - \phi} d\Phi. \end{aligned} \tag{2.76}$$

To determine the asymptotic behaviour of s as $\phi \to \phi_G^+$ the terms in equation (2.76) are examined. By assumption, the term on the LHS is bounded. Assuming that s is well behaved on the domain $(\phi_G, +\infty)$, a physically reasonable expectation, the second term on the RHS converges, and so it too is bounded. It follows that the first term on the RHS must also be bounded as $\phi \to \phi_G^+$. In order for this to be true the exponent $p = 1/2$, since $0 < p < 1$ and $\cot \pi/2 = 0$. Hence

$$s \sim K_4(\phi - \phi_G)^{-1/2} \quad \text{as} \quad \phi \to \phi_G^+, \tag{2.77}$$

and using equation (2.44) it can be seen that

$$H \sim K_5(\phi - \phi_G)^{1/4} \quad \text{as} \quad \phi \to \phi_G^+, \tag{2.78}$$

where K_i are constants. Hence, provided that the velocity along the fluid-fluid interface is well behaved, the profile of any spreading film close to its fronts has the form (2.78). The author notes that the behaviour (2.78) is inconsistent with the assumption that the vertical length scale is much smaller than the horizontal length scale. Hence, it could be argued that the underlying assumptions of the model break down in the vicinity of the front of the films. One approach to rectify this would be to consider an inner problem (local to the front) and match the solution to an outer outer problem (away from the front). However, it is anticipated that the result of this matching would act passively on the outer solution and hence not affect the global behaviour.

2.11 Discussion and conclusions

A systematic derivation has been given for the equations that govern the spreading of several films of viscous fluid on the surface of a deep pool of more dense viscous fluid. In the parameter regime of interest, it has been shown that the dominant force balance is between the gravitational force due to the buoyant films, and the shear stress induced on the films by the viscous stress of the deep pool. As a consequence, the resulting expression for the evolution of the spreading films is independent of their viscosity, and only depends on the density of the films and the density and viscosity of the pool on which they float. It has also been shown that the way in which the films float on the surface of the pool is determined by a relationship that is consistent with Archimedes' principle.

For the special case of a symmetric arrangement of films it has been predicted that the position of any front moves proportional to $t^{1/3}$ and hence the speed of a front is proportional to $t^{-2/3}$. Furthermore, this means that any two adjacent fronts will separate with a distance proportional to $t^{1/3}$. For a single spreading film, two spreading films and an infinite periodic array of films analytical descriptions of the films evolution are derived ((2.47), (2.55) and (2.65)) as well as numerical description of flow generated in the underlying pool. It has also been shown that the model predicts that the gradient of the profile of any fluid film near its front is infinite, and close to this front the profile is proportional to $x^{1/4}$.

Chapter 3

The reversing of fronts in slow diffusion processes with strong drainage

This chapter considers a family of one-dimensional nonlinear diffusion equations with drainage. In particular, the solutions that have fronts that change their direction of propagation are examined. Although this phenomenon of reversing fronts has been seen numerically, and some special exact solutions have been obtained, there was previously no analytical insight into how this occurs in more general cases. The approach taken here is to seek self-similar solutions local to the front and local to the reversing time. The analysis is split into two parts, one for the solution prior to the reversing time and the other for the solution after the reversing time. In each case the governing PDE is reduced to an ODE by introducing a self-similar coordinate system. These ODEs do not readily admit any non-trivial exact solutions and so the asymptotic behaviour of solutions is studied. By doing this the adjustable parameters, or degrees of freedom, which may be used in a numerical shooting scheme are determined. A numerical algorithm is then proposed to furnish solutions to the ODEs and hence the PDE in the limit of interest. As examples of physical problems in which a PDE of this type may be used as a model the author studies the spreading of a viscous film under gravity and subject to evaporation (or equivalently drainage), the dispersion of a population and a nonlinear heat conduction problem. The numerical algorithm is demonstrated using these examples. Results are also given on the possible existence of self-similar solutions and types of reversing behaviour that can be exhibited by PDEs in the family of interest.

3.1 Introduction

This study is concerned with properties of solutions to a one-dimensional slow diffusion equation with strong drainage

$$\frac{\partial h}{\partial t} = \frac{\partial}{\partial x}\left(h^m \frac{\partial h}{\partial x}\right) - h^{1-q}. \tag{3.1}$$

Here h is the concentration of some species, x and t denote space and time respectively, and the exponents m and q are constants. All variables in (3.1) are dimensionless. Boundary conditions and initial conditions to be imposed on (3.1) are discussed below, see (3.2) - (3.4). In this context the term slow diffusion refers to (3.1) with $m > 0$, so that, the fronts of compactly supported solutions have a finite propogation speed [28]. The term strong drainage refers to (3.1) with $q > 0$, as introduced in [22]. The family of equations shown in (3.1) is widely used as a model for many physical situations, including; the spreading of viscous gravity currents (typically $m = 3$ and $q = 0, 1$) [3], fluid flow in porous media (typically $m = 1$ and $q = 0, 1$) [4], population modelling (typically $m = 1$ and $q > 0$) [27] and nonlinear heat conduction (typically $m > 1$ and $q > 0$) [28]. In all cases, the first term on the RHS of (3.1) represents diffusion, whilst the second term on the RHS represents drainage or consumption of h according to a power-law. In section 3.1.1 the derivation of the model for the case of a slowly spreading viscous film under gravity and subject to evaporation (or equivalently drainage) is outlined.

In many problems of practical interest, bounded, continuous, non-negative solutions to (3.1) that have initial data with compact support are sought in infinitely extended regions. In analysing such solutions it is necessary to consider the points of singular behaviour where $h \to 0$. One common approach is to identify such points as fronts, and to only solve the governing PDE on regions between fronts where h is non-zero. The motions of the fronts are then determined as part of the solution to the problem by insisting that h is zero at the fronts and that the fronts move in such a way that the flux of h through them is zero. These conditions, along with the specification of an initial configuration of h complete the problem definition. Using the notation $s(t)$ to denote the location of the left front at any given time the boundary and initial conditions may be written as

$$h = 0 \quad \text{at} \quad x = s(t), \tag{3.2}$$

$$\frac{ds}{dt} = -h^{m-1}\frac{\partial h}{\partial x} + \left(q\frac{\partial}{\partial x}\left(h^q\right)\right)^{-1} \quad \text{at} \quad x = s(t), \tag{3.3}$$

and initial data

$$h(x,0) = h_0(x) \tag{3.4}$$

determining the initial position of the front, $s(0)$. Note that two conditions analogous to (3.2) and (3.3) must also be imposed to determine the motion of the right front of the solution.

Properties of (3.1) have been extensively examined by previous authors. See [39] and the bibliography therein for results on existence and uniqueness of solutions. The behaviour of solutions depends critically on the values of m and q. One result that is particularly relevant to this study states that when $m \leq 0$ solutions with initial conditions that have compact support have fronts that move at an infinite velocity. By contrast, if $m > 0$ the fronts propagate with a finite velocity [28]. Another important result states that for $q > 0$ receding fronts can exist [22]. In this context a receding front refers to circumstances where the front moves in a way that decreases the size of the region of compact support of the solution. For the case $m > 0$ and $0 < q < 1$ it has been shown that $h(x,t) \equiv 0$ for all x after some finite time, so that the problem displays so-called finite extinction time [19], [38]. The asymptotic behaviour of the solution near this extinction time was studied in [26] where it was shown that if $m - q \geq 0$ the behaviour is completely dominated by drainage. However, if $m - q < 0$ then there are regions near the edge of the support where diffusion becomes important. In [41] a generalised version of (3.1) was studied where the growth and connectedness of the support of solutions as $t \to +\infty$ could be determined. It was shown that the compact support can either remain bounded or become unbounded as $t \to +\infty$, depending on the parameters m and q. Predictions for the rate of growth of the compact support were also derived.

Other authors have obtained exact solutions for several special choices of m and q. Essentially, solutions can be found in the case $m + q = 0$, since the effects of diffusion and drainage are matched, in the sense that both are proportional to h^{m+1}. Similarly, in the case $q = 0$ the drainage and time derivative terms are matched in the sense that both are proportional to h. Another special case in which an exact solution can be found occurs when $m - q + 1 = 0$

[40]. In [29] separation of variables and self-similar reductions were used to reduce (3.1) to various ODEs. For two of these ODEs first integrals and exact solutions are obtained. In [53] a special exact solution to a generalisation of (3.1) (in more than one spatial dimension) was found by means of a self-similar reduction. In [55] an exact solution was found for the special case $m = 1$ and $q = 0$ by transforming the spatial coordinates. In the same study another exact solution was found for the case $m = 1$ and $q = 1$ by means of separation of variables. In [50] a numerical scheme is developed to find approximate solutions to (3.1). The numerical solutions are compared to one of the aforementioned exact solutions and a good agreement is shown between the two.

Other relevant studies include [5] and [44], in which the problem of waiting time was considered. This refers to the phenomenon exhibited by the purely diffusive version of (3.1) (i.e. without the term h^{1-q} in the PDE) with $m > 0$ where fronts can remain stationary for some finite time and then begin to move. Using a self-similar reduction to the governing equation, local solutions are found which describe the change in the behaviour of the front.

The author's original interest in equations of this type came about when modelling the spreading of a viscous film over a horizontal plate, under the action of gravity and subject to evaporation. An outline of the derivation of the model is given in section 3.1.1 and gives rise to (3.1) with $m = 3$ and $q = 1$. Initial analysis of this model was concentrated on looking for approximate travelling wave solutions local to the front. The notation $s(t)$ was used to denote the location of the left front at any given time. By transforming to a coordinate system local to this front by writing $x = s(t) + \xi$ the following PDE in the neighbourhood of the front was derived

$$\frac{\partial h}{\partial t} - \frac{ds}{dt}\frac{\partial h}{\partial \xi} = \frac{\partial}{\partial \xi}\left(h^3 \frac{\partial h}{\partial \xi}\right) - 1. \tag{3.5}$$

From equation (3.5), it is relatively straightforward to see that a balance between the second term on the LHS and the first term on the RHS of (3.5) gives rise to a local advancing travelling wave solution of the form

$$h \sim \left(-3\frac{ds}{dt}\right)^{1/3} \xi^{1/3} \quad \text{i.e.} \quad h \sim \left(-3\frac{ds}{dt}\right)^{1/3} (x - s(t))^{1/3} \quad \text{as} \quad x \to s(t)^+. \tag{3.6}$$

Furthermore, a balance between the second term on the LHS and the second term on the RHS of (3.5) gives rise to a receding local travelling wave solution of the form

$$h \sim \left(\frac{ds}{dt}\right)^{-1} \xi \quad \text{i.e.} \quad h \sim \left(\frac{ds}{dt}\right)^{-1} (x - s(t)) \quad \text{as} \quad x \to s(t)^+. \tag{3.7}$$

In addition to this local analysis, numerical experiments were carried out that indicated (for certain initial conditions) numerical solutions exhibit a behaviour in which the front of the solution would change its direction of propagation. Throughout this study such a phenomenon is referred to as the reversing of a front. Although the reversing behaviour of solutions to (3.1) has been observed numerically and some of the aforementioned exact solutions also exhibit this behaviour, there appears to be no analytical explanation of how this occurs in more general cases [47], [50]. In other words, there appears to be no analytical explanation of how the advancing wave (3.6) gives way to the receding wave (3.7). With this in mind a similar approach is taken in this study to that used in [44], namely to seek solutions to (3.1) local to the front and local to the reversing time. To find such solutions a self-similar reduction will be made to (3.1) in the parameter regime $m > 0$, $q > 0$ and $m - q > 0$. The first of these restrictions ensures that the fronts propagate with a finite velocity [28], while the second allows the existence of receding fronts [22]. It will become apparent that the third means that an advancing front moves due to a balance between the time derivative and diffusion. Conversely, a receding front moves due to a balance between the time derivative and drainage. Note that a front may reverse even if the third restriction is not satisfied - however it appears that if $m - q \leq 0$ the solution local to the front and local to the reversing time will behave differently to the case studied here.

For algebraic clarity, the origins of time and space are chosen so that the reversing time is $t = 0$ when the position of the front is $s(0) = 0$. Additionally it is assumed, without loss of generality, that h is non-zero in $x > 0$ and h is zero for all $x \leq 0$. Throughout this study it is assumed that $s(t)$ and its first derivative are continuous. Whilst this seems to be a physically sensible assumption there appears to be no rigorous proof for behaviour. To find a suitable similarity reduction the author refers to [23] which, by consideration of classical point symmetries of (3.1), lists possible reductions for equations of this type. Included in this list is a reduction of the form

$$h = |t|^\alpha H(\phi), \quad \text{with} \quad \phi = x|t|^\beta \quad \text{and} \quad s(t) = \Lambda|t|^{-\beta}, \tag{3.8}$$

where Λ is an arbitrary constant, and α and β are constants that are fixed by the exponents m

and q. Later in this work it will be seen that $\alpha = 1/q$ and $\beta = -(m+q)/2q$. Though in [23] other reductions to (3.1) are derived, these are unsuitable to describe the reversing behaviour since they necessarily give a discontinuity in the velocity of the front as t passes through zero. It is noted, however, that some of these other reductions do give a sensible behaviour of the solution away from $t = 0$. The form of (3.8) means that the position of the front moves in proportion to $|t|^{-\beta}$ with $\beta < -1$ (since $m > 0$, $q > 0$ and $m - q > 0$) and hence the velocity of the front is continuous as t passes through zero.

The analysis is split into two sections. In section 3.2 the solution for $t < 0$ (with an advancing front) is studied. Using a self-similar reduction of the form (3.8) to (3.1) an ODE is derived for the dependent self-similar variable H as a function of ϕ. The asymptotic behaviour of solutions to this ODE as $H \to 0^+$ and $\phi \to +\infty$ are examined by assuming a power-law type expansion in each limit. In section 3.3, a similar analysis is carried out for the solution with $t > 0$ (and a receding front). In order to close the problem, continuity of h across $t = 0$ is enforced so that h is continuous as the front changes its direction of propagation. This is equivalent to insisting that the solutions both prior to and after the reversing time have the same asymptotic behaviour as $\phi \to +\infty$. In section 3.4 a numerical scheme, which makes use of the determined asymptotic behaviours, is proposed to determine solutions local to $x = 0$ and $t = 0$ (see [56] for another example of applying this technique). In sections 3.4.1, 3.4.2 and 3.4.3 this algorithm is demonstrated using several physically motivated examples. Section 3.4.4 discusses the practicalities of finding solutions for other pairs of values of m and q. Finally, in section 3.5 the results and conclusions are discussed. Before proceeding to analyse (3.1) a physical application that leads to a reversing front of the type outlined above is discussed.

3.1.1 The slow spreading of a viscous film with evaporation

Consider the slow spreading of a viscous film along a fixed horizontal plate under the action of gravity and subject to evaporation. The definition diagram for the flow is shown in figure 3.1. By assuming that the Reynolds number is sufficiently small that inertial effects can be neglected, the equations of momentum and continuity are

$$\nabla p = \mu \nabla^2 \mathbf{u} - \rho \mathbf{g}_r, \quad \nabla \cdot \mathbf{u} = 0. \tag{3.9}$$

Here, p is the pressure, μ is the viscosity of the fluid, $\mathbf{u} = (u, v)$ is the velocity vector, ρ is the density of the fluid and $\mathbf{g}_r = (0, g_r)$ is the acceleration due to gravity. The no-slip boundary condition between the film and the plate is

$$\mathbf{u} = 0 \quad \text{on} \quad y = 0. \tag{3.10}$$

It is assumed that the capillary number, $Ca = \mu u_0 \gamma^{-1}$ (where u_0 is the velocity scale of the flow and γ is the interfacial tension) is sufficiently large so that surface tension effects are negligible. The free surface of the film is modelled as stress free and assumed to satisfy a modified kinematic condition, which takes into account the loss of fluid due to a constant evaporation normal to the free surface. Hence

$$\mathbf{t}'\mathbf{T}\mathbf{n} = \mathbf{n}'\mathbf{T}\mathbf{n} = 0 \quad \text{and} \quad v - \frac{Q}{\rho} = u\frac{\partial \eta}{\partial x} + \frac{\partial \eta}{\partial t} \quad \text{on} \quad y = \eta(x, t). \tag{3.11}$$

Here a prime denotes the usual vector transpose operation, $y = \eta(x, t)$ is the free surface of the film, $\mathbf{t}$ and $\mathbf{n}$ are unit vectors tangential and normal to the surface $y = \eta(x, t)$, Q is the evaporation rate per unit area and $\mathbf{T}$ is the stress tensor (defined in the usual way).

Assuming that the film is slender motivates the non-dimensionalisation $x = L\bar{x}$, $y = \epsilon L\bar{y}$ and $\eta = \epsilon L\bar{\eta}$. Here L is a typical length of the film and $\epsilon \ll 1$ is the ratio of typical depth to typical length. An as yet undetermined horizontal velocity scale for the flow is introduced by writing $u = u_0\bar{u}$. In order to conserve mass the vertical velocity scale is $v = \epsilon u_0 \bar{v}$. Pressure and time are scaled the natural way by writing $p = \rho g_r \epsilon L\bar{p}$ and $t = Lu_0^{-1}\bar{t}$. So that the pressure in the film is hydrostatic (to leading order in ϵ) this sets the undetermined velocity scale $u_0 = \rho g_r \epsilon^3 L^2 \mu^{-1}$. To leading order in ϵ the system of equations (3.9), (3.10) and (3.11) may be written as

$$\frac{\partial \bar{p}}{\partial \bar{y}} = -1, \quad \frac{\partial^2 \bar{u}}{\partial \bar{y}^2} = \frac{\partial \bar{p}}{\partial \bar{x}} \quad \text{and} \quad \frac{\partial \bar{u}}{\partial \bar{x}} + \frac{\partial \bar{v}}{\partial \bar{y}} = 0, \tag{3.12}$$

$$\bar{u} = \bar{v} = 0 \quad \text{on} \quad \bar{y} = 0, \tag{3.13}$$

$$\frac{\partial \bar{u}}{\partial \bar{y}} = 0, \quad \bar{p} = 0 \quad \text{and} \quad \bar{v} - \frac{Q}{\epsilon u_0 \rho} = \bar{u}\frac{\partial \bar{\eta}}{\partial \bar{x}} + \frac{\partial \bar{\eta}}{\partial \bar{t}} \quad \text{on} \quad \bar{y} = \bar{\eta}(\bar{x}, \bar{t}). \tag{3.14}$$

The system of equations (3.12), (3.13) and (3.14) can be solved to obtain $\bar{u}$ and $\bar{v}$ in terms of $\bar{y}$ and $\bar{\eta}$. Substitution of these solutions into the third equation in (3.14) yields the following

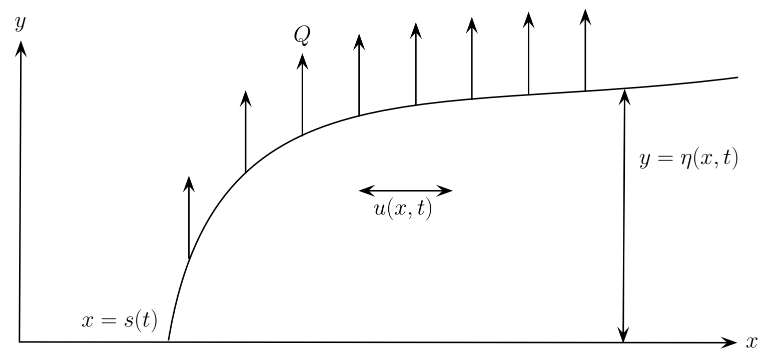

Figure 3.1: Definition diagram for the slow spreading of a viscous film over a plate with evaporation.

equation for $\bar{\eta}$

$$\frac{\partial \bar{\eta}}{\partial \bar{t}} = \frac{\partial}{\partial \bar{x}}\left(\bar{\eta}^3 \frac{\partial \bar{\eta}}{\partial \bar{x}}\right) - \frac{Q}{\epsilon u_0 \rho}. \tag{3.15}$$

This nonlinear PDE for the free surface of the film, $\bar{\eta}(\bar{x}, \bar{t})$, contains one non-dimensional parameter, $Q\epsilon^{-1}u_0^{-1}\rho^{-1}$. This gives a measure of the ratio of the spreading rate to the evaporation rate. Equation (3.15) can be reduced to an equation of type (3.1) for $\bar{\eta}(x^*, t^*)$ with $m = 3$ and $q = 1$ by writing

$$\bar{t} = \frac{\epsilon u_0 \rho}{Q} t^* \quad \text{and} \quad \bar{x} = \sqrt{\frac{\epsilon u_0 \rho}{Q}}\, x^*. \tag{3.16}$$

It is important to note that although equation (3.15) has been derived by considering a situation in which the loss of fluid is due to evaporation through the film's upper surface, one could have arrived at an identical result by considering a situation in which the loss of fluid is through the plate. Put simply, these different physical situations give rise to the same governing PDE because the derivation relies on a thin film approximation. In other words, since the limit that $\epsilon \to 0$ has been taken, the system is reduced to depending on only one spatial coordinate, hence (3.15) is no longer able to differentiate between losses through its upper and lower surfaces.

3.2 Prior to the reversing time

In this section analysis is concentrated on solutions to (3.1) when $t < 0$ and the front is advancing. As discussed in section 3.1 a similarity reduction of the form

$$h = (-t)^{1/q} H(\phi) \quad \text{where} \quad \phi = x(-t)^{-(m+q)/2q} \quad \text{and} \quad s(t) = A(-t)^{(m+q)/2q} \tag{3.17}$$

is employed. Here A is an undetermined constant. Using (3.17), equation (3.1) and its corresponding local boundary condition reduce to

$$-\frac{1}{q}\,H+\frac{m+q}{2q}\,\phi H'=\left(H^m H'\right)'-H^{1-q}\quad\text{with}\quad H(A)=0. \tag{3.18}$$

Equation (3.18) readily admits one exact solution

$$H=\left(\frac{(m+q)^2}{2(2+m-q)}\right)^{1/(m+q)}\phi^{2/(m+q)}. \tag{3.19}$$

However, (3.19) has $H(0)=0$ and as such cannot lead to a solution to (3.1) that exhibits reversing behaviour. Hence, other solutions to (3.18) must be sought. To this end the asymptotic behaviour of solutions near $\phi=A$ and as $\phi\to+\infty$ are examined. As $\phi\to A^+$ an asymptotic solution that has the form of a power-law is sought. It is found that

$$H\sim\left(\frac{m+q}{2q}Am\right)^{1/m}(\phi-A)^{1/m}\quad\text{as}\quad\phi\to A^+. \tag{3.20}$$

The prefactor of the asymptotic behaviour (3.20) depends on the values of both m and q, whereas, the exponent depends on the value of m only. Physically this may be understood by noting that fronts of solutions to (3.1) advance due to diffusion. Since the solution prior to the reversing time has an advancing front it may not come as a complete surprise that the value of m largely determines the behaviour of the solution close to the front.

In the far field a solution that has the the form of a power-law is also sought. It is found that

$$H\sim N\phi^{2/(m+q)}\quad\text{as}\quad\phi\to+\infty. \tag{3.21}$$

Here N is an undetermined constant. A natural question is whether there are solutions to (3.18) that have the behaviour (3.20) near $\phi=A$ and reach the behaviour (3.21) in the far field. In addition, one may also wish to know whether there is an infinite family, countably many or a unique solution with these behaviours. One *ad-hoc* approach to answering this question (which will subsequently be shown to be a valid approach in this case) is to implement a numerical shooting scheme to integrate (3.18) from near $\phi=A$ using (3.20) towards the far field. The value of A can then be adjusted as a shooting parameter with the aim of reaching a solution with behaviour (3.21) in the far field. Alternatively one could integrate (3.18) numerically from the far field using (3.21) and adjust the value of N as a shooting parameter with the aim of reaching a solution with behaviour (3.20) near $\phi = A$. The results of such numerical experiments are shown in figures 3.2 and 3.3. From these results one might conclude that there is only one solution with the aforementioned behaviours, however, this is rather naive. In order to support this claim a more thorough analysis near the point $\phi = A$ and as $\phi \to +\infty$ is presented. The approach will be to linearise about a particular solution, $\bar{H}$, by writing

$$H = \bar{H} + H_1, \tag{3.22}$$

and requiring that $H_1 \ll \bar{H}$. Using (3.18) and (3.22) the following second order linear homogeneous ODE is derived for H_1,

$$-\frac{1}{q}\,H_1 + \frac{m+q}{2q}\,\phi H_1' = \left(\bar{H}^m H_1' + mH_1\bar{H}^{m-1}\bar{H}'\right)' - (1-q)\bar{H}^{-q}H_1. \tag{3.23}$$

By examining the possible asymptotic solutions for H_1 the number of adjustable parameters, or degrees of freedom, when implementing a shooting scheme will be determined.

First consider the asymptotic behaviour (3.20) near $\phi = A$. Linearising about this as follows

$$H \sim \left(\frac{m+q}{2q}Am\right)^{1/m}(\phi - A)^{1/m} + H_1 \quad \text{as} \quad \phi \to A^+, \tag{3.24}$$

and substituting into (3.18) leads to a second order linear homogeneous ODE for H_1 with the following possible asymptotic behaviours

$$H_1 \sim M_1\,(\phi - A)^{(1/m)-1} \quad \text{or} \quad H_1 \sim M_2 \quad \text{as} \quad \phi \to A^+. \tag{3.25}$$

Here M_1 and M_2 are undetermined constants. The first behaviour in (3.25) corresponds to changing A in (3.20) by a small amount. This can be seen by performing a Taylor expansion on (3.20) for small adjustments to A. Hence, without loss of generality M_1 can be set equal to zero. The second behaviour in (3.25) is necessarily larger than (3.20) in the limit that $\phi \to A^+$ unless M_2 is zero. Hence the solution with $M_2 = 0$ is required. Therefore, there is only adjustable parameter (degree of freedom) when shooting from near $\phi = A$, namely the value of A.

An analogous analysis in the far field is performed by linearising about the asymptotic behaviour (3.21) by writing

$$H \sim N\phi^{2/(m+q)} + H_1 \quad \text{as} \quad \phi \to +\infty. \tag{3.26}$$

As before, this leads to a second order linear homogeneous ODE for H_1 with the following possible asymptotic behaviours

$$H_1 \sim N_1\phi^{2/(m+q)} \quad \text{or} \quad H_1 \sim N_2 \exp\left(\frac{(m+q)^2}{4q^2} N^{-m}\phi^{2q/(m+q)}\right)$$

$$\text{as} \quad \phi \to +\infty. \tag{3.27}$$

Here N_1 and N_2 are undetermined constants. The first behaviour in (3.27) is the same as (3.21), hence, without loss of generality N_1 is set equal to zero. For sufficiently large ϕ the second behaviour in (3.27) becomes larger than (3.21) unless N_2 is zero. Therefore the solution with $N_2 = 0$ is required. It is noted that numerical evidence suggests that solutions that do deviate from (3.21) (with N_2 non-zero) have $H = 0$ at some large but finite ϕ. Hence, such solutions are not viable in this problem. Therefore there is only one adjustable parameter (degree of freedom) when shooting from the far field, namely the value of N.

Having determined the adjustable parameters near $\phi = A$ and as $\phi \to +\infty$ the shooting problem from near $\phi = A$ is reconsidered. Picking a particular value of A one might expect that for some large but finite ϕ

$$H \sim N\phi^{2/(m+q)} + N_2 \exp\left(\frac{(m+q)^2}{4q^2} N^{-m}\phi^{2q/(m+q)}\right). \tag{3.28}$$

Hence, as ϕ continues to grow, the solution will deviate from the behaviour (3.21) unless $N_2 = 0$. Examples of such solutions can be seen in figure 3.2. Thus it is anticipated that there are at most countably many values of A that correspond to the far field behaviour (3.21).

Alternatively, consider the shooting problem from the far field. Picking a particular value of N one might expect that for some small but non-zero H

$$H \sim \left(\frac{m+q}{2q} Am\right)^{1/m} (\phi - A)^{1/m} + M_2. \tag{3.29}$$

Hence the solution deviates from the behaviour (3.20) unless $M_2 = 0$. Examples of such solutions can be seen in figure 3.3. Therefore it is expected that there are at most countably many values of N that correspond to the behaviour (3.20) near $\phi = A$.

3.3 After the reversing time

In this section analysis is concentrated on (3.1) when $t > 0$ and the front is receding. In this case a reduction of the same form as that used in section 3.2 is employed, but taking care that t is now positive,

$$h = t^{1/q} H(\phi) \quad \text{where} \quad \phi = x t^{-(m+q)/2q} \quad \text{and} \quad s(t) = B t^{(m+q)/2q}. \tag{3.30}$$

Here B is an undetermined constant. Using (3.30), equation (3.1) and its corresponding local boundary condition reduces to

$$\frac{1}{q} H - \frac{m+q}{2q} \phi H' = (H^m H')' - H^{1-q} \quad \text{with} \quad H(B) = 0. \tag{3.31}$$

This second order nonlinear ODE does not readily admit any exact solutions aside from (3.19). Hence, in a similar manner to the previous section, the asymptotic behaviour of solutions to (3.31) near $\phi = B$ and as $\phi \to +\infty$ are examined. As $\phi \to B^+$ the behaviour is examined by assuming a power-law type expansion. It is found that

$$H \sim \left(\frac{m+q}{2q^2} B \right)^{-1/q} (\phi - B)^{1/q}. \tag{3.32}$$

The prefactor of the asymptotic behaviour (3.20) depends on the values of both m and q, whereas, the exponent depends on the value of q only. Physically, this may be understood by noting that fronts of solutions to (3.1) recede due to drainage effects. Since the solution after the reversing time has a receding front it may not be unexpected that the value of q largely determines the behaviour of the solution close to the front.

As $\phi \to +\infty$ the asymptotic behaviour is also examined by assuming a power-law type expansion. It is found that

$$H \sim Q \phi^{2/(m+q)}. \tag{3.33}$$

Here Q is an undetermined constant. For reasons that have been discussed in section 3.2 the author now linearises about the asymptotic solutions (3.32) and (3.33). Linearising about (3.32) using

$$H \sim \left(\frac{m+q}{2q^2}B\right)^{-1/q}(\phi - B)^{1/q} + H_1 \tag{3.34}$$

and substituting into (3.31) leads to a second order linear homogeneous ODE for H_1 with the following asymptotic behaviours

$$H_1 \sim P_1(\phi - B)^{(1/q)-1} \quad \text{or} \quad H_1 \sim P_2 \exp\left(\left(\frac{B}{2}\right)\frac{m+q}{m-q}\left(\frac{m+q}{2q^2}B\right)^{m/q}(\phi - B)^{-(m-q)/q}\right)$$

$$\text{as} \quad \phi \to B^+. \tag{3.35}$$

The first behaviour in (3.35) corresponds to a small change in B in the behaviour (3.32). This can be seen by performing a Taylor expansion on (3.32) for small adjustments to B. Hence, without loss of generality P_1 is set equal to zero. The second behaviour in (3.35) becomes larger than (3.32) in the limit $\phi \to B^+$ unless P_2 is zero. Hence the solution with $P_2 = 0$ is required. Therefore there is only one adjustable parameter (degree of freedom) when shooting from near $\phi = B$, namely the value of B.

The solution (3.33) in the far field is linearised about by writing

$$H \sim Q\phi^{2/(m+q)} + H_1. \tag{3.36}$$

Again, this leads to a second order linear homogeneous ODE for H_1 with the following asymptotic behaviour

$$H_1 \sim Q_1\phi^{2/(m+q)} \quad \text{or} \quad H_1 \sim Q_2 \exp\left(-\frac{(m+q)^2}{4q^2}Q^{-m}\phi^{2q/(m+q)}\right). \tag{3.37}$$

The first behaviour in (3.37) is the same as (3.33) and so without loss of generality Q_1 is set equal to zero. To fix values for Q and Q_2 it is necessary to discuss a condition of continuity which should be imposed on the solution. On physical grounds it must be insisted that the concentration, h, is continuous as t passes through zero. In terms of the self-similar variables this is equivalent to requiring that solutions to (3.18) and (3.31) have the same behaviour as $\phi \to +\infty$ (corresponding to $t \to 0^+$ and $t \to 0^-$). It was shown in the previous section that solutions to (3.18) take the form (3.21) in the far field. Therefore, continuity across $t = 0$ requires the solution to (3.31) has $Q = N$.

Now consider the shooting problem from near $\phi = B$. Picking a value of B one might expect that for some large but finite ϕ

$$H \sim Q\phi^{2/(m+q)} + Q_2 \exp\left(-\frac{(m+q)^2}{4q^2} Q^{-m} \phi^{2q/(m+q)}\right). \tag{3.38}$$

The value of B must be adjusted as a shooting parameter until the behaviour (3.38) with $Q = N$ is reached in the limit that $\phi \to +\infty$. In doing this a value for Q_2 is also fixed. However, in the far field limit the second term in (3.38) tends to zero, independent of Q_2. As before, one expects there to be at most countably many values of B which correspond to the requisite behaviour (3.33) with $Q = N$ in the far field.

Alternatively, consider the shooting problem from the far field. Fixing the value of $Q = N$ (by virtue of the condition of continuity across $t = 0$) and picking a particular value of Q_2 one might expect that for some small but non-zero H

$$H \sim \left(\frac{m+q}{2q^2} B\right)^{-1/q} (\phi - B)^{1/q} + P_2 \exp\left(\left(\frac{B}{2}\right) \frac{m+q}{m-q} \left(\frac{m+q}{2q^2} B\right)^{m/q} (\phi - B)^{-(m-q)/q}\right). \tag{3.39}$$

Hence the solution deviates from (3.32) unless $P_2 = 0$. Therefore it is expected that there are at most countably many values of Q_2 that correspond to $P_2 = 0$.

3.4 A numerical shooting scheme

In this section, a numerical algorithm is proposed to construct solutions to (3.1) local to the front and local to the reversing time. The approach is to use the asymptotic behaviours (3.20) and (3.21) to formulate an initial value problem for the ODE (3.18). A similar method is then used for the asymptotic behaviours (3.32) and (3.38) and the ODE (3.31). These can then be integrated numerically using the ODE45 package in MATLAB [58]. The details of the method are set out below.

- The solution for $t < 0$ can be determined using two different shooting schemes (i) using the form shown in (3.20) to construct initial values for H and H' so that (3.18) can be integrated from $\phi = A$ towards the far field or (ii) using the form shown in (3.21) to form initial values for H and H' so that (3.18) can be integrated from the far field towards $\phi = A$. However, shooting in either of the aforementioned directions is inherently unstable. In the case (i) this is due to the exponentially large term in (3.27), and in the case (ii) due to the constant M_2 in (3.25). Hence, in practice it is necessary to shoot both from $\phi = A$, adjusting A as a shooting parameter, and from the far field adjusting N as a shooting parameter. By adjusting A and N correctly two solution curves (one using the shooting method (i) and the other using the method (ii)) can be obtained that agree (to within some small error tolerance) on a significant range of ϕ between A and the far field, see for example figure (3.2). It is then reasonable to assume the required solution is very well approximated by the solution (i) for ϕ near A and by (ii) in the far field.

- The solution for $t < 0$ is then fully determined. It is now insisted that the behaviour of the solution as $\phi \to +\infty$ does not change as t passes through zero (and hence the concentration, h, is continuous) so a solution for $t > 0$ must be found with $Q = N$.

- The solution for $t > 0$ can be determined using two different shooting schemes (i) using (3.32) to construct initial values for H and H' so that (3.31) can be integrated from $\phi = B$ towards the far field or (ii) using (3.38) to construct initial values for H and H' so that (3.31) can be integrated from the far field towards $\phi = B$. Due to the presence of the exponentially large term in (3.35) shooting in the direction (ii) is inherently unstable. Therefore, in practice it may be necessary to shoot both from $\phi = B$, adjusting B as a shooting parameter, and from the far field adjusting Q_2. By adjusting B and Q_2 correctly two solution curves (one using the shooting method (i) and the other using method (ii)) can be obtained that agree on a significant range of ϕ between B and the far field. As before, it is then reasonable to assume that the required solution is very well approximated by the solution (i) near $\phi = A$ and the solution (ii) in the far field.

3.4.1 The solution for $m = 3$ and $q = 1$; a spreading viscous film with evaporation

To demonstrate the method proposed in section 3.4 the example that originally motivated this study is used, that is, (3.1) with $m = 3$ and $q = 1$. In this case the forms (3.20), (3.21), (3.32) and (3.33) reduce to

$$H \sim (6A)^{1/3}(\phi - A)^{1/3} \quad \text{as} \quad \phi \to A^+ \quad \text{for} \quad t < 0, \tag{3.40}$$

$$H \sim N\phi^{1/2} \quad \text{as} \quad \phi \to +\infty \quad \text{for} \quad t < 0, \tag{3.41}$$

$$H \sim \frac{1}{2B}(\phi - B) \quad \text{as} \quad \phi \to B^+ \quad \text{for} \quad t > 0, \tag{3.42}$$

$$H \sim Q\phi^{1/2} \quad \text{and} \quad \text{as} \quad \phi \to +\infty \quad \text{for} \quad t > 0. \tag{3.43}$$

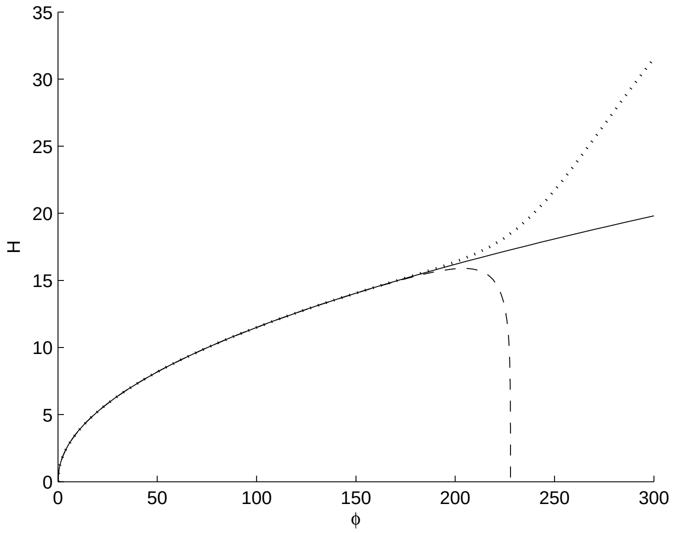

Figure 3.2: Plot of H vs ϕ for $t < 0$ for equation (3.1) with $m = 3$ and $q = 1$. The dashed and dotted curves show the solution computed by integrating (3.18) from $\phi = A$ with $A = 0.14397765 \pm 5 \times 10^{-8}$ respectively. It is noted that the dashed curve shows H tending to infinity in the negative direction whilst the dotted curve shows H tending to infinity in the positive direction corresponding to negative and positive values of N_2. Therefore it is anticipated, although not proven, that the exact value of A which corresponds to $N_2 = 0$ lies in the range $0.14397765 \pm 5 \times 10^{-8}$. The solid line shows the solution computed from integrating from $\phi = 300$ with a value of $N = 1.1435$.

Using the numerical algorithm outlined above (with the default settings in the ODE45 suite) in MATLAB the following values are determined

$$A \approx 0.1440, \quad B \approx 0.0958; \text{ and } N = Q \approx 1.1435. \tag{3.44}$$

When the absolute error tolerances were reduced below the ODE45 default value of 10^{-6} there were no appreciable changes in the computed solutions. The results of the numerical computations are shown in figures 3.2 and 3.3. Figure 3.4 has also been included to show that the condition of continuity across $t = 0$ has been satisfied. Other numerical computations were carried out for a large range of values of the shooting parameters A and N. It was found in all cases that the deviation from the required behaviour was monotone in the shooting parameter. Although this is not a rigorous proof, the numerical evidence strongly suggests that the above values of A, B, N and Q are unique. Figures 3.5 and 3.6 have also been included to show the evolution of the solution $h(x,t)$ and the position of the front during this evolution.

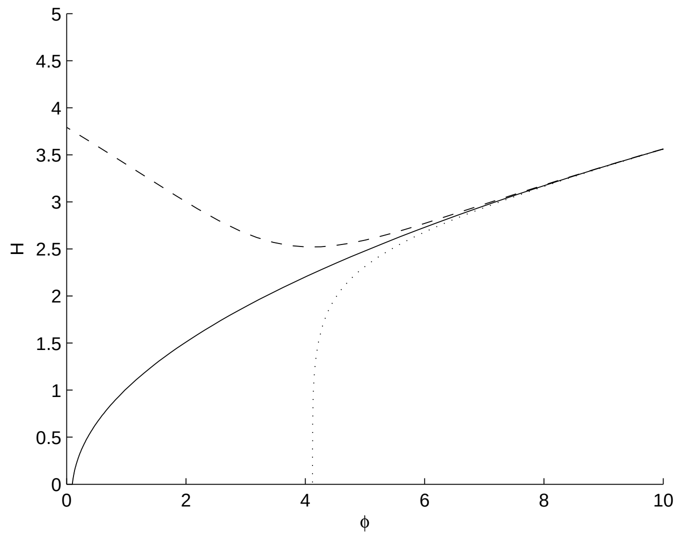

Figure 3.3: Plot of H vs ϕ for $t > 0$ for equation (3.1) with $m = 3$ and $q = 1$. The dashed curve shows the solution computed by integrating (3.18) from $\phi = 30$ with $Q = 1.1435$ and $Q_2 = -16507$. The dotted curve shows the solution computed by integrating (3.18) from $\phi = 30$ with $Q = 1.1435$ and $Q_2 = -16508$. It is noted that although the dotted curve may appear to have the requisite behaviour as H becomes small the solution computed by integrating (3.18) using the corresponding value of A diverges from the required behaviour in the far field. The solid line shows the solution computed from integrating from $\phi = B$ with a value of $B = 0.0958$.

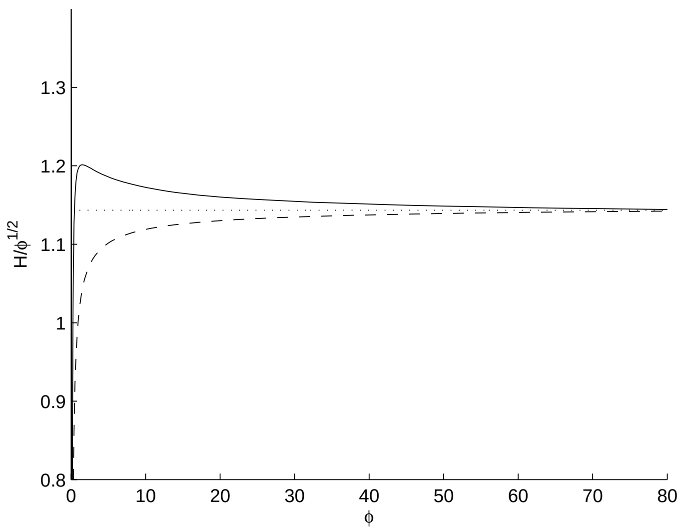

Figure 3.4: Plot of $H/\phi^{1/2}$ vs ϕ for equation (3.1) with $m = 3$ and $q = 1$. The solid curve shows the solution for $t > 0$, the dashed curve shows the solution for $t < 0$ and the dotted curve shows $N\phi^{1/2}$ vs $\phi^{1/2}$.

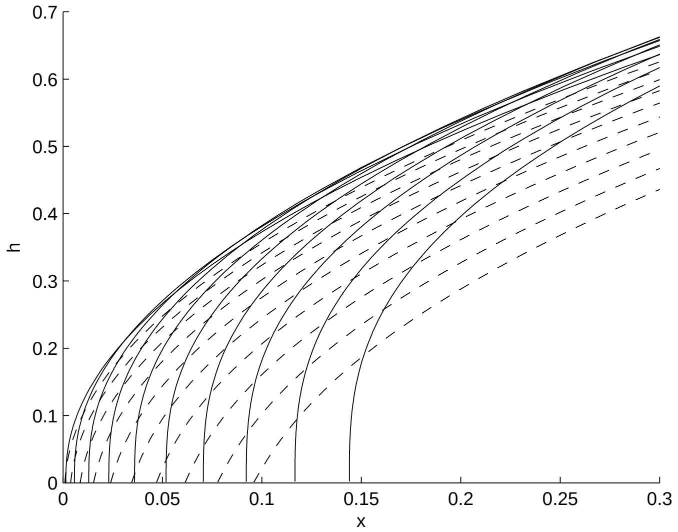

Figure 3.5: Plot of h vs x for equation (3.1) with $m = 3$ and $q = 1$. The solution has been plotted at 20 equally spaced times between $t = -1$ and $t = 1$. The solid curves show the solution for $t < 0$ and the dashed curves for $t > 0$.

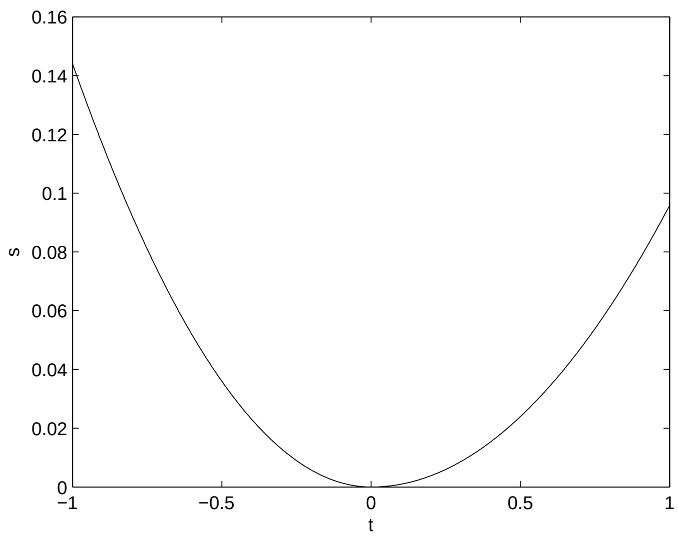

Figure 3.6: Plot of s vs t for equation (3.1) with $m = 3$ and $q = 1$. The position of the front as a function of time.

3.4.2 The solution for $m = 2$ and $q = 1$; a population with constant death rate

For a second demonstration of the numerical scheme proposed in section 3.4 a population model is considered. Many population studies use equation (3.1) with $m = 2$ to model the movement of a species, see for example [17] and the bibliography therein. The derivation of such models are based on the assumption that the dispersion of organisms in a species is prevalent in regions that are densely populated. For simplicity, the case of a population subject to a constant death rate is considered. This gives rise to (3.1) with $q = 1$. In this case the forms (3.20), (3.21), (3.32) and (3.33) reduce to

$$H \sim (3A)^{1/2}(\phi - A)^{1/2} \quad \text{as} \quad \phi \to A^+ \quad \text{for} \quad t < 0, \tag{3.45}$$

$$H \sim N\phi^{2/3} \quad \text{as} \quad \phi \to +\infty \quad \text{for} \quad t < 0, \tag{3.46}$$

$$H \sim \frac{2}{3B}(\phi - B) \quad \text{as} \quad \phi \to B^+ \quad \text{for} \quad t > 0, \tag{3.47}$$

$$H \sim Q\phi^{2/3} \quad \text{and} \quad \text{as} \quad \phi \to +\infty \quad \text{for} \quad t > 0. \tag{3.48}$$

Using the numerical algorithm outlined in section 3.4 and the default settings in the ODE45 the following values are determined

$$A \approx 0.001354, \;\; B \approx 0.01022 \;\text{ and }\; N = Q \approx 1.1445. \tag{3.49}$$

The same convergence and uniqueness checks were carried out as those in section 3.4.1. A plot of the solution is shown in figure 3.7.

3.4.3 The solution for $m = 4$ and $q = 1$; nonlinear heat conduction with drainage

For a further demonstration of the numerical scheme set up in section 3.4 a nonlinear heat conduction problem is considered. Previous authors have modelled the dissipation of heat in media where heat flow is due to radiation and the material is optically thick. For example, [65] considered a problem in which the relevant model was equation (3.1) with $m = 4$ and $q = 1$.

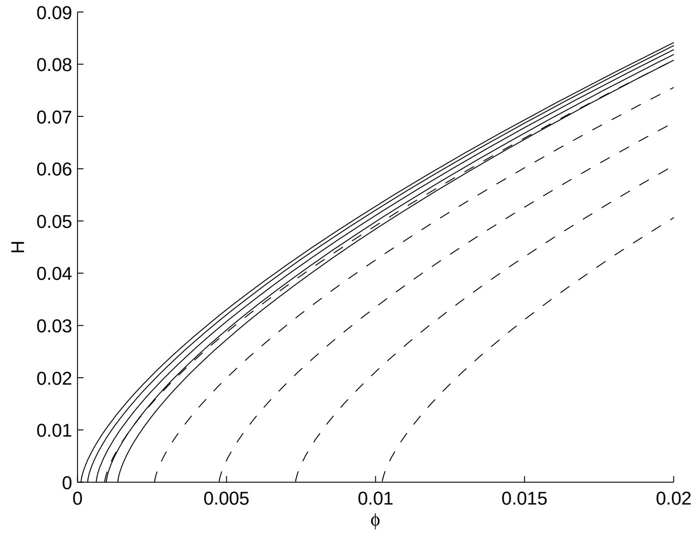

Figure 3.7: Plot of h vs x for equation (3.1) with $m = 2$ and $q = 1$. The solution has been plotted at 10 equally spaced times between $t = -1$ and $t = 1$. The solid curves show the solution for $t < 0$ and the dashed curves for $t > 0$.

In this case the forms (3.20), (3.21), (3.32) and (3.33) reduce to

$$H \sim (10A)^{1/4}(\phi - A)^{1/4} \quad \text{as} \quad \phi \to A^+ \quad \text{for} \quad t < 0, \tag{3.50}$$

$$H \sim N\phi^{2/5} \quad \text{as} \quad \phi \to +\infty \quad \text{for} \quad t < 0, \tag{3.51}$$

$$H \sim \frac{2}{5B}(\phi - B) \quad \text{as} \quad \phi \to B^+ \quad \text{for} \quad t > 0, \tag{3.52}$$

$$H \sim Q\phi^{2/5} \quad \text{and} \quad \text{as} \quad \phi \to +\infty \quad \text{for} \quad t > 0. \tag{3.53}$$

Using the numerical algorithm outlined in section 3.4 and the default settings in the ODE45 the following values are determined

$$A \approx 0.3859, \;\; B \approx 0.3405 \;\text{ and }\; N = Q \approx 1.0101. \tag{3.54}$$

The same convergence and uniqueness checks were carried out as those in section 3.4.1. A plot of the solution is shown in figure 3.8.

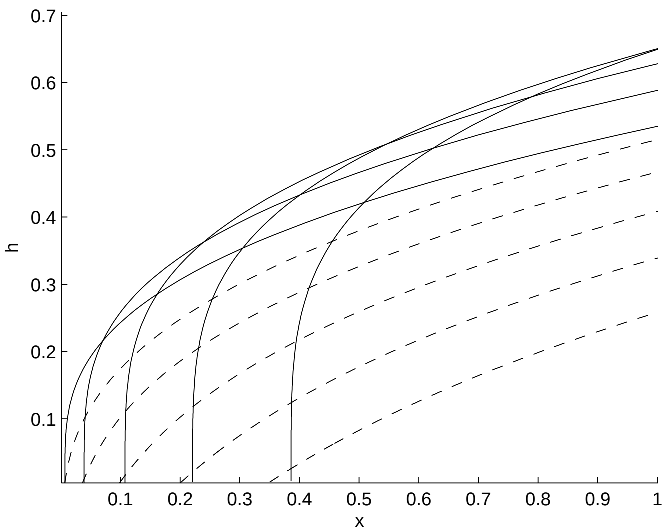

Figure 3.8: Plot of h vs x for equation (3.1) with $m = 4$ and $q = 1$. The solution has been plotted at 10 equally spaced times between $t = -1$ and $t = 1$. The solid curves show the solution for $t < 0$ and the dashed curves for $t > 0$.

3.4.4 Others values of q

It has been shown that there is a similarity reduction to (3.1) capable of describing reversing behaviour (for parameters in the range $m > 0$, $q > 0$ and $m - q > 0$). The work in sections 3.4.1, 3.4.2 and 3.4.3 has demonstrated that this reduction leads to meaningful reversing similarity solutions in the cases; when $m = 3$ and $q = 1$, when $m = 2$ and $q = 1$ and when $m = 4$ and $q = 1$. Further numerical experimentation has indicated that it is also possible to find reversing solutions for all values of $m > 1$ and $q = 1$.

However, whether this is the case for all pairs of values m and q in the range $m > 0$, $q > 0$ and $m - q > 0$ remains an open question. Hence, this section discusses the practicalities of finding solutions to the ODEs (3.18) and (3.31) that satisfy the condition of continuity across $t = 0$ when $q \neq 1$.

This question is explored by setting $m = 3$ and allowing q to increase above 1. Carrying out the numerical scheme outlined in section 3.4 has revealed that when $1 < q < q_3$ (where $q_3 \approx 1.1$) it is possible to find solutions to (3.18) and (3.31) with non-zero values of the parameters A and B and with $Q = N$ in the far field. Hence, this leads to solutions that describe reversing behaviour of solutions to (3.1), see figure 3.9. However, when $q > q_3$ it appears that the value of $B = 0$, and hence the only solution to the problem for $t > 0$ is the exact solution (3.19), see

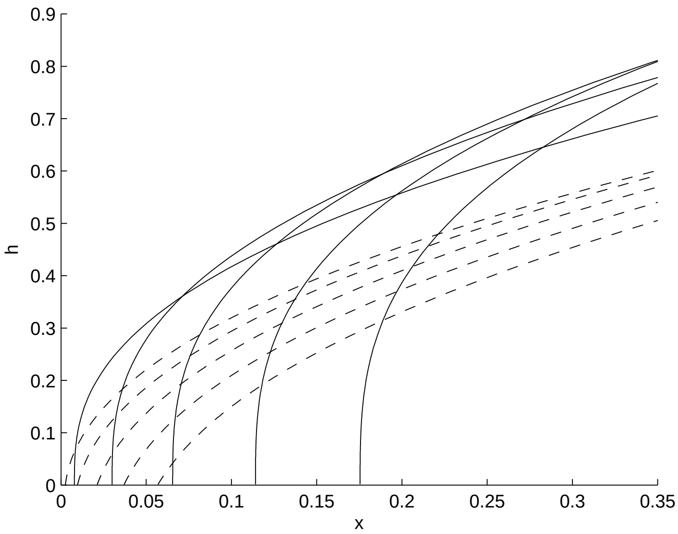

Figure 3.9: Plot of h vs x for equation (3.1) with $m = 3$ and $q = 1.05$. The solution has been plotted at 10 equally spaced times between $t = -1$ and $t = 1$. The solid curves show the solution for $t < 0$ and the dashed curves for $t > 0$.

figure 3.10. Furthermore, it is not possible to find a solution to (3.18) that satisfies the condition of continuity across $t = 0$ (i.e. it is not possible to find solutions with $Q = N$). Therefore it is conjectured, but not proven, that the self-similar solution ceases to exist for $q > q_3$.

Other interesting behaviour has been observed by holding $m = 3$ and decreasing q below 1. In this case it appears that the only solution to (3.18) is the exact solution (3.19). Furthermore, when carrying out the numerical scheme outlined in section 3.4 it has not been possible to find a solution to (3.31) with $Q = N$ and a non-zero value of B. Therefore it is conjectured, but not proven, that the self-similar solution ceases to exist for $q < 1$.

Further numerical experimentation has been carried out for values of $m \neq 3$. It appears that the lack of solutions for $q < 1$ is generic for all values of m. It also appears that for any given value of m there is a critical value of q, $q_m > 1$ say, such that if $q > q_m$ then the self-similar solution does not exist. Note that these conjectures are based on numerical evidence and as such do not constitute rigorous proofs. Why this set of values, q_m, are critical in determining the behaviour of solutions close to a reversing time is an interesting and open question.

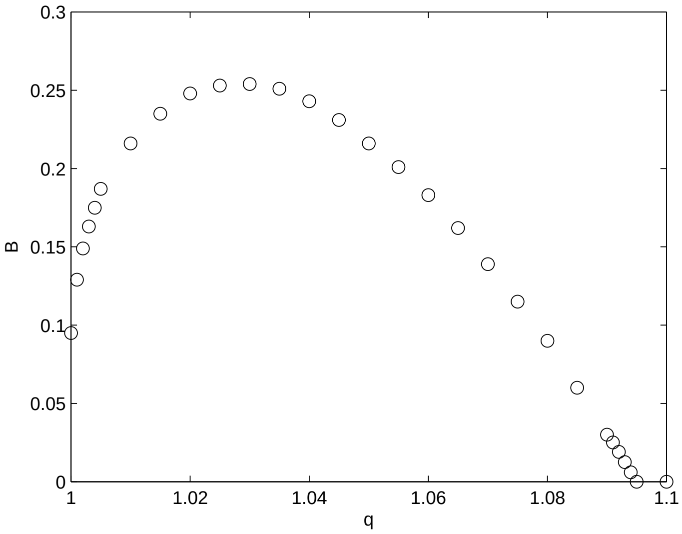

Figure 3.10: Plot of B vs q for $m = 3$.

3.5 Discussion and conclusions

This study has been concerned with solutions to the family of equations (3.1) with $m > 0$, $q > 0$ and $m - q > 0$. These restrictions were placed on the exponents m and q to ensure that the fronts of the solution travel with a finite velocity, that receding fronts can exist, that an advancing front moves due to diffusion and that a receding front moves due to drainage. In particular, solutions to these equations local to the front and local to the reversing time have been examined. By doing this, an analytical explanation of how a front reversal occurs has been given. To do this, self-similar reductions were made to the governing equation (3.1) to derive ODEs for the dependent self-similar variable, H, as a function of ϕ. The analysis was split into two parts, one for the solution prior to the reversing time and the other for the solution after the reversing time. In each case the asymptotic behaviour of solutions as $H \to 0^+$ and as $\phi \to +\infty$ were studied. A numerical algorithm which made use of the determined asymptotic behaviours was then put forward as a method for furnishing solutions to (3.1) local to $x = 0$ and $t = 0$. This algorithm was then demonstrated using the examples of $m = 3$ and $q = 1$, $m = 2$ and $q = 1$, and $m = 4$ and $q = 1$. Finally, some remarks have been made on the existence and practicalities of finding solutions for any pair of values of m and q in the range under consideration.

In section 3.2 the solution prior to the reversing time was studied. By making a self-similar reduction to the governing equation a second order nonlinear ODE was derived for the dependent self-similar variable H. By studying the asymptotic behaviours of this ODE as $\phi \to A^+$ and as $\phi \to +\infty$ it was demonstrated that close to the front the solution takes the form

$$h(x,t) \sim \left(\frac{m+q}{2q}Am\right)^{1/m} (-t)^{(m-q)/2mq} \left(x - A(-t)^{(m+q)/2q}\right)^{1/m}$$

$$\text{as} \quad x \to A(-t)^{(m+q)/2q}. \tag{3.55}$$

For large negative time this has the form of a travelling wave, with velocity proportional to $t^{(m-q)/2q}$. From (3.55) it can also be seen that h increases proportional to $x^{1/m}$ close to this front. It was also shown that the far field behaviour of the solution is

$$h(x,t) \sim Nx^{2/(m+q)} \quad \text{as} \quad x|t|^{-(m+q)/2q} \to +\infty. \tag{3.56}$$

Hence, local to the reversing time and close to, but away from, the front the solution is stationary with behaviour proportional to $x^{2/(m+q)}$.

In section 3.3 the solution after the reversing time was studied. In a similar fashion to section 3.2, a self-similar reduction was made to the governing equation. By studying the asymptotic behaviour of solutions as $\phi \to B^+$ and as $\phi \to +\infty$ it was shown that close to the front

$$h(x,t) \sim \left(\frac{m+q}{2q^2}B\right)^{-1/q} t^{-(m-q)/2q^2} \left(x - Bt^{(m+q)/2q}\right)^{1/q}$$

$$\text{as} \quad x \to Bt^{(m+q)/2q}. \tag{3.57}$$

It can again be seen that for large positive time this takes the form of a travelling wave with velocity proportional to $t^{(m-q)/2q}$. Also, the concentration, h, close to the front increases proportional to $x^{1/q}$. It was shown that the far field solution necessarily took the same form as the solution prior to the reversing time, that is, proportional to $x^{2/(m+q)}$. Furthermore, so that the concentration, h, was continuous as t passed through zero, the constant of proportionality was chosen so that the far field behaviour was the same as that prior to the turning time.

In section 3.4 knowledge of the aforementioned asymptotic behaviours was used in order to formulate a numerical algorithm to furnish meaningful solutions to (3.1). This algorithm was demonstrated using the examples of (3.1) with $m = 3$ and $q = 1$, $m = 2$ and $q = 1$, and $m = 4$ and $q = 1$. In section 3.4.4 the practicalities of finding solutions for all pairs of values of m and

q in the range of interest were considered. Based on numerical evidence it has been conjectured that the self-similar solution proposed in this study does not exist when $q < 1$. Furthermore, for each value of m, there exists a q, q_m say, such that for $q > q_m$ the self-solution does not exist. For $m = 3$, numerical evidence suggests the $q_3 \approx 1.1$, see figure 3.10. An interesting and open question exists as to why these values, q_m, are critical in determining the behaviour of solutions close to a reversing time.

Attention is also drawn to another notable result from the analysis that applies to any equation of the form (3.1) with $q = 1$. It appears that there is only one form of reversing behaviour for each value of m. Note that the asymptotic forms (3.20), (3.21), (3.32) and (3.38) depend only on the values of m, A, B, N, Q and Q_2. Numerical evidence suggests that all these values are uniquely determined for any given equation in the family (3.1) with $q = 1$. In other words, so long as the solution exhibits a reversing of a front at some time in its evolution, the solution local to this front and local to the reversing time is generic.

Finally, the author discusses the implication of the results in the context of the physical problem, the spreading of a viscous film under gravity and subject to evaporation. It has been shown that the behaviour near the front changes dramatically as t passes through zero. In particular the slope at the front is infinite before $t = 0$ and finite after $t = 0$. While the position of the front is quadratic in time, the quadratic coefficient changes as t passes through zero. Any numerical scheme that attempts to solve (3.1) must capture these non-trivial changes. Therefore, equations (3.55), (3.56) and (3.57) provide a way of validating the accuracy of such numerical scheme's accuracy near the front.

Chapter 4

The spreading and draining of viscous films on the surface of a deep viscous pool

In this chapter, a model for the slow spreading and draining of viscous films on the surface of a quiescent deep pool due to gravity is considered. In a similar manner to the analysis in chapter 2, it is assumed that the densities and viscosities of the fluids in the films and pool are comparable and that surface tension effects are negligible. Asymptotic techniques that exploit the slender geometry of the spreading films are employed to analyse the flow. One of the main results from chapter 2, namely, that the dominant forces controlling the spreading are gravity and the tangential stress induced by the underlying pool is shown to apply when the drainage rate is comparable to the vertical component of the fluid velocity in the film. As a consequence, the spreading of the films is independent of their viscosity. The model is systematically reduced to a singular integro-differential equation (SIDE). A special case is then considered in which a steady state exists. This steady state is maintained by balancing the flux of fluid draining from the film with a flux being added at the center of the film. In this special case, a solution to the problem is obtained using a combination of asymptotic and numerical techniques. Finally, some general results on the existence of advancing and receding fronts are derived. The existing literature relevant to this study is discussed in chapters 2 and 3 and so to avoid repetition we proceed directly to formulate the model.

4.1 Problem formulation

The incompressible flow is modelled in the limit of zero Reynolds number by assuming that the fluids in both the films and pool obey the Stokes flow equations. Hence

$$\nabla p = \mu_1 \nabla^2 \mathbf{u} - \rho_1 \mathbf{g}_r \quad \text{and} \quad \nabla \cdot \mathbf{u} = 0 \quad \text{in the pool and} \tag{4.1}$$

$$\nabla p = \mu_2 \nabla^2 \mathbf{u} - \rho_2 \mathbf{g}_r \quad \text{and} \quad \nabla \cdot \mathbf{u} = 0 \quad \text{in the films.} \tag{4.2}$$

Where p is the pressure, $\mathbf{u} = (u, v)$ is the fluid velocity vector, $\mathbf{g}_r = (0, g_r)$ is the acceleration due to gravity, μ_1 and ρ_1 are the viscosity and density of the fluid in the pool and μ_2 and ρ_2 are the viscosity and density of the fluid in the spreading films. As shown in figure 4.1 the surfaces at the top of the films and the top of the pool, denoted by $y = h(x,t)$ and $y = f(x,t)$ respectively, are both assumed to be stress free and evolve as material surfaces. Hence,

$$\mathbf{n}_h' \mathbf{T} \mathbf{n}_h = \mathbf{t}_h' \mathbf{T} \mathbf{n}_h = 0 \quad \text{and} \quad \frac{D}{Dt}(y - h) = 0 \quad \text{on} \quad y = h(x,t) \tag{4.3}$$

and

$$\mathbf{n}_f' \mathbf{T} \mathbf{n}_f = \mathbf{t}_f' \mathbf{T} \mathbf{n}_f = 0 \quad \text{and} \quad \frac{D}{Dt}(y - f) = 0 \quad \text{on} \quad y = f(x,t). \tag{4.4}$$

Where $\mathbf{T}$ is the stress tensor (defined in the usual way), $\mathbf{n}_f$, $\mathbf{t}_f$, $\mathbf{n}_h$ and $\mathbf{t}_h$ are the unit vectors normal and tangential to the surfaces $y = f(x,t)$ and $y = h(x,t)$ respectively, a prime denotes the usual vector transpose operation and D/Dt is the material derivative with respect to the fluid velocity. Across the interfaces between the films and pool, denoted by $y = g(x,t)$, stresses are continuous. Due to the drainage normal to this surface a modified kinematic condition and conditions of conservation of mass are imposed. Hence,

$$[\mathbf{n}_g' \mathbf{T} \mathbf{n}_g] = [\mathbf{t}_g' \mathbf{T} \mathbf{n}_g] = 0, \quad \frac{D}{Dt}(y - g) = -d,$$

$$[\mathbf{u} \cdot \mathbf{t}_g] = 0 \quad \text{and} \quad g_t + [\mathbf{u} \cdot \mathbf{n}_g] = 0 \quad \text{on} \quad y = g(x,t). \tag{4.5}$$

Here $\mathbf{n}_g$ and $\mathbf{t}_g$ are unit vectors normal and tangential to the surface $y = g(x,t)$, square brackets denote the jump in the enclosed quantity across the surface $y = g(x,t)$ and d is the drainage velocity normal to the surface $y = g(x,t)$. As a result of the lack of externally driven flows, it is imposed that the velocity of the fluid far from the evolving films vanishes. Specification of

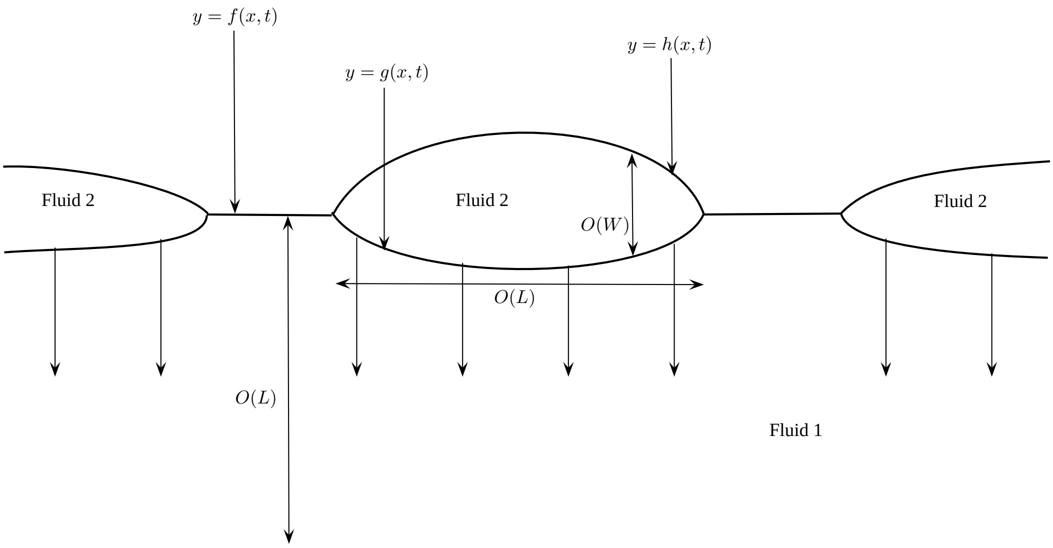

Figure 4.1: A schematic diagram of the flow showing the characteristic length scales.

the initial data completes the problem definition.

The problem is non-dimensionalised in the same way as the model in chapter 2 by setting $x = L\bar{x}$ and $y = W\bar{y}$, where L and W are a typical length and typical depth of the film, $p = \rho_2 g_r W\bar{p}$, $u = u_0\bar{u}$ and $v = \epsilon u_0\bar{v}$. The problem in the pool is non-dimensionalised by setting $x = L\hat{x}$, $y = L\hat{y}$, $p = \rho_2 g_r L\hat{p}$, $u = u_0\hat{u}$ and $v = u_0\hat{v}$ and $t = \mu_2 L\rho_2^{-1} g_r^{-1} W^{-2}\bar{t}$. Here $u_0 = \rho_2 g_r W^2 \mu_2^{-1}$. By scaling in this manner, three dimensionless parameters are introduced that characterise the flow. The ratio of the viscosity and density of the two fluids are denoted by $\mu = \mu_1/\mu_2$ and $\rho = \rho_1/\rho_2$ and the inverse aspect ratio of the film is denoted by $\epsilon = W/L$. Note that in the following analysis the limit that ϵ tends to zero will be taken, and so in the interests of brevity, terms of $O(\epsilon^2)$ and smaller are not shown explicitly. Equations (4.1) and (4.2) become

$$\frac{\partial \hat{p}}{\partial \hat{x}} = \epsilon^2 \mu \frac{\partial^2 \hat{u}}{\partial \hat{x}^2} + \epsilon^2 \mu \frac{\partial^2 \hat{u}}{\partial \hat{y}^2}, \quad \frac{\partial \hat{p}}{\partial \hat{y}} = \epsilon^2 \mu \frac{\partial^2 \hat{v}}{\partial \hat{x}^2} + \epsilon^2 \mu \frac{\partial^2 \hat{v}}{\partial \hat{y}^2} - \rho \quad \text{and} \quad \frac{\partial \hat{u}}{\partial \hat{x}} + \frac{\partial \hat{v}}{\partial \hat{y}} = 0 \tag{4.6}$$

in the pool and

$$\epsilon \frac{\partial \bar{p}}{\partial \bar{x}} = \epsilon^2 \frac{\partial^2 \bar{u}}{\partial \bar{x}^2} + \frac{\partial^2 \bar{u}}{\partial \bar{y}^2}, \quad \frac{\partial \bar{p}}{\partial \bar{x}} = \epsilon^3 \frac{\partial^2 \bar{v}}{\partial \bar{x}^2} + \epsilon \frac{\partial^2 \bar{v}}{\partial \bar{y}^2} - 1 \quad \text{and} \quad \frac{\partial \bar{u}}{\partial \bar{x}} + \frac{\partial \bar{v}}{\partial \bar{y}} = 0 \tag{4.7}$$

in the films. In non-dimensional variables the boundary conditions (4.3) on $y = h(x,t)$ become

$$\bar{p} + 2\epsilon\left(\frac{\partial\bar{h}}{\partial\bar{x}}\frac{\partial\bar{u}}{\partial\bar{y}} - \frac{\partial\bar{v}}{\partial\bar{y}}\right) + O(\epsilon^2) = 0, \tag{4.8}$$

$$\frac{\partial\bar{u}}{\partial\bar{y}} + O(\epsilon^2) = 0 \tag{4.9}$$

$$\frac{\partial\bar{h}}{\partial\bar{t}} + \bar{u}\frac{\partial\bar{h}}{\partial\bar{x}} = \bar{v}. \tag{4.10}$$

On the interfaces between the films and the pool, $y = g(x,t)$, the jump conditions become

$$\epsilon\bar{p} = \hat{p} + O(\epsilon^2), \tag{4.11}$$

$$\frac{\partial\bar{u}}{\partial\bar{y}} = \epsilon\bar{\mu}\left(\frac{\partial\hat{u}}{\partial\hat{x}} + \frac{\partial\hat{v}}{\partial\hat{y}}\right) + O(\epsilon^2) \tag{4.12}$$

$$\frac{\partial\bar{h}}{\partial\bar{t}} + \bar{u}\frac{\partial\bar{h}}{\partial\bar{x}} = \bar{v} - \bar{d} \tag{4.13}$$

$$\bar{u} = \hat{u} + \epsilon\frac{\partial\bar{g}}{\partial\bar{x}}\hat{v} + O(\epsilon^2)$$

$$\epsilon(\rho - 1)\frac{\partial\bar{g}}{\partial\bar{t}} + \rho\left(\hat{v} - \epsilon\frac{\partial\bar{g}}{\partial\bar{x}}\hat{u}\right) + \epsilon\left(\bar{v} - \frac{\partial\bar{g}}{\partial\bar{x}}\bar{u}\right) = 0. \tag{4.14}$$

Where $\bar{d} = \mu_2 L \rho_2^{-1} g_r^{-1} H^{-3} d$ so that the drainage rate is $O(\epsilon u_0)$. Finally, on the free surface of the pool, $y = f(x,t)$ the boundary conditions become

$$\hat{p} + O(\epsilon) = 0, \tag{4.15}$$

$$\frac{\partial\hat{u}}{\partial\hat{y}} + O(\epsilon) = 0. \tag{4.16}$$

Note that the boundary conditions in (4.16) only apply along the surface $y = f(x,t)$ (or in the scaled coordinate system $\hat{y} = 0$) in regions where both $h(x,t)$ and $g(x,t)$ are both zero. In the regime that the spreading films are sufficiently slender, $\epsilon \ll 1$, therefore the flow is considered in the distinguished limit that ϵ tends to zero. In this limit the parameters μ and ρ are taken to be $O(1)$, so that the subsequent analysis is relevant to situations where the viscosities and densities of the pool and films are comparable. Following the analysis in chapter 2 regular asymptotic expansions of the dependent variables are made in the small parameter, ϵ, of the form

Region 1:	Region 2:
$\hat{u} \sim \hat{u}_0 + \epsilon \hat{u}_1 + \cdots$	$\bar{u} \sim \bar{u}_0 + \epsilon \bar{u}_1 + \cdots$
$\hat{v} \sim \hat{v}_0 + \epsilon \hat{v}_1 + \cdots$	$\bar{v} \sim \bar{v}_0 + \epsilon \bar{v}_1 + \cdots$
$\hat{p} \sim \hat{p}_0 + \epsilon \hat{p}_1 + \cdots$	$\bar{p} \sim \bar{p}_0 + \epsilon \bar{p}_1 + \cdots$
$\hat{g} \sim -\epsilon g_0 - \epsilon^2 g_1 + \cdots$	$\bar{g} \sim -g_0 - \epsilon g_1 + \cdots$
$\hat{h} \sim \epsilon h_0 + \epsilon^2 h_1 + \cdots$	$\bar{h} \sim h_0 + \epsilon h_1 + \cdots$
$\hat{f} \sim \epsilon f_0 + \epsilon^2 f_1 + \cdots$	

The problem for the flow in the films can then be analysed at lowest order in ϵ. Integrating equations (4.7) and imposing that to lowest order in ϵ there is zero normal stress on $y = h(x,t)$, zero tangential stress on either $y = g(x,t)$ or $y = h(x,t)$, continuity of mass tangential to the interface $y = g(x,t)$ and using the kinematic conditions on both $y = g(x,t)$ and $y = h(x,t)$ it can be shown that the pressure in the films is hydrostatic and

$$(g_0 + h_0)\frac{\partial h_0}{\partial \bar{t}} + \frac{\partial}{\partial \bar{x}}\left((g_0 + h_0)\hat{u}_0(\hat{x}, 0, \hat{t})\right) = -\bar{d}. \tag{4.17}$$

This is the equation of conservation of mass in the spreading films (with the addition of a source/sink term and driven at a velocity $\hat{u}_0(\hat{x}, 0, \hat{t})$). Due to the degenerate nature of the tangential stress conditions on the top and bottom fronts of the films (at lowest order in ϵ) it is not possible to close the problem for finding the lowest order evolution of the films. Therefore, a solvability condition is sought by studying the equations governing the flow in the films at first order in ϵ. Integration of the first equation in (4.7) (at first order in ϵ) and imposing that there is zero tangential stress on $y = h(x,t)$ and that stress is continuous across $y = g(x,t)$ it can be shown that

$$(g_0 + h_0)\frac{\partial h_0}{\partial \bar{x}} + \mu \frac{\partial \hat{u}_0}{\partial \hat{y}}(\hat{x}, 0, \hat{t}) = 0. \tag{4.18}$$

This equation is a balance of forces acting on a film in the horizontal direction. The first term in (4.18) represents the effect of gravity, and the second term represents the tangential stress induced in the film by the underlying pool. Equations (4.17) and (4.18) are two relationships between the four quantities g_0, h_0, $\hat{u}(\hat{x}, 0, \hat{t})$ (the interfacial velocity) and $\partial \hat{u}/\partial \hat{y}(\hat{x}, 0, \hat{t})$ (the interfacial tangential stress). In order to derive two further relationships between these four quantities the problem for the flow in the pool is explored.

Balancing equations (4.6) - (4.14) at lowest order in ϵ shows that

$$\hat{p}_0 = -\hat{y}, \tag{4.19}$$

i.e. the leading order pressure in the pool is hydrostatic. In a similar manner to the analysis in chapter 2, a first order balance of the equations for the flow in the pool gives rise to a relation consistent with Archimedes' principle

$$h_0 = (\rho - 1)g_0. \tag{4.20}$$

Note that equation (4.20) may also be derived physically by applying Archimedes' principle to a infinitesimally thin vertical *slice* of a spreading film. In order to derive a fourth relation between g_0, h_0, the interfacial velocity and the interfacial tangential stress the equations (4.6) - (4.14) are balanced at order ϵ^2. Equation (4.6) is recast in terms of a stream function, ψ, such that

$$\hat{u}_0 = \frac{\partial \psi}{\partial \hat{y}} \quad \text{and} \quad \hat{v}_0 = -\frac{\partial \psi}{\partial \hat{x}}. \tag{4.21}$$

By rewriting equations (4.6), (4.14), (4.15), (4.16), (4.18) and (4.20) in terms of ψ and identifying $s_n(\bar{t})$ and $s_{n+1/2}(\bar{t})$ as the left and right fronts of the n^{th} film (where $g(x,t)$ and $h(x,t)$ both become zero) and $\mathcal{F} = \cup_{n=0}^{n=N}(s_n(\bar{t}), s_{n+1/2}(\bar{t}))$ the following problem is posed.

$$\nabla^4 \psi = 0 \quad \text{for} \quad \hat{x} \in (-\infty, +\infty),\ \hat{y} \in (-\infty, 0) \tag{4.22}$$

with

$$\psi = \frac{\partial \psi}{\partial \hat{y}} = 0 \quad \text{on} \quad \hat{y} = 0 \quad \text{for} \quad \hat{x} \notin \mathcal{F}, \tag{4.23}$$

$$\psi = 0 \quad \text{and} \quad \frac{\partial^2 \psi}{\partial \hat{y}^2} = -\frac{1}{\mu}\left(\frac{\rho}{\rho - 1}\right)\frac{\partial}{\partial \bar{x}}\left(\frac{h_0^2}{2}\right) \quad \text{on} \quad \hat{y} = 0 \quad \text{for} \quad \hat{x} \in \mathcal{F}, \tag{4.24}$$

$$\frac{\partial \psi}{\partial \hat{x}}, \frac{\partial \psi}{\partial \hat{y}} \to 0^+ \quad \text{as} \quad \hat{x} \to \pm\infty \quad \text{and} \tag{4.25}$$

$$\frac{\partial \psi}{\partial \hat{x}}, \frac{\partial \psi}{\partial \hat{y}} \to 0^+ \quad \text{as} \quad \hat{y} \to -\infty. \tag{4.26}$$

In order to solve the problem posed by (4.22) - (4.26) boundary integral techniques are employed. Consider the stream function of a Stokeslet singularity, ψ_s, of unit strength oriented in the direction of positive $\hat{x}$ and positioned at $\hat{x} = x_0$ and $\hat{y} = 0$,

$$\psi_s = -\frac{\hat{y}}{4\pi} \ln \left(|\hat{x} - x_0|^2 + |\hat{y}|^2 \right). \tag{4.27}$$

Provided $x_0 \in \mathcal{F}$, the stream function (4.27) solves satisfies the problem (4.22) - (4.26), except the condition on the interfacial tangential stress (4.24). Therefore, due to the linearity of the problem, a solution to (4.22) - (4.26) may be obtained by finding a superposition of Stokeslet singularities that satisfy (4.24). Since the stream function (4.27) is a stress singularity of unit strength, and the flow in the pool is driven purely by the spreading of the films, the problem may be reduced to the singular integral equation

$$\psi = \lim_{\hat{y} \to 0^-} \int_{\mathcal{F}} \frac{\partial \hat{u}_0}{\partial \hat{y}}(x_0, 0, \hat{t}) \psi_s dx_0 \quad \text{for} \quad x \in \mathcal{F}. \tag{4.28}$$

Taking the derivative of (4.28) with respect to $\hat{y}$ and taking the limit that $\hat{y}$ tends to zero from below yields

$$\hat{u}_0 = \frac{1}{2\pi} \int_{\mathcal{F}} \frac{\partial \hat{u}_0}{\partial \hat{y}}(x_0, 0, \hat{t}) \ln |\bar{x} - x_0| dx_0 \quad \text{for} \quad x \in \mathcal{F}. \tag{4.29}$$

Differentiating (4.29) with respect to $\hat{x}$ yields

$$\frac{\partial \hat{u}_0}{\partial \hat{x}} = \frac{1}{2\pi} \fint_{\mathcal{F}} \frac{\partial \hat{u}_0}{\partial \hat{y}}(x_0, 0, \bar{t}) \frac{1}{\bar{x} - x_0} dx_0 \quad \text{for} \quad x \in \mathcal{F}. \tag{4.30}$$

Integrating equation (4.29) by parts, substituting equations (4.18) and (4.20), and assuming that h_0 tends to zero sufficiently quickly near the fronts $s_n(\bar{t})$ and $s_{n+1/2}(\bar{t})$ yields

$$\hat{u}_0 = \frac{1}{4\pi} \frac{1}{\mu} \frac{\rho}{\rho - 1} \fint_{\mathcal{F}} \frac{h_0(x_0, \bar{t})^2}{\bar{x} - x_0} dx_0 \quad \text{for} \quad x \in \mathcal{F}. \tag{4.31}$$

At this stage in the analysis the problem for the evolution of the spreading films may be formulated either as a set of three coupled equations or as a SIDE. In the interest of algebraic clarity the following changes of variable are made

$$\sigma(\chi, \tau) = 2\mu \frac{\rho - 1}{\rho} \frac{\partial \hat{u}_0}{\partial \hat{y}}(\bar{x}, 0, \bar{t}), \quad D = 4\pi\mu \left(\frac{\rho - 1}{\rho} \right)^2 \bar{d}, \quad \upsilon(\chi, \tau) = 4\pi\mu \frac{\rho - 1}{\rho} \hat{u}_0(\bar{x}, 0, \bar{t}), \tag{4.32}$$

$$\tau = \frac{1}{4\pi\mu} \frac{\rho}{\rho - 1} \bar{t}, \quad \chi = \bar{x}, \quad \chi_0 = x_0, \quad F(\tau) = \mathcal{F}(\bar{t}) \quad \text{and} \quad \eta(\chi, \tau) = h_0(\bar{x}, \bar{t}). \tag{4.33}$$

Using equations (4.17), (4.18), (4.20) and (4.30) the problem for the evolution of the films may be reduced to the the following system of three equations

$$\frac{\partial \eta}{\partial \tau} + \frac{\partial}{\partial \chi}(\upsilon\eta) = -D \quad \text{for} \quad \chi \in F, \tag{4.34}$$

$$\sigma = -\frac{\partial}{\partial \chi}\left(\eta^2\right) \quad \text{for} \quad \chi \in F, \tag{4.35}$$

$$\frac{\partial \upsilon}{\partial \chi} = \fint_F \frac{\sigma(\chi_0, \tau)}{\chi - \chi_0} d\chi_0 \quad \text{for} \quad \chi \in F. \tag{4.36}$$

Alternatively, by substituting (4.20) and (4.31) into (4.17) a SIDE is derived for the evolution of the films

$$\frac{\partial \eta}{\partial \tau} + \frac{\partial}{\partial \chi}\left(\eta\left(\fint_F \frac{\eta(\chi_0, \tau)^2}{\chi - \chi_0} d\chi_0\right)\right) = -D \quad \text{for} \quad \chi \in F. \tag{4.37}$$

4.2 A paradigm problem

In this section a paradigm problem is considered in which there is a single film spreading on the surface of the pool and $D = 1 - 2\delta(\chi)$ (here $\delta(\chi)$ is the Dirac delta function), so that there is a constant rate of drainage from the film, and two units of flux entering the film at $\chi = 0$. Physically, this could correspond to a fluid film being poured onto the surface of a pool at a rate comparable to the rate at which the fluid is draining. The problem is also simplified to studying a steady state that may occur when the mass of fluid draining from the film balances the mass being added at $\chi = 0$. Due to the symmetric nature of the function D, it is assumed that η is an even function and hence σ and υ are odd functions of the spatial coordinate χ. Under the assumption that a steady state exists a simple mass conservation argument may be employed to reveal that the location of the fronts are $s_1(\bar{t}) = -1$ and $s_{3/2}(\bar{t}) = 1$, hence equations (4.34) and (4.37) may be integrated with respect to χ and the locations of the fronts imposed to give

$$\upsilon\eta = 2\mathcal{H}(\chi) - 1 - \chi \quad \text{for} \quad \chi \in F, \tag{4.38}$$

$$\eta\left(\fint_{-1}^{+1} \frac{\eta(\chi_0)^2}{\chi - \chi_0} d\chi_0\right) = 2\mathcal{H}(\chi) - 1 - \chi \quad \text{for} \quad \chi \in F. \tag{4.39}$$

Here $\mathcal{H}$ is the Heaviside step function. Even with these simplifications the problem does not readily admit any exact non-trivial solutions. Hence, a numerical solution to the problem is sought. However, before doing so it is instructive (and, as shall become apparent later, necessary) to examine the points of singular behaviour in the problem asymptotically.

Difficulties arise near the fronts at $\chi = \pm 1$. The source of these difficulties are revealed by introducing $\delta \ll 1$ and rewriting equation (4.31) as

$$\upsilon(\chi) = \fint_{-1}^{1} \frac{\eta(\chi_0)^2}{\chi - \chi_0} d\chi_0 = \fint_{-1}^{1-\delta} \frac{\eta(\chi_0)^2}{\chi - \chi_0} d\chi_0 + \fint_{1-\delta}^{1} \frac{\eta(\chi_0)^2}{\chi - \chi_0} d\chi_0. \tag{4.40}$$

Taking $\chi \in (1-\delta, 1)$ and assuming a power series expansion for η near $\chi = 1$ of the form

$$\eta \sim A(1-\chi)^\alpha \quad \text{as} \quad \chi \to 1^- \tag{4.41}$$

we may write

$$\upsilon(\chi) = \int_{-1}^{1-\delta} \frac{\eta(\chi_0)^2}{\chi - \chi_0} d\chi_0 + A^2 \fint_{1-\delta}^{1} \frac{(1-\chi_0)^{2\alpha}}{\chi - \chi_0} d\chi_0. \tag{4.42}$$

Consider the first integral on the LHS of equation (4.42). On the domain of integration $\eta^2 \geq 0$ and $\chi - \chi_0 > 0$ hence this integral is some positive constant, B say. The second integral on the LHS of equation (4.42) may be computed straightforwardly in the limit that $\chi \to 1^-$ and takes the value $\delta^{2\alpha}/\alpha$ [18]. Hence, in the limit that $\delta \to 0^+$

$$\upsilon(1) = \fint_{-1}^{+1} \frac{\eta(\chi_0)^2}{1 - \chi_0} d\chi_0 = B > 0. \tag{4.43}$$

As $\eta \to 0^+$ near $\chi = 1$ it has been shown that υ tends to some positive constant, B. Hence, an appropriate power series expansion for υ near $\chi = 1$ takes the form

$$\upsilon \sim B \quad \text{as} \quad \chi \to 0^-. \tag{4.44}$$

To determine the asymptotic behaviour of η near this point the asymptotic forms (4.41) and (4.44) are substituted into equation (4.34) to give

$$AB(1-\chi)^\alpha + \cdots = 2\theta(\chi) - 1 - \chi. \tag{4.45}$$

In the limit that $\chi \to 1^-$ the RHS of (4.45) tends to zero linearly, hence $\alpha = 1$ and $A = 1/B$. Using equation (4.36) it is then straightforward to determine a suitable power series expansion for σ near $\chi = 1$. In summary

$$\eta \sim \frac{1}{B}(1-\chi) + \cdots, \quad \upsilon \sim B + \cdots, \quad \sigma \sim \frac{2}{B^2}(1-\chi) + \cdots \quad \text{as} \quad \chi \to 1^-. \tag{4.46}$$

Note that retrospectively it can be seen that the assumption on η (and hence h_0) tending to zero sufficiently quickly near the fronts was justified, see equation (4.30) and the explanation therein. Also note that although an expression for the constant B has been derived, its value cannot be determined until the solution has been computed over $\chi \in (-1, +1)$. Put simply, this is due to the non-local nature of the singular integral operator in (4.37) (or equivalently (4.36)).

By examination, it can be seen that problems occur near $\chi = 0$. By the even properties of the interfacial velocity $v(0) = 0$ and hence, by equation (4.38), η must blow up as χ tends to zero. Therefore, the behaviour of η as $\chi \to 0^+$ is considered. To do this, we take $0 < \chi \ll 1$ and introduce $\delta \ll 1$ but $\chi < \delta$ so that the singularity in the integral operator is *trapped* on the domain $(-\delta, \delta)$. So equation (4.39) may be written as

$$\eta(\chi)\left(\int_{-1}^{-\delta} \frac{\eta(\chi_0)^2}{\epsilon - \chi_0} d\chi_0 + \fint_{-\delta}^{\delta} \frac{\eta(\chi_0)^2}{\chi - \chi_0} d\chi_0 + \int_{\delta}^{1} \frac{\eta(\chi_0)^2}{\chi - \chi_0} d\chi_0\right) = 1 - \chi. \tag{4.47}$$

In the first integral on the LHS of (4.47) the variable of integration is changed from χ_0 to $-\chi_0$, and, in the second integral on the LHS of (4.47) the variable of integration is changed from χ_0 to χp. Hence (4.47) becomes

$$\eta(\chi)\left(\int_{\delta}^{1} \frac{\eta(-\chi_0)^2}{\chi + \chi_0} d\chi_0 + \fint_{-\delta/\chi}^{+\delta/\chi} \frac{\eta(\chi p)^2}{1 - p} dp + \int_{\delta}^{1} \frac{\eta(\chi_0)^2}{\chi - \chi_0} d\chi_0\right) = 1 - \chi. \tag{4.48}$$

Using the even properties of η and changing the integration variable p to $s + 1$ in the second integral in (4.48) leads to

$$h(\chi)\left(2\chi \int_{\delta}^{1} \frac{\eta(\chi_0)^2}{\chi^2 - \chi_0^2} d\chi_0 - \fint_{-\delta/\chi-1}^{+\delta/\chi-1} \frac{\eta(\chi(s+1))^2}{s} ds\right) = 1 - \chi. \tag{4.49}$$

Assuming a power series expansion of η near the $\chi = 0$ leads to contradictions. Therefore, a local expansion of the form

$$\eta \sim A(-\ln|\chi|)^{\alpha} + \cdots \quad \text{as} \quad \chi \to 0^+ \tag{4.50}$$

is sought. Substitution of the assumed asymptotic form (4.50) into (4.49) gives

$$A(-\ln|\chi|)^{\alpha}\left(2\chi \int_{\delta}^{1} \frac{\eta(\chi_0)^2}{\chi^2 - \chi_0^2} d\chi_0 - A^2 \fint_{-\delta/\chi-1}^{+\delta/\chi-1} \frac{(-\ln|\chi(s+1)|^{2\alpha}}{s} ds\right) = 1 - \chi. \tag{4.51}$$

Analysis is now concentrated on the second integral in (4.51),

$$I = \int_{-\delta/\chi-1}^{+\delta/\chi-1} \frac{(-\ln|\chi(s+1)|^{2\alpha}}{s} ds. \tag{4.52}$$

Some algebraic rearrangement gives

$$I = \ln|\chi^{-1}|^{2\alpha} \int_{-\delta/\chi-1}^{+\delta/\chi-1} \frac{1}{s}\left(1 - \frac{\ln|(s+1)|}{\ln|\chi^{-1}|}\right)^{2\alpha} ds. \tag{4.53}$$

Since $\chi \ll 1$, $\ln|\chi^{-1}| \gg 1$ the parenthesis in (4.53) are expanded and the largest two terms retained

$$\begin{aligned} I &\approx (-\ln|\chi|)^{2\alpha} \int_{-\delta/\chi-1}^{+\delta/\chi-1} \frac{1}{s}\left(1 - 2\alpha\frac{\ln|(s+1)|}{\ln|\chi^{-1}|}\right) ds & (4.54)\\ &= (-\ln|\chi|)^{2\alpha} \int_{-\delta/\chi-1}^{+\delta/\chi-1} \frac{1}{s}\, ds - 2\alpha(-\ln|\chi|)^{-1} \int_{-\delta/\chi-1}^{+\delta/\chi-1} \frac{\ln|(s+1)|}{s} ds & (4.55)\\ &= (-\ln|\chi|)^{2\alpha}\left(-2\chi - \pi^2\alpha(-\ln|\chi|)^{-1}\right). & (4.56) \end{aligned}$$

Replacing this expression in (4.51) yields

$$A(-\ln|\chi|)^{\alpha}\left(2\chi\int_{\delta}^{1} \frac{\eta(\chi_0)^2}{\chi^2-\chi_0^2} d\chi_0 - A^2\left((-\ln|\chi|)^{2\alpha}\left(-2\chi - \pi^2\alpha(-\ln|\chi|)^{-1}\right)\right)\right) \approx 1-\chi. \tag{4.57}$$

In taking the limit that $\chi \to 0^+$ the leading order balance is between

$$A^3\alpha\pi^2(-\ln|\epsilon|)^{3\alpha-1} \sim 1. \tag{4.58}$$

Hence $\alpha = 1/3$ and $A = (\alpha^{-1}\pi^{-2})^{1/3}$. Using equations (4.35) and (4.38) it is straightforward to find the corresponding asymptotic behaviours of υ and σ near $\chi = 0$. In summary

$$\eta \sim \frac{3^{1/3}}{\pi^{2/3}}(-\ln|\chi|)^{1/3} + \cdots, \quad \upsilon \sim \frac{\pi^{2/3}}{3^{1/3}}(-\ln|\chi|)^{-1/3} + \cdots, \quad \sigma \sim \frac{2}{3^{1/3}\pi^{4/3}}\frac{(-\ln|\chi|)^{-1/3}}{\chi} + \cdots \tag{4.59}$$

$$\text{as} \quad \chi \to 0^+.$$

Note that in contrast to the analysis near the fronts at $\chi = \pm 1$ the coefficients of the asymptotic behaviours may be determined exactly. This is due to the symmetric nature of η and hence the cancellation of the integral operator in (4.37) (or equivalently (4.36)) on either side of $\chi = 0$.

Having determined the behaviour of the solution near the singular points the problem may be solved numerically using a collocation method, the details of which are outlined below.

4.2.1 Numerical solution

Before tackling the problem numerically it is recast, exploiting the symmetry of η, and hence avoiding any numerical difficulties that may arise due to the discontinuities associated with the Heaviside function at $\chi = 0$. The integral term in (4.39) is split into the sum of integrals from $\chi_0 = -1$ to 0 and from $\chi_0 = 0$ to 1. By changing the variable of integration over the domain $\chi_0 = -1$ to 0, from χ_0 to $-\chi_0$ the problem may be written as

$$\eta\left(\fint_0^1 \frac{\eta(\chi_0)^2}{\chi-\chi_0}d\chi_0 + \fint_0^1 \frac{\eta(\chi_0)^2}{\chi+\chi_0}d\chi_0\right) = 1-\chi \quad \text{for} \quad \chi \in (0,1). \tag{4.60}$$

An approximate numerical solution to equation (4.60) is now sought by means of a collocation method.

The interval $(0, 1)$ is divided into N equally sized sub-intervals $((i-1)\Delta\chi, i\Delta\chi)$, where $i = 1...N$ and $\Delta\chi = 1/N$. The integral operators in (4.60) are discretised by identifying

$$I_1 = \fint_0^1 \frac{\eta(\chi_0)^2}{\chi-\chi_0}d\chi_0 = \sum_{i=1}^{i=N}\fint_{(i-1)\Delta\chi}^{i\Delta\chi} \frac{\eta(\chi_0)^2}{\chi-\chi_0}d\chi_0, \tag{4.61}$$

$$I_2 = \int_0^1 \frac{\eta(\chi_0)^2}{\chi+\chi_0}d\chi_0 = \sum_{i=1}^{i=N}\int_{(i-1)\Delta\chi}^{i\Delta\chi} \frac{\eta(\chi_0)^2}{\chi+\chi_0}d\chi_0. \tag{4.62}$$

Bearing in mind the determined asymptotic behaviours, (4.46) and (4.59), η is approximated as a piece-wise linear function on each subinterval, except the interval $(0, \Delta\chi)$ where η^2 is approximated as $\bar{\eta}_1(-\log\chi)^{2/3}$. By assigning the values of η^2 at the mid-points of each subinterval as $\bar{\eta}_i$ respectively the integral operators I_1 and I_2 may be written as

$$I_1 = \bar{\eta}_1\fint_0^{\Delta\chi} \frac{(-\log\chi_0)^{2/3}}{\chi-\chi_0}d\chi_0 + \sum_{i=2}^{i=N}\bar{\eta}_i\fint_{(i-1)\Delta\chi}^{i\Delta\chi}\frac{1}{\chi-\chi_0}d\chi_0$$

$$= \bar{\eta}_1\fint_0^{\Delta\chi} \frac{(-\log\chi_0)^{2/3}}{\chi-\chi_0}d\chi_0 + \sum_{i=2}^{i=N}\bar{\eta}_i\log\left|\frac{\chi-(i-1)\Delta\chi}{\chi-i\Delta\chi}\right|, \tag{4.63}$$

$$I_2 = \bar{\eta}_1\int_0^{\Delta\chi} \frac{(-\log\chi_0)^{2/3}}{\chi+\chi_0}d\chi_0 + \sum_{i=2}^{i=N}\bar{\eta}_i\int_{(i-1)\Delta\chi}^{i\Delta\chi}\frac{1}{\chi+\chi_0}d\chi_0$$

$$= \bar{\eta}_1 \int_0^{\Delta\chi} \frac{(-\log\chi_0)^{2/3}}{\chi+\chi_0} d\chi_0 + \sum_{i=2}^{i=N} \bar{\eta}_i \log\left|\frac{\chi+i\Delta\chi}{\chi+(i-1)\Delta\chi}\right|. \tag{4.64}$$

Due to the form of the integrand on the first subinterval, $(0, \Delta\chi)$, values for these terms must be computed numerically using, for example, the quadgk or Hilbertf routines in MATLAB. By evaluating these expressions at each point $\chi = (j-1/2)\Delta\chi$ (for $j = 1...N$) the problem may be written as a system of N nonlinear equations of the form

$$\boldsymbol{\eta}^{1/2} (\mathbf{I_1}\,\boldsymbol{\eta} + \mathbf{I_2}\,\boldsymbol{\eta}) = \mathbf{1} - \boldsymbol{\chi}. \tag{4.65}$$

Where $\boldsymbol{\eta} = (\eta_1, ..., \eta_N)$, $\mathbf{1} = (1, ..., 1)$ and $\boldsymbol{\chi} = (\Delta\chi/2, ..., (N-1/2)\Delta\chi)$ are vectors of length N. Note that the power notation in (4.65) is to be understood in an element-wise sense. $\mathbf{I_1}$ is a $N \times N$ matrix with entries

$$\mathbf{I_1} = \int_0^{\Delta\chi} \frac{(-\log\chi_0)^{2/3}}{(j-1/2)\Delta\chi+\chi_0} d\chi_0 \quad \text{for} \quad i = 1, \forall j,$$

$$\mathbf{I_1} = \log\left|\frac{(j-i+1/2)}{(j-i-1/2)}\right| \quad \text{for} \quad i \neq 1, \forall j. \tag{4.66}$$

Whilst $\mathbf{I_2}$ is a $N \times N$ matrix with entries

$$\mathbf{I_2} = \int_0^{\Delta\chi} \frac{(-\log\chi_0)^{2/3}}{(j-1/2)\Delta\chi+\chi_0} d\chi_0 \quad \text{for} \quad i = 1, \forall j,$$

$$\mathbf{I_2} = \log\left|\frac{(i+j-1/2)}{(i+j-3/2)}\right| \quad \text{for} \quad i \neq 1, \forall j. \tag{4.67}$$

By rearranging the equations (4.65) in the form

$$\boldsymbol{\eta} = F(\boldsymbol{\eta}) = \boldsymbol{\eta}^{1/2} (\mathbf{I_1}\,\boldsymbol{\eta} + \mathbf{I_2}\,\boldsymbol{\eta}) - \mathbf{1} + \boldsymbol{\chi} + \boldsymbol{\eta}, \tag{4.68}$$

a direct iteration scheme may be applied with a relaxation coefficient λ of the form

$$\boldsymbol{\eta}_{n+1} = \boldsymbol{\eta}_n + \lambda(\boldsymbol{\eta}_n - F(\boldsymbol{\eta}_n)). \tag{4.69}$$

Carrying out the numerical scheme outlined above yields the result in figure 4.2. The solution was computed with $N = 100$ and a relaxation coefficient $\lambda = 10^{-4}$. As a test on the convergence of the result computations were also carried out with other values of N. Provided $N > 50$ there

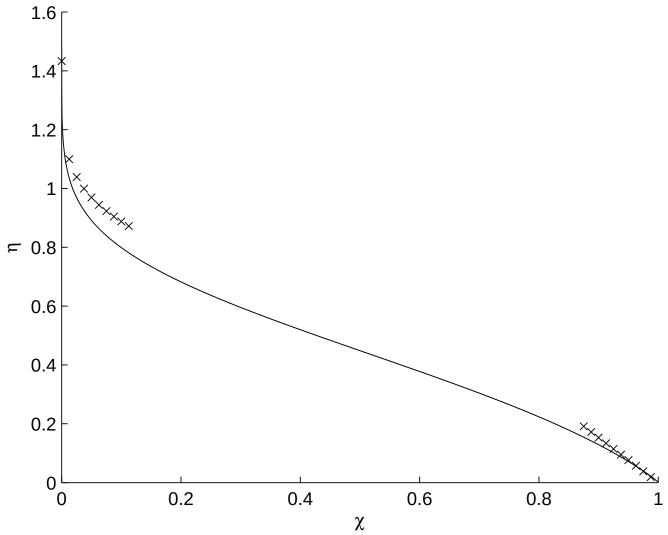

Figure 4.2: A steady solution to (4.37) with $D = 1-2\delta(\chi)$. The solid curve shows the numerical solution and the crosses show the asymptotic behaviours (4.46) and (4.59).

were no appreciable changes in the solution. The numerical solution was also robust to changes in the initial guess $\boldsymbol{\eta}_0$. The result shown in figure 4.2 was computed with $\boldsymbol{\eta}_0 = \mathbf{1} - \mathbf{x}$ and took approximately $10,000$ iterations to converge.

4.3 Advancing and receding travelling waves

In section 4.2, a special case was considered in which a steady state solution to (4.37) existed. In general, solutions to (4.37) may exhibit behaviour in which the fronts of the solution may advance and/or recede (in the sense introduced in chapter 3). It is therefore instructive to examine travelling wave solutions local to a moving front. For simplicity, our interest is restricted to cases in which the drainage rate is related to the film depth by a power law by putting $D = \eta^{1-q}$ with q a constant (this unorthodox notation is used in the interests of consistency with the analysis in chapter 3). Note that most physically motivated examples will give rise to a drainage term of this form. For simplicity the case when there is one spreading film, with a left front at position $\chi = s_1(\bar{t}) = L(\tau)$, and a right front at position $\chi = s_{3/2}(\bar{t}) = R(\tau)$ is studied. In this case equations (4.34) - (4.37) become

$$\frac{\partial \eta}{\partial \tau} + \frac{\partial}{\partial \chi}(\upsilon \eta) = -\eta^{1-q} \quad \text{for} \quad \chi \in (L(\tau), R(\tau)), \tag{4.70}$$

$$\sigma = -\frac{\partial}{\partial \chi}\left(\eta^2\right) \quad \text{for} \quad \chi \in (L(\tau), R(\tau)), \tag{4.71}$$

$$\frac{\partial \upsilon}{\partial \chi} = \fint_L^R \frac{\sigma(\chi_0, \tau)}{\chi - \chi_0} d\chi_0 \quad \text{for} \quad \chi \in (L(\tau), R(\tau)), \tag{4.72}$$

and

$$\frac{\partial \eta}{\partial \tau} + \frac{\partial}{\partial \chi}\left(\eta\left(\fint_L^R \frac{\eta(\chi_0, \tau)^2}{\chi - \chi_0} d\chi_0\right)\right) = -\eta^{1-q} \quad \text{for} \quad \chi \in (L(\tau), R(\tau)). \tag{4.73}$$

In order to examine advancing and receding solutions local to a moving front the behaviour of the solution as $\chi \to R(\tau)^-$ is studied. To do so a local solution of the form

$$\eta \sim A(R-\chi)^\alpha\,, \quad \upsilon \sim B(R-\chi)^\beta \quad \text{and} \quad \sigma \sim G(R-\chi)^\gamma \quad \text{as} \quad \chi \to R^-, \tag{4.74}$$

is sought. Here A, B, G, α, β and γ are constants and $\alpha > 0$ so that $\eta(R(\tau), \tau) = 0$.

4.3.1 Advancing waves

In chapter 3, it was shown that the motion of an advancing front is driven by diffusive effects and conversely a receding travelling wave is driven by drainage. On this basis it is assumed that the same result applies in this case, a physically reasonable assumption, and hence an advancing front is governed by a balance between the terms on the LHS of (4.70) (or equivalently (4.37)). Substituting the assumed local behaviours (4.74) into (4.70) it can be seen that the two terms on the LHS of (4.70) have a dominant balance if

$$\beta = 0\,, \quad B = \frac{dR}{d\tau} \quad \text{and} \quad 1 - \alpha q > 0. \tag{4.75}$$

Hence, local to an advancing front, $\partial \upsilon / \partial \chi \sim 0$. Hence, the analysis carried out in section 2.10 can be applied directly to equation (4.72). Therefore

$$\gamma = -1/2. \tag{4.76}$$

Finally, by substituting the assumed asymptotic forms (4.74) into equation (4.71) it is relatively straightforward to see that

$$\alpha = 1/4 \quad \text{and} \quad G = \frac{A^2}{2}. \tag{4.77}$$

In summary

$$\eta \sim A(R-\chi)^{1/4}, \quad \upsilon \sim \frac{dR}{d\tau} \quad \text{and} \quad \sigma \sim \frac{A^2}{2}(R-\chi)^{-1/2} \quad \text{as} \quad \chi \to R^-. \tag{4.78}$$

Note that the undetermined constant A can, in principle, be found using equation (4.71) (or equivalently (4.73)). However, due to the non-local nature of the integral operator, its value depends on the solution over the domain $(L(\tau), R(\tau))$. Hence, its value cannot be determined with a local analysis alone. Note also that the requirement $1 - \alpha q > 0$ (derived in (4.75)) amounts to requiring $q < 4$. This result seems to indicate that either an advancing front may not exist if the effects of drainage are too strong near to the front (i.e. as the $\eta \to 0^+$), or else an advancing front does exist, but its local behaviour is not of the form $\eta \sim A(R-\chi)^{\alpha}$.

4.3.2 Receding waves

The behaviour of solutions local to a receding front is now studied. As discussed in section 4.3.1, the motion of a receding front is driven by drainage, hence a balance between the term on the RHS with the first term on the LHS of equation (4.70) (or equivalently (4.37)) is sought. Substitution of the assumed asymptotic forms (4.74) into (4.70) gives the prerequisite dominant balance provided

$$\alpha = \frac{1}{q}, \quad A = \left(-\frac{1}{q}\frac{dR}{d\tau}\right)^{-1/q} \quad \text{and} \quad \beta > 0 \tag{4.79}$$

so that $\upsilon(R(\tau), \tau) = 0$. Substitution of the asymptotic forms (4.74) into equation (4.72) gives an asymptotic balance provided

$$\gamma = \frac{2-q}{q} \quad \text{and} \quad G = \frac{2}{q}\left(-\frac{1}{q}\frac{dR}{d\tau}\right)^{-2/q}. \tag{4.80}$$

Due to the non-local nature of the integral operator in equation (4.71) (or equivalently (4.73)) it is not possible to determine a value for the exponent $\beta(>0)$ or the constant B. However the result that β must be positive does imply that the fluid velocity at the receding front is zero. In summary

$$\eta \sim \left(-\frac{1}{q}\frac{dR}{d\tau}\right)^{-1/q}(R-\chi)^{1/q} \quad \text{and} \quad \sigma \sim \frac{2}{q}\left(-\frac{1}{q}\frac{dR}{d\tau}\right)^{-2/q}(R-\chi)^{(2-q)/q} \quad \text{as} \quad \chi \to R^-. \tag{4.81}$$

Note that the requirement that $\alpha > 0$ and result (4.79) seems to indicate that a receding front may only exist for $q > 0$, or, if a receding front does it exist, its local behaviour is not of the form $\eta \sim A(R-\chi)^{\alpha}$. Observe the contrast in the behaviour of the interfacial stress near the front as q passes through 2.

Having carried out this local analysis one natural question arises; how does an advancing wave (4.78) give way to a receding wave (4.81). In other words, how does a front reverse? In chapter 3, reversing solutions to the nonlinear PDE that governs the spreading of a viscous film over a flat plate subject to drainage were obtained, see section 3.4.1. The analysis showed that reversing solutions was theoretically possible for $0 < q < 3$. However, in practice it was not possible to find these solution unless $1 < q < q_3$, where $q_3 \approx 1.1$. A similar analysis in this section has shown that it is theoretically possible to find reversing solutions to (4.37) if $0 < q < 4$. Whether this turns out to be possible in practice is an open question that, in order to answer, requires a careful analysis local to a reversing time. In light of the complexity of the analysis carried out in chapter 3 it is anticipated that would be a lengthy process.

4.4 Discussion, conclusions and future work

A systematic derivation has been given for the equations that govern the spreading of several films of viscous fluid on the surface of a deep pool subject to drainage. In the parameter regime of interest, it has been shown that the full model may be reduced to a SIDE (or equivalently a set of three coupled equations) for the films' evolution. It has also been shown that the two dominant forces controlling the spreading are the gravitational force due to the buoyant films, and the shear stress induced on the films by the viscous stress of the deep pool. As a consequence, the resulting reduced equations for the evolution of the spreading films are independent of their viscosity, and only depend on the density of the films and the density and viscosity of the pool on which they float. It has also been shown that the way in which the films float on the surface of the pool is determined by a relationship that is consistent with Archimedes' principle.

In section 4.2, a special case was considered in which a steady state solution to the governing equations existed. A solution to this special problem was obtained using a combination of asymptotic and numerical techniques. At this point, it is relevant to discuss other special cases in which solutions to (4.37) (or equivalently ((4.70) - (4.72)) may be readily obtained. One way to simplify the problem from two independent variables to a single independent variable is to introduce a self-similar coordinate system such that $\eta(\chi, \tau) = \tau N(\phi)$ where $\phi = \chi\tau^{-3}$. Furthermore, one can then readily perform a first integral of the problem by setting the drainage rate proportional to either N or $dN/d\phi$. Another possibility for obtaining further solutions to (4.37) is to consider the Lie Group symmetries of the problem. It is anticipated, though not proven, that a family of other possible self-similar reductions may also exist.

In section 4.3, the behaviour of solutions local to a moving front was considered. It was shown that the existence of both advancing and receding fronts is possible when the drainage rate $D = \eta^{1-q}$ with $0 < q < 4$. The analysis also indicated that if $q < 0$ receding fronts may not exist. Physically this can be understood since if $q < 0$ the effects of drainage (the mechanism driving the front to recede) is weak local to the front. In contrast it was shown that if $q > 4$ then advancing fronts may not exist since the effects of drainage are strong enough to dominate the diffusive effects local to the front.

It is also relevant to discuss how one might approach finding unsteady solutions to (4.37). Aside from the aforementioned special cases it is anticipated that this is, in general, a problem that must be solved numerically. Some of the major challenges inherent in doing so include, dealing with the singular integral operator, and, accurately dealing with the behaviour of the solution close to the moving fronts. In order to overcome these challenges it is first necessary to examine the asymptotic behaviour of the solution close to the moving fronts, and close to any other points of singular behaviour that may exist. The ideas used in section 4.2 and 4.3 form a basis for doing this. Another idea which the author anticipates to be useful is to pose the problem in a coordinate system that can expand or contract in agreement with the compact support of the solution. By doing this the problem can then be solved on a fixed grid rather than an adaptive grid. Usually numerical schemes based on a fixed grid are less intensive computationally.

Lastly, it is also worth discussing interesting behaviours that could be exhibited by full unsteady solutions to (4.37). As was alluded to in section 4.3 it is anticipated that the behaviour of solutions to (4.37) as an advancing front (4.78) gives way to the receding front (4.81) may be of interest. Another interesting question is whether a film may rupture, or whether two films can coalesce. As far as the author is aware there are currently no results on these phenomena and so another potentially fruitful avenue is to seek to prove whether such behaviours can occur.

Chapter 5

Summary and conclusions

This thesis has considered the spreading and draining of films of slowly flowing incompressible viscous fluid. The models were motivated by the industrial float glass process and aimed to gain insight into the spreading of the blanket and foam logs that float on the surface of a pool of molten glass. The ethos of the work was to consider simplified models that allowed analytical progress to be made, yet still retained the essence of the fluid behaviour. The models considered parts of the blanket and logs that were sufficiently melted that their effective viscosity and density were comparable to that of the underlying molten glass pool. Furthermore, it was assumed that both the foam and molten glass phases could be modelled as fluids that obey the Navier-Stokes equations. The interface between the spreading films and pool was modelled as being sharp, and the drainage across this interface was modelling by imposing mass flux and conservation of mass conditions. Since the constituent fluid in the foam is the same as the fluid in the pool on which the films float surface tension effects were assumed to be negligible. In this chapter, a summary of the results of the work in chapters 2, 3 and 4 is given followed by a discussion of how the results of the work were implemented in the context of the industrial float glass process.

In the introductory chapter, a description of the float glass process was given and the need for the development of mathematical models of the blanket and separated logs was discussed. To explore some initial ideas, a paradigm model for the spreading of a viscous film over a flat surface was considered. This model, albeit unphysical, gave an introduction to the mathematical techniques that were used throughout this thesis. This model also served as a simple analogy to the more complex models that were considered in chapters 2, 3 and 4.

In the first technical chapter, a model for the spreading of viscous films on the surface of a deep viscous pool was explored. In this model, the effects of drainage were neglected. Hence, the model examined solely how the spreading of logs interacted with one another and the flow driven in the underlying pool. It was shown that for sufficiently melted logs, the dominant forces controlling the spreading were gravity, and the tangential stress induced in the logs by the molten glass pool. Hence, it was demonstrated that the rate of spreading of the logs is independent of their viscosity, and only depends on the logs density and the viscosity and density of the deep pool. For a symmetric configuration of logs, it was shown that the flow induced in the pool by the spreading foam films acts to push the logs apart. Hence, the distance between adjacent logs increases proportional to $t^{1/3}$. For the special cases of a single log, two symmetric logs and an infinite periodic array of logs an analytic expression for the evolution of the flow was developed. In each of these special cases, it was found that local to any front the thickness of the log was proportional to $x^{1/4}$. This result prompted an investigation into the behaviour of the flow near the front of a log subject to a more general flow. It was shown, that provided the logs are symmetrically arranged on the pool's surface, the thickness of the log (near its front) is proportional to $x^{1/4}$. Although the model in this chapter gave rise to some interesting mathematical problems, and some novel results were derived, it did not gain insight into the effects of drainage.

The next technical chapter considered the spreading of a draining viscous film over a flat surface. The governing Navier-Stokes equations were systematically reduced to a nonlinear diffusion PDE. This result prompted the analysis to be presented in some generality, since the mathematical techniques that were employed also applied to a broad family of PDEs. The inclusion of the effects of drainage into the model was an initial step towards understanding how the rising of bubbles (the effective drainage of the fluid in the logs and blanket) has an impact on the flow in a float glass furnace. The family of PDEs that were studied exhibit an interesting behaviour in which the front of a solution changes its direction of propagation. This corresponds to a film initially spreading then subsequently retreating due to drainage. To this end, an analysis local to the time at which a front reverses was carried out by looking for self-similar solutions that change their direction of propagation. Using a combination of asymptotic and numerical techniques, solutions were found for the special case of a constant rate of drainage. Comments were also made on the more general case when the drainage is related to the film depth by a power law.

The model in the final technical chapter incorporated both the effects of drainage and the interactions of logs via the underlying molten glass pool. Guided by the analysis in the previous chapters, a SIDE was derived for the evolution of the logs on the pool's surface. In agreement with the model considered in chapter 2, it was shown that gravity and the tangential stress of the underlying pool are the dominant forces controlling the spreading, provided; the viscosities and densities of the logs and pool are comparable and that the drainage rate is comparable to the typical vertical component of the fluid velocity in the logs. For the special case of a constant rate of drainage, a steady solution was obtained using a combination of asymptotic and numerical techniques. Finally, to complement the analysis in the previous chapters, solutions local to a travelling front of this SIDE were examined. In agreement with the previous models, it was shown that an advancing front was driven by spreading, and close to the front the thickness of the log is proportional to $x^{1/4}$. It was also shown that, for the case of a constant rate of drainage, the thickness of a log close to a receding front is proportional to x.

To summarise, the models have gained new insight into the fluid dynamic processes that occur in float glass furnaces and have also given rise to novel mathematical results. Although the models are simplistic, they are based on systematic reductions to the Navier-Stokes equations, and so they retain the essence of the fluid behaviour observed in the industrial process that motivated the study.

5.1 Practical implementation

In this final section the implementation and extension of the results from the previous chapters are discussed in the context of the float glass process. In the interests of confidentiality the full details cannot be disclosed, but, it is appropriate to outline the ways in which the results of this thesis are of industrial interest. As discussed in section 1.1, it is of industrial concern to be able to predict the motion of the blanket and logs that exist in float glass furnaces. Previously, an in-house numerical code had been developed at the Pilkington Technical Centre to solve for the bulk flow in a float glass furnace. However, due to the complex nature of the physics of the blanket and logs (as described in section 1.1) their numerical treatment was either crude (and hence unrealistic) or else was based on solutions to the full Navier-Stokes equations (and hence very computationally expensive). To this end, it was of great interest to develop a simplified model that could accurately replicate the movement of the blanket and logs without requiring a lengthy compute time.

The models in the previous chapters have all been based on the assumption that the viscosity of the fluid in the films is comparable to the viscosity of the pool on which they float. As such, they are appropriate for describing the evolution of the blanket and logs when they have been melted sufficiently that their effective viscosity is comparable to the viscosity of the molten glass pool. However, this assumption is invalid when the blanket is relatively cool (and hence viscous), or when the blanket consists of solid grains. In the latter case, it is not obvious if the blanket can be appropriately modelled using the Navier-Stokes equations rather than a granular flow model.

The models in chapters 2 and 4 were extended to allow the blanket to be treated as a fluid, with a temperature dependent viscosity, and to incorporate situations in which the floating films (blanket and logs) can be much more viscous than the underlying pool. In this case a system of three equations relating; the depth of the film above the pool surface, the depth of the film below the pool surface, the interfacial stress and the interfacial velocity could be derived. These three equations are conservation of mass, Archimedes' principle and a relationship between the dominant horizontal forces acting on the films. Using the notation introduced in chapter 4 the three equations are

$$(g_0 + h_0)\frac{\partial h_0}{\partial \bar{t}} + \frac{\partial}{\partial \bar{x}}\left((g_0 + h_0)\hat{u}_0(\hat{x}, 0, \hat{t})\right) = -\bar{d}, \tag{5.1}$$

$$h_0 = (\rho - 1)g_0, \tag{5.2}$$

$$(g_0 + h_0)\frac{\partial h_0}{\partial \bar{x}} + \frac{\partial \hat{u}_0}{\partial \hat{x}}(\hat{x}, 0, \hat{t}) = \frac{4\epsilon}{\mu}\left((g_0 + h_0)\frac{\partial \hat{u}_0}{\partial \hat{x}}(\hat{x}, 0, \hat{t})\right). \tag{5.3}$$

Here $\mu = \mu_1/\mu_2$, is the ratio of viscosities of the pool and films and $\bar{d}$ is the dimensionless drainage rate. In general, both μ and $\bar{d}$ can be functions of space, time, temperature and any of the other physical parameters of the flow. Equation (5.3) can be interpreted as a force balance (analogous to that seen in section 1.2.2) between the effects of gravity (represented by the first term on the left-hand side), the shear stress induced by the underlying pool (represented by the second term on the left-hand side) and the resistance due to extensional forces (represented by the term on the right-hand side). The factor of 4 on the RHS of (5.3) arises as a Trouton viscosity [33]. Note that in the case where $\mu = O(1)$, equation (5.3) reduces to the same dominant horizontal force balance derived in chapters 2 and 4 (see equations (2.18) and (4.18)). The problem of finding g_0, h_0, $\hat{u}_0(\hat{x}, 0, \hat{t})$ and $\partial\hat{u}_0/\partial\hat{y}(\hat{x}, 0, \hat{t})$ is closed by coupling the system of equations (5.1) - (5.3) to the problem for the bulk flow in the molten glass pool in the furnace.

The equations (5.1) - (5.3) have been derived by considering the flow in the blanket and logs in the limit that the inverse aspect ratio of the films tends to zero. As a consequence, they depend on only one spatial coordinate that varies along the flat top surface of the underlying pool. Hence, when these equations are coupled to the problem for the flow in the underlying pool, they appear as conditions along the pool's top surface. This means that the geometry in which the problem for the flow in the pool must be solved is a rectangle. This makes the numerical simulation of the flow in the pool far simpler than if one was to attempt to find a solution using an unsimplified model, and then resolve the position of the interfaces between the films and pool numerically. Hence, this simplified model has the benefit of significantly reducing the computation time. However, the model still retains the essence of the fluid dynamic behaviour. It is noted that the model discussed in this section is currently actively used by the modelling group at the Pilkington Technical Centre to make predictions regarding the dynamics of the blanket and logs in their glass furnaces.

Bibliography

[1] M. Abramowitz and I. Stegun. *Handbook of Mathematical Functions.* Dover Publications, 1965.

[2] D. J. Acheson. *Elementary Fluid Dynamics.* Oxford University Press, 1990.

[3] J. M. Acton, H. E. Huppert and M. G. Worster. Two dimensional viscous gravity currents flowing over a deep porous medium. *Journal of Fluid Mechanics*, 440:359–380, 2001.

[4] D. G. Aronson. Regularity properties of flows through porous media. *SIAM Journal of Applied Mathematics*, 17:461–467, 1969.

[5] D. G. Aronson, L. C. Caffarelli and S. Kamin. How an initially stationary interface begins to move in porous medium flow. *SIAM Journal of Mathematical Analysis*, 14:639–658, 1983.

[6] B. C. Berndt. On the Hurwitz-Zeta Function *Rocky Mountain Journal of Mathematics*, 2:151–157, 1972.

[7] J. F. Blowey, J. R. King, and S. Langdon. Small and waiting-time behaviour of the thin film equation. *Journal of Fluid Mechanics*, 59:481–491, 2007.

[8] C. G. Broyden. On the discovery of the "good Broyden" method. *Mathematical Programming*, 87:209–213, 1973.

[9] J. Buckmaster. Viscous-gravity spreading of an oil slick. *Journal of Fluid Mechanics*, 59:481–491, 1973.

[10] R. Chebbi. Viscous-gravity spreading of oil on water. *AIChE Journal*, 47(2):288–294, 2001.

[11] S. Chiu-Webster, E. J. Hinch, and J. R. Lister. Very viscous horizontal convection. *Under consideration for publication in Journal of Fluid Mechanics.*

[12] J. A. Cuminato, A. D. Fitt, M. J. S. Mphaka, and A. Nagamine. A singular integro-differential equation model for dryout in LMFBR boiler tubes. *IMA journal of applied mathematics*, 75(2):269–290, 2010.

[13] L. J. Cummings, and P. D. Howell. On the evolution of non-axisymmetric viscous fibres with surface tension, inertia and gravity. *Journal of Fluid Mechanics*, 389:361–389, 1999.

[14] S. H. Davis, and L. M. Hocking. Spreading and inhibition of viscous liquid on a porous base. *Physics of Fluids*, 11(1):48–57, 1999.

[15] J. N. Dewynne, P. D. Howell, and P. Wilmott. Slender viscous fibres with inertia and gravity. *The Quarterly Journal of Mechanics and Applied Mathematics*, 47(4):541–555, 1994.

[16] N. Didden and T. Maxworthy. The viscous spreading of plane and axisymmetric gravity currents. *Journal of Fluid Mechanics*, 121:27–42, 1981.

[17] L. Edelstein-Keshet. Mathematical models in Biology. *SIAM Classics in Applied Mathematics*, 2005.

[18] R. Estrada and R. P. Kanwal *Singular Integral Equations.* Birkhäuser Publishers, 1999.

[19] R. Ferreira, and J. L. Vazquez. Extinction behaviour for fast diffusion equations with absorption. *Nonlinear Analysis*, 43:943–985, 2001.

[20] A. D. Fitt, K. Furusawa, T. M. Monro, C. P. Please, and D. J. Richardson. The mathematical modelling of capillary drawing for holey fibre manufacture. *Journal of Engineering Mathematics*, 43:201–227, 2002.

[21] M. Foda and R. G. Cox. The spreading of thin liquid films on a water-air interface. *Journal of Fluid Mechanics*, 101:33–51, 1980.

[22] V. A. Galaktionov, S. I. Shmarev and J. L. Vazquez. Regularity of interfaces in diffusion processes under the influence of strong absorption. *Archive for Rational Mechanics and Analysis*, 149:183–212, 1999.

[23] M. L. Gandarias. Classical point symmetries of a porous medium equation. *Journal of Physics A: Mathematical and Theoretical*, 29:607–633, 1994.

[24] M. A. Goldshtik. Viscous-flow paradoxes. *Annual Review of Fluid Mechanics*, 22:441–472, 1990.

[25] H. J. J. Gramberg, P. D. Howell, and J. R. Ockenden. Convection by a horizontal thermal gradient. *Journal of Fluid Mechanics*, 586:41–57, 2007.

[26] R. E. Grundy. The asymptotics of extinction in nonlinear diffusion reaction equations. *Journal of the Australian Mathematical Society*, 33:413–428, 1992.

[27] M. E. Gurtin. On the diffusion of biological populations. *Mathematical Biosciences*, 33:35–49, 1977.

[28] M. A. Herrero and J. L. Vazquez. The one-dimensional nonlinear heat equation with absorption: regularity of solutions and interfaces. *SIAM Journal of Mathematical Analysis*, 18:149–167, 1987.

[29] J. M. Hill, A. J. Avagliano and M. P. Edwards. Some exact results on nonlinear diffusion with absorption. *SIAM Journal of Mathematical Analysis*, 18:149–167, 1987.

[30] E. Hinch. *Perturbation Methods*. Cambridge University Press, 1991.

[31] J. Y. Holyer and H. E. Huppert. Gravity currents entering a two-layer fluid. *Journal of Fluid Mechanics*, 100(4):739–767, 1980.

[32] D. P. Hoult. Oil spreading on the sea. *Annual Review of Fluid Mechanics*, 4:341–368, 1972.

[33] P. D. Howell. Extensional Thin Layer Flows. *D.Phil thesis, St. Catherine's College, Oxford, 1994.*

[34] P. D. Howell. Models for thin viscous sheets. *European Journal of Applied Mathematics*, 7:321–343, 1996.

[35] H. E. Huppert. The propogation of two-dimensional and axisymmetric viscous gravity currents over a rigid horizontal surface. *Journal of Fluid Mechanics*, 121:43–58, 1981.

[36] H. E. Huppert. Gravity currents: A personal perspective. *Journal of Fluid Mechanics*, 554(1):299–322, 2005.

[37] G. A. Jones, and D. Singerman Complex Functions: an algebraic and geometric viewpoint. Cambridge University Press, 1987.

[38] A. S. Kalashnikov. The propagation of disturbances in problems of nonlinear heat conduction with absorption. *USSR Computational Mathematics and Mathematical Physics*, 14:70–85, 1974.

[39] S. Kamin and L. Veron. Existence and uniqueness of the very singular solution of the porous medium equation with absorption. *Journal d'Analyse Mathematique*, 51(1):245–258, 1988.

[40] R. Kersner. On the behaviour of temperature fronts in media with nonlinear heat conductivity with absorption. *Vestnik Moskovskogo Universitetor Matematika*, 33:44–51, 1978.

[41] B. F. Knerr. The behaviour of the support of solutions of the equation of nonlinear heat conduction with absorption in one dimension. *Transactions of the American Mathematical Society*, 249:409–424, 1979.

[42] D. Krause, and H. Loch. *Mathematical simulation in glass technology.* Springer, 2002.

[43] A. A. Lacey. Initial motion of a free boundary for a nonlinear diffusion equation. *Journal of Applied Mathematics*, 31:113–119, 1983.

[44] A. A. Lacey, J. R. Ockendon and A. B. Tayler. Waiting time solutions of a nonlinear diffusion equation. *SIAM Journal of Applied Mathematics*, 42:1252–1264, 1982.

[45] H. Lamb. *Hydrodynamics.* Cambridge University Press, 1952.

[46] T. Maxworthy, J. Leilich, J. E. Simpson, and E. H. Meiburg. The propogation of a gravity current into a linearly stratified fluid. *Journal of Fluid Mechanics*, 453:371–394, 2002.

[47] K. Mikula. Numerical solution of nonlinear diffusion with finite extinction phenomenon. *Acta Mathematica Universitatis Comenianae*, 64(2):173–184, 1995.

[48] A. Münch, B. Wagner, and T. P. Witelski. Lubrication models with small to large slip lengths. *Journal of Engineering Mathematics*, 53:359–383, 2005.

[49] N. I. Muskhelishvili. *Singular Integral Equations.* P. Noordhoff N. V, Groningen, 1953.

[50] T. Nakaki. Numerical interfaces in nonlinear diffusion equations with finite extinction phenomena. *Hiroshima Mathematical Journal*, 18:373–397, 1988.

[51] C. Nakaya. *Spread of Fluid Drops over a Horizontal Plate.* Journal of the Physical Society of Japan, 1974.

[52] J. Ockenden, S. Howison, A. Lacey, and A. Movchan. *Applied Partial Differential Equations.* Oxford University Press, 2003.

[53] R. E. Pattle. Diffusion from an instantaneous point source with a concentration dependent coefficient. *Quarterly Journal of Mechanics and Applied Mathematics*, 12:407–410, 1958.

[54] C. Pozrikidis. *Boundary Integral and Singularity Methods for Linearised Viscous Flow.* Cambridge Texts In Applied Mathematics, 1992.

[55] D. Pritchard, A. W. Woods, and A. J. Hogg. On the slow draining of a gravity current moving through a layered permeable medium. *Journal of Fluid Mechanics*, 444:23–47, 2001.

[56] G. Richardson, and J. R. King. The Evolution of space curves by curvature and torsion. *Journal of Physics A: Mathematical and General*, 35:9857–9879, 2002.

[57] L. F. Shampine. Vectorized Adaptive Quadrature in MATLAB. *Journal of Computational and Applied Mathematics*, 211:131-140, 2008.

[58] L. F. Shampine and M. W. Reichelt. The MATLAB ODE suite. *SIAM Journal on Scientific Computing*, 18:1–22, 1997.

[59] J. E. Simpson. Gravity currents in the laboratory, atmosphere, and ocean. *Annual Review of Fluid Mechanics*, 14:213–234, 1982.

[60] G. G. Stokes. *Mathematical and Physical Papers. Cambridge University Press*, 3:55–67, 1880 - 1905.

[61] F. G. Tricomi. *Integral Equations.* Interscience Publishers, 1957.

[62] J . L. Vazquez. *The Porous Medium Equation : Mathematical Theory.* Oxford Mathematical Monographs, 2006.

[63] B. Wagner. Asymptotic approach to second-kind similarity solutions of the modified porous medium equation. *Journal of Engineering Mathematics*, 53:201–220, 2006.

[64] E. T. Whittaker, and G. N. Watson. *A course of Modern Analysis, 4th edition* Cambridge University Press, 1958.

[65] Y. B. Zel'dovich and Y. P. Raizer. Physics of shock waves and high-temperature hydrodynamic phenomena. *Dover publications*, 2002.